# NATIONAL ADVISORY COMMITTEE FOR AERONAUTICS

## TECHNICAL NOTE 3235

LOW-SPEED YAWED-ROLLING AND SOME OTHER ELASTIC

CHARACTERISTICS OF TWO 56-INCH-DIAMETER,

24-PLY-RATING AIRCRAFT TIRES

By Walter B. Horne, Bertrand H. Stephenson,
and Robert F. Smiley

Langley Aeronautical Laboratory
Langley Field, Va.

NACA

Washington

August 1954

NATIONAL ADVISORY COMMITTEE FOR AERONAUTI

TECHNICAL NOTE 3235

LOW-SPEED YAWED-ROLLING AND SOME OTHER ELASTIC

CHARACTERISTICS OF TWO 56-INCH-DIAMETER,

24-PLY-RATING AIRCRAFT TIRES

By Walter B. Horne, Bertrand H. Stephenson,
and Robert F. Smiley

## SUMMARY

The low-speed (up to 4 miles per hour) cornering characteristics of two 56 × 16, type VII, extra-high-pressure, 24-ply-rating tires were determined for a range of vertical loadings, yaw angles, and tire inflation pressures. Locked-wheel drag tests were also made for one vertical-load condition. The quantities measured included cornering force, drag force, self-alining torque, pneumatic caster, vertical tire deflection, rolling radius, and relaxation length. Some supplementary tests were made which included measurements of tire footprint area, vertical-load-deflection characteristics, and the variation of tire radius and width with inflation pressure.

Results indicated that the normal force reached a maximum at between 14° and 18° yaw. The self-alining torque increased with yaw angle up to between 5° and 8° yaw where a maximum was reached. Increasing the yaw angle beyond this point tended to decrease the self-alining torque considerably. The pneumatic caster was a maximum at small yaw angles and tended to decrease in value with increasing yaw angle. The yawed-rolling and sliding drag coefficients of friction both tended to decrease in magnitude with increasing average bearing pressure. In general, the test results indicate that the relaxation length decreases with increasing vertical tire deflection and increasing inflation pressure.

## INTRODUCTION

Existing experimental data on aircraft tire behavior under static, kinematic, and dynamic conditions, most of which are discussed in reference 1, are limited in both scope and quantity particularly for large tires. This lack of scope has hindered those engaged in design problems concerning landings with yaw, ground handling, and wheel shimmy. A program was therefore undertaken to determine values of the essential tire parameters for a range of tire sizes under static, kinematic, and dynamic

conditions. Some static force-deflection tests of the program have been completed and the results were reported in reference 2. The present paper presents results from part of the kinematic test program for two 56-inch-diameter, 56 × 16, type VII, extra-high-pressure, 24-ply-rating tires.

Most of the test consisted of towing the tire specimens in a yawed condition. The yaw-angle range covered was from about 0° to 18° and the inflation-pressure range, from about 30 psi to 230 psi. The vertical loads covered ranged from about 10,000 to 45,000 pounds per tire. The towing speed was held constant for each run and did not exceed 4 miles per hour. The quantities measured included vertical tire deflection, side force, drag force, self-alining torque, pneumatic caster, rolling radius, and relaxation length. Relaxation-length measurements were also determined for the case of approximately zero yaw for both a standing and rolling tire.

Drag tests were conducted with the wheels locked to obtain measurements in the fore-and-aft direction of the sliding coefficient of friction and the stiffness of the tires. Some supplementary tests were made which included measurements of footprint area, vertical-load—deflection characteristics, and the variation of tire radius and width with inflation pressure.

## SYMBOLS

$A_g$          gross footprint area, sq in.

$A_n$          net footprint area, sq in.

b             overall tire-ground contact width, in.

d             outside diameter of free tire, in.

F             force, lb

$F_R$          resultant force, $\sqrt{F_x^2 + F_y^2}$, lb

$F_x$          drag or fore-and-aft force (ground force parallel to direction of motion), lb

$F_y$          cornering force (steady-state ground force perpendicular to direction of motion), lb

$F_{y_i}$      instantaneous ground force perpendicular to direction of motion, lb

$F_z$      vertical load on tire, lb

$F_\psi$      normal force (ground force perpendicular to wheel plane, $F_y \cos \psi + F_x \sin \psi$), lb

$2h$      overall tire-ground contact length, in.

$K_x$      fore-and-aft spring constant, $\left(\dfrac{dF_x}{dx}\right)_{x \to 0}$, lb/in.

$L$      relaxation length, in.

$L_f$      unyawed-rolling-force relaxation length of tire, in.

$L_s$      static relaxation length of tire, in.

$L_y$      yawed-rolling relaxation length of tire, in.

$L_\lambda$      unyawed-rolling-deflection relaxation length of tire, in.

$\Delta M_z$      measured portion of self-alining torque, lb-in.

$M_{z_0}$      self-alining torque for $\psi = 0.35^\circ$, lb-in.

$M_z$      self-alining torque, $\Delta M_z + M_{z_0}$, lb-in.

$N$      cornering power (rate of change of cornering force or normal force with yaw angle for small yaw angles, $dF_y/d\psi$ or $dF_\psi/d\psi$ for $\psi \to 0$), lb/deg

$p$      tire inflation pressure, lb/sq in.

$p_0$      tire inflation pressure at zero vertical load ($F_z = 0$), lb/sq in.

$p_g$      average gross footprint pressure, $F_z/A_g$, lb/sq in.

$p_n$      average tire-ground bearing pressure, $F_z/A_n$, lb/sq in.

$p_r$      rated tire inflation pressure, lb/sq in.

$q$          pneumatic caster, $M_z/F_\psi$, in.

$r$          outside radius of free tire, in.

$r_e$        rolling radius, in.

$s$          circumferential distance around the tire, ft

$v$          rolling velocity, ft/sec

$w$          maximum tire width, in.

$x$          displacement in direction of motion, in. or ft

$\delta$          vertical tire deflection due to combined vertical and yaw loads, in.

$\delta_0$        vertical tire deflection due to vertical load only, in.

$\eta$          interpolation factor, in.$^3$/deg

$\lambda$          lateral distortion of the tire equator, in.

$\lambda_0$        lateral distortion of tire equator at center of contact, in.

$\mu_x$        sliding drag coefficient of friction, $F_{x_{max}}/F_z$

$\mu_\psi$        yawed-rolling coefficient of friction, $F_{R_{max}}/F_z$

$\psi$          angle of yaw, deg

$\omega$         wheel rotation, radians

Subscript:

max      maximum

    Bars over symbols denote the average value of the quantities involved for tires A and B.

## DEFINITIONS OF CONCEPTS

Inasmuch as some of the quantities used in this paper are not generally very well known, the following definitions are given to aid the reader.

Footprint area.- The tire contacts the ground in a finite area the shape of which is illustrated in figure 1. Because the tires tested had a rib-type tread, this area consists of alternate strips where the tire contacts the ground and where it does not contact the ground (corresponding to the spaces between the treads). The total area, including the spaces between the treads, is designated as the gross footprint area of the tire. The actual ground-contact area, or bearing area, is referred to as the net footprint area.

Yawed-rolling characteristics.- If a pneumatic-tired wheel is towed unbraked in a straight line while yawed by an angle $\psi$, it develops an elastic side force which, for small yaw angles, is roughly proportional to the yaw angle. The component of this side force perpendicular to the direction of motion is called the cornering force $F_y$. The initial rate of change of cornering force with yaw angle is called the cornering power $N$ $\left[\text{that is, } N = \left(\dfrac{dF_y}{d\psi}\right)_{\psi \to 0}\right]$. The yawed-rolling condition also produces a ground moment on the tire which is called the self-alining torque $M_z$. Other yawed-rolling forces are the drag force $F_x$ (parallel to the direction of motion) and the component of the side force perpendicular to the wheel center plane or normal force $F_\psi$.

Relaxation length.- The relaxation length is a tire property which has been defined by Temple in reference 3. Consider the situation where the base or ground-contact area of an unyawed tire is laterally deflected relative to the wheel and the wheel is then rolled straight ahead in its initial plane. After the tire has rolled forward a distance equal to the footprint length, then, from that point on, according to the experiments of Kantrowitz (ref. 4) and others, the lateral tire deflection $\lambda_0$ dies out exponentially with the distance $x$ rolled. The distance that the tire must roll forward in order for the lateral deflection $\lambda_0$ to drop to a fraction $1/e$ of its initial value has been defined by Temple as the relaxation length of the tire. In other words, the variation of lateral deflection $\lambda_0$ with distance $x$ rolled is governed by an equation of the type

$$\lambda_o = A_1 e^{-x/L} \qquad\qquad (1)$$

where $A_1$ is a constant depending on the initial lateral tire deflection and $L$ is the relaxation length.

The preceding definition of relaxation length in terms of the result of an unyawed-rolling experiment is only one of a number of ways in which this quantity might be defined. Four other slightly different methods of defining this quantity which were employed in the present investigation will now be described. From the point of view of the theory of reference 5, these definitions and the corresponding experiments should lead to the same numerical value of relaxation length; however, because this theory is not completely rigorous, it is not unexpected that the different definitions to be given will not lead to precisely the same value of relaxation length. In order to distinguish these different values of relaxation length to be discussed, they are assigned different names and symbol subscripts.

Static relaxation length $L_s$.- Consider the experiment where the ground-contact area of a stationary tire is deflected laterally with respect to the wheel plane. The different parts of the center band or equator of the tire are then deflected sidewise from the wheel center plane in the manner illustrated in figure 2. From the available experimental data, it is found that, except in and near the edge of the ground-contact area and near the top of the tire, this distortion curve is essentially an exponential curve of the form

$$\lambda = A_2 e^{-s/L_s} \qquad\qquad (2)$$

where $\lambda$ is the lateral distortion of the tire equator, $A_2$ is a constant, and $s$ is the circumferential distance about the tire. The exponential constant $L_s$ is called the static relaxation length of the tire.

Unyawed-rolling-deflection relaxation length $L_\lambda$.- The next definition of relaxation length to be considered is a minor modification of the original definition for the unyawed-rolling case (eq. 1) which is designed to take into account the fact that, owing to experimental difficulties, it was not possible to attain exactly the condition of zero yaw angle in the tests of the present paper. Actually, the minimum yaw angle attained was about $0.35^\circ$. In order to take this small yaw angle into account in the definition of relaxation length, the theory of reference 5 indicates that equation (1) should be replaced by the equation

$$\lambda_0 = \lambda_\infty + A_3 e^{-x/L_\lambda} \tag{3}$$

where $A_3$ is a constant depending on the initial tire deflection, $\lambda_\infty$ is the measured tire deflection for steady yawed rolling at the small angle of yaw, and $L_\lambda$ is a constant which will be called the unyawed-rolling-deflection relaxation length.

Unyawed-rolling-force relaxation length $L_f$.- In view of the fact that tire lateral force is approximately proportional to tire lateral deflection, the relaxation length for the unyawed-rolling-deflection relaxation-length test could also be determined by measuring the rate of decay of the lateral force $F_{y_i}$ with distance $x$ rolled. This decay proceeds in accordance with the equation

$$F_{y_i} = F_y + A_4 e^{-x/L_f} \tag{4}$$

analogous to equation (3) where $F_y$ is the measured side force for steady yawed rolling at the small angle of yaw and $A_4$ is a constant. The corresponding relaxation length $L_f$ is called the unyawed-rolling-force relaxation length.

Yawed-rolling relaxation length $L_y$.- Another definition of relaxation length may be obtained in connection with the experiment where a wheel is set up at an angle of yaw and is then rolled straight ahead. If no skidding occurs, then, according to theory (ref. 5) and to the present test results, after the wheel has rolled forward a distance approximately equal to the footprint length $2h$, the tire builds up a side force which exponentially approaches an end-point condition for steady yawed rolling; that is, the side force $F_{y_i}$ builds up with distance $x$ rolled according to a relation of the form

$$F_{y_i} = F_y - A_5 e^{-x/L_y} \tag{5}$$

where the constant $A_5$ depends on the initial tire distortion and $L_y$ is called the yawed-rolling relaxation length.

Rolling radius.- The rolling radius of a tire is defined as the ratio of the component of the rolling velocity parallel to the plane of the wheel $v \cos \psi$ to the angular velocity of the wheel about the axle $\omega$

or as the ratio of the component of the rolling displacement parallel
to the plane of the wheel to the angular rotation of the wheel.


## APPARATUS

### Test Vehicle

The basic test vehicle consisted of the fuselage and wing center
section of a surplus cargo airplane; general views of this vehicle are
shown in figures 3 to 5. The airplane was towed tail first by a tractor
truck at an attitude such that the original airplane shock struts were
vertical. This attitude was necessary in order to use the existing
landing-gear structure and still keep the tires in a vertical plane at
varying angles of yaw. The original yokes and torque links of the
landing-gear struts along with the wheel assemblies were replaced by
steel wheel housings which held the tires and wheels tested. A rigid
truss pinned at four points to the two wheel housings held the wheel
housings in a fixed relative position during towing operations. Holes
located in the wheel housings at angular intervals of $3\frac{1}{2}^{O}$ permitted the
wheel frames to be rotated through a nominal yaw-angle range of $0^{O}$ to
$24\frac{1}{2}^{O}$. Actual measurements on the completed test rig, however, showed
the yaw-angle range to be from $0.35^{O}$ to $24.9^{O}$.

The towing loads were taken by two steel cables attached between
the wheel housings and the tow truck chassis. At high yaw angles with
the heavy-weight condition, an additional truck was attached to the tow
truck to provide increased power for towing. The maximum towing force
required was approximately 8,000 pounds.

The airplane tail was supported by the original swiveling tail-
wheel-strut assembly which was modified so that the tail-wheel assembly
rotated about a vertical axis. The axle rested in a slot on the top of
the tow-truck support structure. This slot and pin arrangement permitted
the entire towing load, with the exception of a relatively small amount
of friction force, to be carried by the drag cables.

The weight of the test vehicle acting on the tires was approximately
20,000 pounds in the lightest condition. This weight was varied in incre-
ments by the addition of six steel and concrete weight cans (each weighing
about 8,000 pounds) which were mounted on the airplane structure as shown
in figure 3. Additional weights were also added in the fuselage to obtain
the heaviest weight condition of 90,000 pounds.

For the locked-wheel drag-force investigation, the test setup was as shown in figure 5. The drag cables were disconnected from the tow truck and attached to a hydraulic ram which was anchored to several stationary heavy vehicles. The airplane wheels were locked by means of rods passing through the spokes and bearing on the wheel frames. Pressure was supplied to the ram by the electrically driven pump shown in figure 5.

## Instrumentation

The test vehicle was equipped with instruments for measuring side force, self-alining torque, drag, vertical tire deflection, horizontal translation, and wheel rotation. An explanation of the method by which each of the quantities was measured is given in the following sections. Measurements of these quantities were recorded simultaneously on a 14-channel oscillograph mounted in the test vehicle. This oscillograph was equipped with a 0.01-second timer. A sample oscillograph record for a yawed-rolling run is shown in figure 6.

Side force.- The side force acting on the two tires was measured by means of a rigid truss structure which was installed between the two wheel housings and which was equipped with four strain-gage dynamometers. (See fig. 7.)

Self-alining torque.- The same dynamometers used for the side-force measurements were used to obtain the self-alining torque (that is, the moment about a vertical axis through the center of the wheel).

Vertical load.- The vertical load on the tires was measured by a portable commercial strain-gage dynamometer kit.

Drag forces.- Two separate strain-gage dynamometers, indicated as 5 and 6 in figure 7, were used for measuring the drag forces.

Vertical tire deflection.- Vertical-tire-deflection measurements were obtained during the test runs by use of the wheel and strut assembly shown in figure 4(a). Vertical motion of the small solid swiveling wheel, which represents the large tire deflection, is recorded by means of a variable-resistance slide-wire potentiometer.

Fore-and-aft translation.- Fore-and-aft translation of the test vehicle from the initial starting point, during the early stages of each run, was recorded by means of the circular slide-wire potentiometer device which is shown in figure 4(a). This device consists of a drum with a string wound around it, one end of the string being tied to a weight resting on the taxi strip. Translation of the test vehicle thus produces rotation of the drum. This rotation produces a sawtooth-type record (see fig. 6), each sawtooth of which corresponds to a single revolution of the drum.

Horizontal translation during later stages of each run was measured
by means of trailing bicycle wheels attached behind the wheel frames.
These bicycle wheels are equipped with an electrical device which gives
a pulse on the oscillograph for each 0.39 foot of distance traveled.

Wheel rotation.- Rotation of the test wheels was obtained from
revolution-counter devices installed on each of the wheels. These
devices furnished indications on the oscillograph for each 10° of wheel
rotation.


Tires

General description.- The tires tested in this investigation were two
56-inch-diameter, 56 × 16, type VII, extra-high-pressure, 24-ply-rating,
rib tread tires which were made by different manufacturers. One tire was
new and unused. This tire is referred to in this paper as tire A. The
other tire, which will be referred to as tire B, was previously subjected
to the static tests which are reported in reference 2. The specifica-
tions for these tires given in table I were either obtained from refer-
ence 6 or by direct measurement after the conclusion of the tests. Fig-
ure 8 shows the deflated and inflated cross sections of the tires tested.
These cross sections were obtained from plaster casts taken after the
conclusion of the tests and, consequently, they show the tire cross sec-
tion for a worn condition. There appears to be no appreciable difference
in the inflated outer profiles for the two tires. However, there is seen
to be an appreciable difference in cross-sectional thickness of the two
tire treads.

Tire wear.- During the course of the present investigation, there
was an appreciable progressive change in the cross-sectional shape of
the tires due to skidding and working of the tires. Therefore, the
chronological order in which the test data was collected is of some
importance in the interpretation of the data. This chronological order
is indicated in this paper by a series letter which is assigned to all
test data. Specifically, series A represents conditions at the beginning
of the tests; series B represents conditions for a later period of time,
and so forth.

The change in tire-tread pattern due to tire wear throughout the
tests is illustrated in figure 9. At the beginning of the tests both
tires had a rectangular cross-sectional tread pattern (fig. 9(a)) and
this pattern was substantially preserved throughout most of series A
to C. Toward the end of series C, however, the side of the tread in
intimate contact with the ground began to wear away and produced the
tread pattern illustrated in figure 9(b). This wear increased substan-
tially during series D and for series E to G the tire profile remained
approximately as indicated in figure 9(c). The small projecting edges

of the tread were then cut off and for the remainder of the tests
(series H and I) the tread cross section was again essentially rectan-
gular with rounded-off corners, as shown in figure 9(d).

Tire radius.- The variation of the unloaded tire radii with infla-
tion pressure and tire wear is shown in figure 10.  Each measurement
shown was taken after the tires had been left at constant pressure for
at least 24 hours.  For test series E to H, the radius of the tires is
defined as the maximum radius less the height of the small projecting
edge shown in figure 9(c); thus, the indicated difference in tire radius
for series A to C and E to I is largely due to the wearing off of the
tread.  It should also be noted that the tire radii during the later
stages of this investigation (series E to I in fig. 10) differ slightly
from the radii measured after the conclusion of the tests (table I and
fig. 8).  The difference, approximately 1 percent, is probably due to
the fact that the earlier measurements were made during a period of
time when the tires were being regularly subjected to severe loadings
whereas the later measurements were made after the tires had been com-
pletely unloaded for a long period of time.

A radius-pressure hysteresis loop for tire B is shown in figure 11.
The elapsed time from start is shown for a few of the measurements pre-
sented.  The variation in tire radius for a given pressure is seen to
amount to as much as 1 percent for this relatively slow rate of change
of pressure (roughly, four hours for most of the cycle).

Tire width.- The variation of maximum tire width with inflation
pressure is shown in figure 12 for both tires.  These measurements were
all made after the conclusion of testing (tires well worn) and each
measurement was taken after the tires had been kept at constant pressure
for at least 24 hours in order to minimize hysteresis effects.

Test Surface

All yawed-rolling and drag tests were conducted by towing the test
vehicle along the center of a 9-inch-thick reinforced-concrete taxi strip.
This taxi strip had a slight crown such that the tires on the test vehi-
cle were subject to a slight tilt.  However, this tilt was less than $1^\circ$.
The texture of the taxi strip, a boarded concrete surface, as determined
from plaster casts, is shown in figure 13 for three random positions on
the strip.  All other tests were conducted on a much smoother, level,
reinforced-concrete surface.

Precision of Data

The instruments used in these tests and the methods of reducing data are believed to yield results usually accurate within the following limits:

Vertical load on tires, $F_z$, percent . . . . . . . . . . . . . . . . . . . .  ±3

Cornering force, $F_y$, percent  . . . . . . . . . . . . . . . . . . . . .  ±3

Force perpendicular to wheel plane, $F_\psi$, percent . . . . . . . . . .  ±3

Drag force per tire, $F_x$, lb . . . . . . . . . . . . . . . . . . . . . .  ±300

Measured moment, $\Delta M_z$, lb-in. . . . . . . . . . . . . . . . . . . . . . ±3,000

Tire inflation pressure, $p_o$ or $p$, lb/sq in. . . . . . . . . . . . . .  ±3

Free radius, $r$, in.  . . . . . . . . . . . . . . . . . . . . . . . . . .  ±0.02

Rolling radius, $r_e$, in.  . . . . . . . . . . . . . . . . . . . . . . . .  ±0.1

Horizontal translation, $x$, in.  . . . . . . . . . . . . . . . . . . . . .  ±3

Vertical tire deflection, $\delta_o$ or $\delta$, in. . . . . . . . . . . . . . . .  ±0.2

Yaw angle, $\psi$, deg . . . . . . . . . . . . . . . . . . . . . . . . . . .  ±0.1

TEST PROCEDURE

The present investigation of tire characteristics is divided into the following parts:  yawed-rolling tests, relaxation-length tests, locked-wheel drag tests, and supplementary measurements.

Yawed-Rolling Tests

For each run of the yawed-rolling tests, the test vehicle was moved into towing position on the dry, clean, concrete taxi strip and the wheel housings were rotated and locked at the particular yaw angle desired.  The tires were adjusted to the test inflation pressure and the vertical tire deflections noted.  The vehicle was then towed a distance of approximately 50 feet within a speed range of from 1 to 4 miles per hour.  Figure 4 shows one of the tires during a run at 17.9° yaw.

All test runs at yaw angles of 0.35°, 3.9°, 7.4°, 10.9°, 14.4°, and 17.9° were made with both wheels symmetrically yawed with respect to the longitudinal axis of the test vehicle.  Because these particular yaw angles were the only angles attainable on the test vehicle, the only way that intermediate yaw angles could be obtained was by unsymmetrically yawing the two wheels with respect to the longitudinal axis of the test vehicle.  This was done to obtain intermediate yaw angles of 2.1° and 5.7° (that is, in order to obtain 2.1°, one wheel was yawed by 0.35° and

the other, by $3.9°$).  When towed ahead in this unsymmetrically yawed
condition, the test vehicle first veers off to the side because of the
unsymmetrical forces.  After a short run, however, the vehicle runs
smoothly with the longitudinal axis of the test vehicle yawed with
respect to the direction of motion such that both wheels have the same
final intermediate yaw angle with respect to the direction of motion.

In general, at the beginning of each run, the tires could not
practically be set in an equilibrium condition but were instead subject
to a certain amount of distortion (and thus, forces and moments) which
appeared as a consequence of residual stresses left over from the previ-
ous runs and from moments resulting from the changing of the yaw angles
of the wheels.

The following measurements were recorded continuously from the
start of the run:  side force, self-alining torque, drag force, verti-
cal tire deflection, wheel rotation, and vehicle translation in the
direction of motion.

All runs except one (run 185 of table II) were made with the tires
toed out in the direction of motion.  For this one particular run, the
usual direction of motion was reversed in order to give an indication
of the effects of unsymmetrical tread wear.  In order to investigate
this unsymmetrical wear effect more thoroughly, each of the tires was
removed from its wheel housing after test series G and was replaced so
that the former outboard side of the tire became the inboard side.  Tow
tests were then continued in the usual toed-out condition throughout
test series H and I.

### Relaxation-Length Tests

Four types of relaxation length were determined in this investiga-
tion (see section entitled "Definitions of Concepts").  The methods used
to determine these types of relaxation length were as follows:

Static relaxation length  $L_s$.- The standing tires were given initial
lateral deflection by pulling outward, by means of hydraulic rams, plates
placed underneath the tire.  The lateral distortion of each tire center
tread relative to the wheel center plane was then measured for several
points around the tire circumference between the footprint edge and a
point $180°$ from the center of contact.

Unyawed-rolling-force relaxation length  $L_f$.- With the wheel housings
positioned close to $0°$ yaw (actually $0.35°$), the tires were given initial
lateral deflections by pulling out on plates placed underneath (as for

the static relaxation-length tests). The test vehicle was then rolled ahead off the plates for a distance of about 50 feet with the recording oscillograph taking a continuous record of side force and horizontal translation.

Unyawed-rolling-deflection relaxation length $L_\lambda$.- This procedure entailed rubbing the center tread of each tire with chalk so that a trace of each center tread would appear on the concrete surface as the tires were rolled ahead. The chalked tires were first given an initial lateral deflection. The test vehicle was then towed forward about 50 feet and the distance between the tire-center-tread traces was measured at intervals from the start up to the point of constant distance between tread traces.

(The rolling procedure for this relaxation length is the same as that for the unyawed-rolling-force relaxation length. Actually, the same test runs were used to obtain test data for determining both of these relaxation lengths.)

Yawed-rolling relaxation length $L_y$.- The basic data for the yawed-rolling relaxation length were obtained from the initial (force buildup) phase of the $3.9^\circ$ yawed-rolling tests. This constant was evaluated in this paper for this yaw angle only, since, for larger angles, skidding appeared to be too significant and for smaller angles the accuracy of measurement was usually too poor.

## Locked-Wheel Drag Tests

The method used to determine tire stiffness and sliding drag in the fore-and-aft direction was as follows: The setup for the locked-wheel drag tests previously described was used, the test vehicle being pulled forward on the taxi strip with the wheels set at approximately $0^\circ$ yaw ($\psi = 0.35^\circ$) and locked to prevent wheel rotation. As the test vehicle was pulled forward at a speed less than 10 inches per minute, a continuous record was taken of drag force and horizontal displacement. This procedure was repeated throughout a range of tire inflation pressures for one weight condition. In addition, several runs were made with the concrete surface in a wet condition.

During these tests, the weight of the test vehicle remained constant; however, the vertical load on the tires decreased slightly with increasing drag force as a consequence of the moment produced by the drag force. This change in vertical load was taken into account in the computation of friction coefficients. (It was not taken into account in the other tests since the effect was very small for those conditions.)

Supplementary Tests and Measurements

In addition to the tests just described, several supplementary tests were made. These tests included vertical-load-deflection measurements and footprint-area determinations. The vertical-load-deflection characteristics of the two tire specimens were determined for one inflation pressure (about 220 lb/sq in.) with the tires mounted on the test vehicle. Tire-contact or footprint-area measurements were made for the tire specimens at several inflation pressures and vertical tire deflections. These measurements were obtained from the imprint left on a piece of heavy paper placed between a chalked portion of the tires and a smooth concrete hangar floor. Several typical imprints are shown in figure 1.

## RESULTS AND DISCUSSION

Most of the experimental data obtained from this investigation are presented in tables II to VI and figures 8 to 47.

### Yawed-Rolling Tests

Table II contains all test data obtained during the final steady-state stage of each yawed-rolling run. Data are presented for 9 different test series (A to I) which represent either different vertical loadings, different tire wear, or different orientation of the tires. The variation of normal force $\bar{F}_\psi$, self-alining torque $\bar{M}_\psi$, and pneumatic caster $\bar{q}$ with yaw angle are shown in figure 14 for all vertical loads and inflation pressures. Some details pertinent to the interpretation of these data are discussed in the appendix. Sample rolling-radius data for two typical test conditions are plotted in figure 15 as functions of yaw angle and vertical tire deflection.

The buildup of cornering force with horizontal distance rolled during the initial stages of the yawed-rolling runs is illustrated in figure 16 for typical runs at several pressures and for three test series. Inasmuch as for most runs there was an initial residual force or preload in the tires, the original test curves did not usually pass through the origin. In order to take this fact into consideration, the test curves shown in this figure have been horizontally shifted (if necessary) so that the extrapolation of each curve is made to pass through the origin. For most of these curves, the initial rate of buildup appears to increase with increasing yaw angle (as is predicted by theory, that is, ref. 5) and that the force generally approaches close to its maximum value before the tires have rolled more than 6 feet.

## Relaxation-Length Tests

Samples of the test data obtained from the four different methods used to determine the relaxation length of the tire specimens are shown in figure 17 for test series A, B, and E. In parts (a), (b), and (c) of figure 17, these data are plotted in semilogarithmic coordinates in order that the expected exponential curves (according to theory) should appear as straight lines. The relaxation lengths for the conditions shown here and for all other conditions of this investigation were obtained by fitting straight lines to such semilogarithmic plots for each test run and are tabulated together in tables II to IV.

It is seen from figure 17 that usually the test results do appear to give substantially straight lines in these semilogarithmic plots; thus, the theoretical exponential variation of force with distance rolled (for the rolling relaxation lengths) or distance around the tire periphery (for the static relaxation length) is supported. The same data shown for series B in figure 17(b) is replotted in linear coordinates in figure 17(d). The solid lines drawn on these plots (fig. 17(d)) are the same solid faired lines which were fitted through the data in figure 17(b).

It should be noted that, for the static-relaxation-length data, the test data do not agree well with the assumed exponential variation near the two endpoint conditions at the edge of the tire footprint and at the top of the tire (for example, see fig. 17(a)). This discrepancy is due largely to the finite bending stiffness of the tire which requires that the slope of the tire-distortion curve must be zero at the edge of the tire footprint $(s = h)$ and also at the top of the tire and both of these factors conflict with an exponential variation.

## Locked-Wheel Drag Tests

Most of the experimental data obtained from the locked-wheel drag tests are presented in table V. Also, typical data are shown in figure 18 for the buildup of fore-and-aft force with horizontal distance pulled for several runs.

## Supplementary Tests

The vertical-load—vertical-tire-deflection characteristics curves for the two tires are given in figures 19 to 21 and the tire-footprint data are given in table VI.

Discussion of Parameters

Normal force $F_\psi$.- The variation of the steady-state normal force
with yaw angle, obtained from the data in table II, is shown in fig-
ure 14 for all test series. For each condition of initial vertical tire
deflection $\bar{\delta}_0$ and inflation pressure $\bar{p}$, it is seen that the normal
force increases with increasing yaw angle and reaches a maximum value at
between $14^\circ$ and $18^\circ$ yaw. The maximum normal force tends to decrease with
increasing inflation pressure. (This observation is discussed later in
more detail under the subject of yawed-rolling coefficient of friction.)
For the case of constant inflation pressure, shown in figure 22,
increasing the vertical load increases the maximum normal force.

Cornering force $F_y$.- The cornering force follows substantially
the same trends that were described for the normal force, as is shown
in figure 23, for a typical loading condition.

Cornering power $N$.- The variation of cornering power with verti-
cal tire deflection and inflation pressure for the different series
tested is shown in figures 24(a) and 24(b), respectively. These data
are derived from the initial slope of the normal-force—yaw-angle curves
given in figure 14. In order to show more clearly the trends of these
data, the effects of inflation pressure and vertical tire deflection,
respectively, on cornering power have been isolated in figures 25 and
26. For the constant vertical tire deflection of 3.2 inches considered
in figure 25, the cornering power increases nonlinearly with increasing
inflation pressure. The data for other constant vertical tire deflec-
tions seem to follow this same trend. For the constant-pressure range
shown in figure 26, the cornering power increases with increasing verti-
cal tire deflection up to a vertical tire deflection of around 3.0 inches
where a maximum is reached. Increasing the vertical tire deflection
beyond this point tends to reduce the cornering power.

Self-alining torque $M_z$.- The variation of self-alining torque with
yaw angle is shown in figure 14 for all test series. The self-alining
torque generally increases with increasing yaw angle for yaw angles less
than $5^\circ$ to $8^\circ$. Between $5^\circ$ and $8^\circ$, a maximum is reached and increasing
the yaw angle beyond this range usually decreases the self-alining torque
considerably. For constant vertical load, the data indicate that
increasing the tire inflation pressure tends to reduce the magnitude of
the self-alining torque at most yaw angles. In the case of constant
inflation pressure, illustrated in figure 22, increasing the vertical
load tends to increase the self-alining torque.

Effect of tire wear on normal force and self-alining torque.- The
influence of tire wear on normal force and self-alining torque can be
seen in figure 27 which presents data both for the unworn tire condition

(series A) and for a considerably worn condition (series F). For the most part, this comparison indicates no extremely large changes in either normal force or self-alining torque; however, reversing the tire tread (reversing the tires in the wheel housings) decreased the maximum normal force considerably as is illustrated in figure 28. A likely explanation for this phenomenon could lie in the fact that the tire-tread beads resulting from unsymmetrical tread wear (see fig. 9) fold over on top of the treads under towing conditions with the tires reversed as is shown schematically in figure 29. Such a folding of the tread bead would tend to reduce the tread-contact area considerably and thus increase the bearing pressure between the tire and the ground. This increase in bearing pressure would result in a reduced friction coefficient (to be discussed later) and would thus reduce the maximum attainable normal force.

Maximum self-alining torque $M_{z_{max}}$.- The variation of maximum self-alining torque with inflation pressure is shown in figure 30(a) and with vertical tire deflection by figure 30(b) for the test series investigated. These data are taken from the faired curves drawn through the data presented in figure 14. In order to show more clearly the trends of the maximum self-alining-torque data, the effects of vertical tire deflection and inflation pressure on the maximum self-alining torque have been isolated in figures 31 and 32. For constant inflation pressure (see fig. 31), the maximum self-alining torque tends to increase nonlinearly with increasing vertical tire deflection whereas, for constant vertical tire deflection (see fig. 32), the maximum self-alining torque increases more or less linearly with increasing inflation pressure.

Pneumatic caster $\bar{q} = \bar{M}_z \big/ \bar{F}_\psi$.- The variation of pneumatic caster with yaw angle for all test conditions is shown in figure 14. The variation of pneumatic caster with vertical tire deflection for the vertical load and inflation pressure range tested is shown in figure 33 for each test yaw angle (data obtained from table II). This figure shows that, for a constant yaw angle, the pneumatic caster increases with increasing vertical tire deflection. For constant vertical tire deflection, any systematic pressure effect on the pneumatic caster is obscured by the scatter of the test data. Faired values of pneumatic caster taken from figure 33 for several constant vertical tire deflections are plotted against yaw angle in figure 34. Figure 34 shows that the pneumatic caster is a maximum at small angles of yaw and generally decreases with increasing yaw angle for the test range covered.

Drag force $\bar{F}_x$.- The variation of drag force with yaw angle for the rated-vertical-load condition (test series B) for the three different inflation pressures tested is shown in figure 35. The data in figure 35 indicate that the drag force, except at small yaw angles, increases more or less linearly with increasing yaw angle for the yaw-angle range covered.

Essentially the same results were obtained for the other test series and inflation pressures investigated. In order to show trends more clearly, the ratio of drag force to cornering force $\bar{F}_x/\bar{F}_y$ is plotted against yaw angle in figure 36 for the different test series and tire inflation pressures investigated. If the total horizontal ground force under yawed rolling was normal to the wheel plane, then the drag force $\bar{F}_x$ would be equal to the cornering force $\bar{F}_y$ multiplied by the tangent of the yaw angle or $\dfrac{\bar{F}_x}{\bar{F}_y} = \tan \psi$. Tan $\psi$ is represented in this figure by a solid line. In general, the data fall near or above this line and indicate that a small force parallel to the wheel plane usually is present throughout the yaw-angle range investigated.

Yawed-rolling coefficient of friction $\bar{\mu}_\psi = \dfrac{\bar{F}_{R_{max}}}{\bar{F}_z}$.- The variation of the yawed rolling coefficient of friction with average bearing or ground pressure is shown in figure 37. The data shown in this figure are derived from data given in table II and in figures 19 and 41 (to be discussed later). The trend of the data shown indicates that the yawed-rolling friction coefficient decreases with increasing bearing pressure from approximately 0.94 at 60 pounds per square inch down to approximately 0.56 at an average bearing pressure of 320 pounds per square inch.

Sliding drag (fore-and-aft) coefficient of friction $\bar{\mu}_x = \dfrac{\bar{F}_{x_{max}}}{\bar{F}_z}$.- The variation of sliding drag coefficient of friction with average bearing pressure for both dry and wet concrete for the one condition of constant vertical load tested is shown in figure 38. The data shown in this figure was obtained from table V. The sliding drag coefficient of friction for the dry-concrete condition appears to decrease with increasing bearing pressure from approximately 0.85 at a bearing pressure of 50 pounds per square inch down to approximately 0.75 at a bearing pressure of 200 pounds per square inch. The friction coefficients found for the limited number of tests made with the concrete in a wet condition indicate a reduction in the sliding drag coefficient of friction of about 10 to 15 percent over that for the dry-concrete condition.

A comparison of the sliding drag coefficient of friction with the yawed-rolling coefficient of friction is shown in figure 39. Both coefficients seem to show approximately the same trends.

Fore-and-aft spring constant $\bar{K}_x$.- The variation of fore-and-aft spring constant with tire inflation pressure, obtained from data in table V, for the one constant vertical load condition tested is shown

in figure 40. These data are derived from the initial slope of the fore-
and-aft (drag) force $\bar{F}_x$ against horizontal displacement $\bar{x}$ curves.
Samples of these curves for three test inflation pressures are presented
in figure 18. For the one constant-vertical-load condition tested, fig-
ure 40 indicates that the fore-and-aft spring constant does not change
markedly with inflation pressure for the range of conditions investigated.

Vertical-load—vertical-tire-deflection characteristics.- The aver-
age vertical-load—vertical-tire-deflection characteristics of the two
tire specimens are shown in figure 19 by means of a family of constant-
vertical-load curves where the ordinate is the initial vertical tire
deflection $\bar{\delta}_0$ and the abscissa is the tire inflation pressure $\bar{p}$.
Each constant-vertical-load curve represents one of the test series or
constant-vertical-load conditions tested. These curves are faired curves
obtained by averaging the data taken from yaw, relaxation length, and
footprint area tests. (Test data for yaw angles greater than 2.1° were
omitted because, under such yaw angles, large cornering-force preloads
were sometimes encountered which could affect the accuracy of the initial
vertical tire deflection considerably.) The scatter of the test data was
·found to range approximately ±0.2 inches and is mainly attributed to hys-
teresis effects, although tire wear and accuracy of measurement also con-
tribute to the scatter to some extent. Figure 20 shows the hysteresis
effects on the test data obtained from the locked-wheel drag tests
(table V). The difference between the increasing and decreasing pressure
curves is considerable and amounts to as much as 0.5 inch vertical tire
deflection. Vertical-load—vertical-tire-deflection data for the one con-
dition of constant tire inflation pressure investigated (p = 219 lb/sq in.,
unloaded) is shown in figure 21. These data indicate that tire A is
slightly stiffer than tire B.

Footprint area $A_g$, $A_n$.- The variation of gross footprint area $A_g$,
net footprint area $A_n$, and the ratio of net footprint area to gross foot-
print area $A_n/A_g$ with vertical tire deflection for the test tires,
obtained from the data in table VI, is shown in figure 41. Both the gross
footprint area and the net footprint area appear to increase linearly with
increasing vertical tire deflection for vertical tire deflections greater
than 1 inch. The ratio of net footprint area to gross footprint area
appears to decrease slightly with increasing vertical tire deflection and
averages approximately 70 percent of the gross footprint area. This
ratio will, of course, change for tires having tread designs different
from the ones tested.

Footprint length 2h and width b.- The variation of footprint
length and width with vertical tire deflection, obtained from data in
table VI, is shown in figure 42. These data indicate that both the
footprint length and the width increase nonlinearly with increasing ver-
tical tire deflection. Also shown in this figure as solid lines are the

lengths of chords of circles having diameters equal to the free diam-
eter  d  and maximum width  w, respectively, of the tire at its rated
inflation pressure and located at a distance  $r - \delta_0$  from the center
of the circles.  A comparison of these quantities indicates that the
experimental values of footprint length and width are smaller than the
corresponding chord lengths over the vertical-tire-deflection range
tested.

Average bearing pressure  $\bar{p}_n = \overline{F_z/A_n}$  and average gross footprint
pressure  $\bar{p}_g = \overline{F_z/A_g}$.- The variation of average bearing pressure and
average gross footprint pressure with tire inflation pressure is given
in figure 43.  The data shown in figure 43 are derived from the faired
vertical-tire-deflection—inflation-pressure curves given in figure 19
and from the faired footprint-area—vertical-tire-deflection curves
given in figure 41.  The heavy solid line shown represents  $\bar{p}_n$  or  $\bar{p}_g = \bar{p}$.
Comparison of this line with the average-bearing-pressure curves indicates
that the average bearing pressure becomes increasingly larger than the
inflation pressure with increasing inflation pressure.  The average gross
footprint pressure, on the other hand, decreases as the inflation pres-
sure increases from being slightly larger at low inflation pressures to
being smaller than the inflation pressure at high inflation pressures.
The offset of both the average bearing pressure and the gross footprint
pressure at zero inflation pressure is indicative of the inherent carcass
stiffness of the tire.

Increasing the vertical tire deflection is seen to increase both the
average-bearing-pressure and the average-gross-footprint-pressure curves.

Relaxation length  L.- The variation of the four types of relaxation
length with tire inflation pressure is shown in figure 44.  The variation
for the static relaxation length with tire inflation pressure is shown in
figure 44(a), for the unyawed-rolling-force and the unyawed-rolling-
deflection relaxation lengths in figure 44(b), and for the yawed-rolling
relaxation length in figure 44(c).  In order to show trends more clearly,
the effects of vertical tire deflection on the relaxation length has
been isolated in figure 45 where the relaxation length is plotted against
tire inflation pressure for several constant vertical tire deflections.
For comparative purposes, the same faired lines drawn through the data
in figure 45(a) are reproduced in figures 45(b) and 45(c).  The agreement
between the static and the unyawed-rolling relaxation lengths is fairly
good for the vertical-tire-deflection range shown.  The yawed-rolling
relaxation lengths appear to average about 25 percent less than the static
relaxation lengths for the vertical-tire-deflection range shown.  Some
of this difference is thought to be caused by the twisting moment or
self-alining torque present in the yawed-rolling case.  As evidence for
this fact, some previously unpublished data for a 45-inch diameter tire

(tire C of ref. 2) is presented in figure 46 where the variation of
static relaxation length with twisting moment or twist is shown for one
condition of combined constant vertical force and constant side force.
The moment for this data was applied in a direction such as to tend to
simulate the yawed-rolling condition. These data indicate that the
static relaxation length decreases with increasing twisting moment or
twist.

Figure 47 presents a comparison of static relaxation lengths
obtained from reference 2 for a 56 × 16, 32-ply-rating tire with the
data for the 56 × 16, 24-ply-rating tire specimens used in the present
tests. Because the rated inflation pressures differ for these two tire
types, a direct comparison of their respective relaxation lengths on
the basis of equal inflation pressures would be of dubious significance.
Therefore, in order to provide a more significant comparison, the data
are shown in figure 47 in terms of the pressure ratio $p/p_r$ where $p_r$
is the rated inflation pressure for the tire specimen. Fairly good
agreement is seen to exist between the different tires for the pressure
ratios considered.

In general, the test results indicate that the relaxation length
decreases with increasing vertical tire deflection and increasing infla-
tion pressure.

Rolling radius $r_e$.- The variation of rolling radius with yaw angle,
obtained from data in table II, for two typical test conditions is shown
in figure 15(a). The rolling radii for both test tires appear to be
in good agreement and remain more or less constant in magnitude with
increasing yaw angle up to at least a yaw angle of 14.4°. The trend of
the data at the higher yaw angles is uncertain because one tire, usually
tire A, was observed to be slipping more than the other at this condition.
The variation of rolling radius with vertical tire deflection for several
of the test inflation pressures is shown in figure 15(b). The data pre-
sented in figure 15(b) were obtained from table II and are for yaw angles
of 0.35° and 2.1°. The trends of these data indicate that, for constant
pressure, the rolling radius decreases with increasing vertical tire
deflection and that, for constant vertical tire deflection, the rolling
radius increases with increasing inflation pressure.

Speed effects.- Within the speed range tested (1 to 4 miles per
hour), no apparent effects of speed were found to exist for the quan-
tities measured.

CONCLUSIONS

Tow tests were made at the Langley Aeronautical Laboratory primarily to determine the yawed-rolling characteristics of two 56 × 16, type VII, extra-high-pressure, 24-ply-rating airplane tires. The results of these tests indicated the following conclusions:

1. The normal force reached a maximum at between 14° and 18° yaw for the vertical load range tested, and this maximum tended to decrease with increasing tire inflation pressure.

2. The cornering power under constant tire inflation pressure increased with increasing vertical tire deflection up to about 3.0 inches vertical tire deflection where a maximum was reached. Increasing the vertical tire deflection beyond this point tended to decrease the cornering power. For the case of constant vertical tire deflection, the cornering power increased with increasing tire inflation pressure.

3. The self-alining torque generally increased with increasing yaw angle for yaw angles less than 5° to 8°. Between 5° and 8°, a maximum was reached and increasing the yaw angle beyond this range tended to decrease the self-alining torque considerably.

4. The maximum self-alining torque for the case of constant vertical tire deflection increased more or less linearly with increasing tire inflation pressure whereas for the case of constant inflation pressure the maximum self-alining torque increased nonlinearly with increasing vertical tire deflection.

5. The pneumatic caster was a maximum at small angles of yaw and generally decreased with increasing yaw angle for the test range covered.

6. The yawed-rolling friction coefficient decreased with increasing bearing pressure from approximately 0.94 at a bearing pressure of 60 pounds per square inch down to approximately 0.56 at a bearing pressure of 320 pounds per square inch.

7. The sliding drag coefficient of friction for the dry concrete condition also decreased with increasing bearing pressure from approximately 0.85 at a bearing pressure of 50 pounds per square inch down to 0.75 at a bearing pressure of 200 pounds per square inch. The limited number of tests made with the concrete in the wet condition indicated a 10 to 15 percent reduction in the sliding drag friction coefficient over the dry-concrete condition.

8. In general, the test results indicate that the relaxation length decreases with increasing vertical tire deflection and increasing inflation pressure.


Langley Aeronautical Laboratory,
    National Advisory Committee for Aeronautics,
        Langley Field, Va., June 11, 1954.

. APPENDIX

DETAILS OF CORNERING-FORCE AND SELF-ALINING-TORQUE MEASUREMENTS

In conducting the yawed-rolling tests a certain amount of difficulty was encountered as a consequence of the fact that it was impractical to set the wheels on the test vehicle exactly to a zero yaw condition; the minimum attainable angle was about $0.35^{\circ}$. This fact is important because, in order to obtain cornering-force and self-alining-torque data for any yaw angle, it is necessary to subtract the dynamometer-record deflections for the yawed-rolling case from those for the reference zero yaw case. In the case of cornering force, this difficulty was resolved by rolling the test vehicle both forward and backward at the minimum yaw angle $(0.35^{\circ})$ and by taking the average record deflection for the two cases as corresponding to the zero yaw condition. The cornering force for this $0.35^{\circ}$ yaw angle was taken as half the difference in force for the rolled-forward and rolled-backward conditions.

For the self-alining torque, the record deflections for the zero yaw condition could not be accurately determined; consequently, it was not possible to obtain direct measurements of the self-alining torque. Instead all moment measurements were made with reference to the $0.35^{\circ}$ minimum yaw condition; that is, the measured moment (designated as $\Delta M_Z$) represents the difference in self-alining torque for the yaw angle considered and for the $0.35^{\circ}$ condition. In order to obtain the actual self-alining torque $M_Z$, it is necessary to add to the measured quantity $\Delta M_Z$ the self-alining torque for $0.35^{\circ}$ yaw (designated as $M_{Z_O}$) or $M_Z = M_{Z_O} + \Delta M_Z$. The quantity $M_{Z_O}$ was estimated from the static-torsional-elasticity-test data for one of the test tires which is given in reference 2. This procedure for correcting the measured moment $\Delta M_Z$ to $M_Z$ is believed to be fairly satisfactory both because the torsional elastic properties of static and slowly rolling tires are at least approximately similar (for example, see experimental data in ref. 5) and because the correction term $M_{Z_O}$ is usually relatively small in comparison with the measured term $\Delta M_Z$.

## REFERENCES

1. Hadekel, R.: The Mechanical Characteristics of Pneumatic Tyres.
   S & T Memo. No. 5/50, British Ministry of Supply, TPA 3/TIB,
   Mar. 1950.

2. Horne, Walter B.: Static Force-Deflection Characteristics of Six
   Aircraft Tires Under Combined Loading. NACA TN 2926, 1953.

3. Temple, G.: Note on American Work on Kinematic and Dynamic Shimmy.
   Rep. No. A.D. 3158, British R.A.E., Nov. 1940.

4. Kantrowitz, Arthur: Stability of Castering Wheels for Aircraft
   Landing Gears. NACA Rep. 686, 1940.

5. Von Schlippe, B., and Dietrich, R.: Zur Mechanik des Luftreifens.
   Junkers Flugzeug- und Motorenwerke, A.G., Dessau. (Available from
   CADO as ATI 105296.)

6. Anon.: Military Specification Casings; Aircraft Pneumatic Tire.
   Military Specification, MIL-C-5041, Sept. 16, 1949; Amendment-2,
   Feb. 8, 1951.

TABLE I.- TIRE SPECIFICATIONS

| Specifications | Military specification (ref. 6) | End of test, tires in worn condition | |
|---|---|---|---|
| | | Tire A | Tire B |
| Tire: | | | |
|   Type[a] . . . . . . . . . . . . . . . . . . . | VII | ----- | ----- |
|   Ply rating . . . . . . . . . . . . . . . | 24 | ----- | ----- |
|   Static load, lb . . . . . . . . . . . . | 45,000 | ----- | ----- |
|   Inflation pressure, lb/sq in. . . . . . | 178 | ----- | ----- |
|   Burst pressure, lb/sq in. . . . . . . | 712 (minimum) | ----- | ----- |
|   Moment of static unbalance, oz-in. . . | 90 | ----- | ----- |
|   Diameter, deflated, in. . . . . . . . | --------------- | 54.40 | 53.70 |
|   Diameter, inflated, in. . . . . . . . | 55.26 (minimum) 56.40 (maximum) | 56.16 | 56.24 |
|   Maximum width, deflated, in. . . . . . | --------------- | 15.36 | 15.87 |
|   Maximum width, inflated, in. . . . . . | 16.00 (maximum) | 16.00 | 16.06 |
|   Bead width, in. . . . . . . . . . . . | 3.88 (maximum) | 2.80 | 3.00 |
|   Minimum wall thickness, in. . . . . . | --------------- | 1.1 | 0.9 |
|   Wall thickness at tread center line | | | |
|     (including tread), in. . . . . . . . | --------------- | 1.3 | 1.0 |
|   Depth of tread (at tread center | | | |
|     line), in. . . . . . . . . . . . . . | 0.35 (maximum) | 0.15 | 0.15 |
|   Casing weight, lb . . . . . . . . . . | 268 (maximum) | 253 | 247 |
|   Tread pattern . . . . . . . . . . . . | Rib or nonskid | Rib | Rib |
| Innertube: | | | |
|   Thickness, in. . . . . . . . . . . . . | | 0.2 | |
|   Weight, lb . . . . . . . . . . . . . . | | 26.7 | |
| Wheel: | | | |
|   Rim diameter, in. . . . . . . . . . . | | 32.5 | |
|   Weight, lb . . . . . . . . . . . . . . | | 217 | |

[a]Type VII is an extra high pressure tire.

## TABLE II.- YAW TEST DATA

(a) SERIES A: $\bar{F}_z = 17{,}000$ lb; $(F_z)_{tire\ A} = 17{,}000$ lb; $(F_z)_{tire\ B} = 16{,}900$ lb.

| Run | Average Values | | | | | | | | | | | Tire A | | | | Tire B | | | |
|---|---|---|---|---|---|---|---|---|---|---|---|---|---|---|---|---|---|---|---|
| | $\bar{p}$, lb/sq in. | $\bar{\delta}_0$, in. | $\bar{\delta}$, in. | $\bar{\psi}$, deg | $\bar{F}_y$, lb | $\bar{F}_x$, lb | $\bar{F}_\psi$, lb | $\Delta\bar{M}_z$, lb-in. | $\bar{M}_z$, lb-in. | $\bar{q}$, in. | $\bar{L}_y$, in. | p, lb/sq in. | $\delta_0$, in. | $\delta$, in. | $r_e$, in. | p, lb/sq in. | $\delta_0$, in. | $\delta$, in. | $r_e$, in. |
| 1 | 61 | 3.5 | 3.3 | 0.35 | 620 | * | 620 | 0 | 4,300 | 6.94 | ** | 58 | 3.5 | 3.3 | ----- | 63 | 3.5 | 3.5 | ----- |
| 2 | 62 | 3.7 | 3.7 | .35 | 580 | * | 580 | 0 | 4,700 | 8.10 | ** | 63 | 3.7 | 3.7 | ----- | 61 | 3.7 | 3.7 | ----- |
| 3 | 62 | 3.7 | 3.7 | .35 | 530 | * | 530 | 0 | 4,700 | 8.87 | ** | 63 | 3.7 | 3.7 | ----- | 61 | 3.7 | 3.7 | ----- |
| 4 | 61 | --- | --- | .35 | 620 | * | 620 | 0 | ------ | ---- | ** | 61 | --- | --- | ----- | 60 | --- | --- | ----- |
| 5 | 56 | 3.8 | 3.8 | .35 | 690 | * | 690 | 0 | 4,700 | 6.81 | ** | 56 | 3.8 | 3.8 | 25.5 | 55 | 3.9 | 3.9 | 25.3 |
| 6 | 57 | 3.9 | 3.9 | .35 | 530 | * | 530 | 0 | 4,900 | 9.25 | ** | 55 | 4.0 | 4.0 | 25.4 | 58 | 3.8 | 3.8 | 25.4 |
| 7 | 60 | 3.6 | 3.6 | .35 | 640 | * | 640 | 0 | 4,500 | 7.03 | ** | 60 | 3.7 | 3.7 | 25.5 | 60 | 3.5 | 3.5 | 25.5 |
| 8 | 60 | 3.6 | 3.4 | 2.1 | 2,980 | 400 | 2,990 | 17,500 | 21,600 | 7.22 | ** | 60 | 3.7 | 3.4 | 25.5 | 60 | 3.5 | 3.4 | 25.5 |
| 9 | 59 | 3.6 | --- | 3.9 | 5,030 | 600 | 5,060 | 37,600 | ------ | ---- | ---- | 57 | 3.6 | --- | 25.5 | 61 | 3.6 | --- | 25.6 |
| 10 | 57 | 3.7 | 3.8 | 3.9 | 4,950 | 600 | 4,980 | 33,400 | 38,100 | 7.65 | ---- | 55 | 3.9 | 4.0 | 25.5 | 58 | 3.6 | 3.5 | 25.5 |
| 11 | 61 | 3.5 | 3.8 | 7.4 | 8,920 | 1,200 | 9,000 | 37,900 | 42,700 | 4.74 | ** | 58 | 3.5 | 3.8 | 25.7 | 63 | 3.5 | 3.8 | 25.8 |
| 12 | 54 | 3.7 | 3.9 | 7.4 | 8,760 | 1,800 | 8,920 | 39,500 | 44,400 | 4.98 | ** | 54 | 3.7 | 3.8 | 25.6 | 54 | 3.7 | 4.1 | 25.6 |
| 13 | 62 | 3.7 | --- | 10.9 | 11,900 | 2,400 | 12,140 | 21,600 | ------ | ---- | ** | 63 | 3.7 | --- | ----- | 61 | 3.7 | --- | ----- |
| 14 | 59 | 3.7 | 4.2 | 10.9 | 11,680 | 2,500 | 11,940 | 29,100 | 34,600 | 2.90 | ** | 60 | 3.6 | 4.1 | 25.7 | 57 | 3.7 | 4.2 | 25.8 |
| 15 | 60 | 3.6 | 4.3 | 14.4 | 12,610 | 3,200 | 13,010 | 13,800 | 19,300 | 1.50 | ** | 61 | 3.6 | 4.3 | ----- | 60 | 3.6 | 4.2 | ----- |
| 16 | 60 | 3.6 | 4.2 | 14.4 | 12,680 | 3,300 | 13,100 | 12,500 | 18,100 | 1.38 | ** | 61 | 3.6 | 4.3 | 25.9 | 60 | 3.6 | 4.1 | 25.5 |
| 17 | 59 | 3.6 | 4.3 | 14.4 | 12,340 | 3,100 | 12,720 | 18,400 | 24,100 | 1.89 | ** | 59 | 3.6 | 4.6 | 25.7 | 59 | 3.6 | 4.0 | 25.7 |
| 18 | 89 | 2.7 | 2.7 | .35 | 760 | * | 760 | 0 | 3,300 | 4.34 | ** | 94 | 2.7 | 2.7 | ----- | 84 | 2.7 | 2.7 | ----- |
| 19 | 87 | 2.9 | 2.7 | 2.1 | 3,840 | 400 | 3,850 | 17,200 | 20,500 | 5.32 | ** | 87 | 3.1 | 2.7 | 26.1 | 87 | 2.8 | 2.6 | 26.1 |
| 20 | 85 | 2.8 | 3.0 | 3.9 | 6,780 | 700 | 6,810 | 28,500 | 32,300 | 4.74 | 12.8 | 84 | 2.9 | 2.9 | 26.1 | 86 | 2.8 | 3.1 | 26.1 |
| 21 | 82 | 2.8 | 3.2 | 7.4 | 10,380 | 1,500 | 10,490 | 27,900 | 32,100 | 3.06 | ** | 80 | 2.8 | 3.4 | 26.2 | 83 | 2.8 | 2.9 | 26.2 |
| 22 | 84 | 2.8 | 3.2 | 10.9 | 12,210 | 2,000 | 12,370 | 19,700 | 23,900 | 1.93 | ** | 85 | 2.8 | 3.1 | 26.2 | 83 | 2.8 | 3.3 | 26.2 |
| 23 | 89 | 2.7 | 3.2 | 14.4 | 12,580 | 3,100 | 12,960 | 11,000 | 15,300 | 1.18 | ** | 94 | 2.7 | 3.1 | 26.7 | 84 | 2.7 | 3.2 | 26.0 |
| 24 | 174 | 1.9 | 1.9 | .35 | 730 | * | 730 | 0 | 2,400 | 3.29 | ** | 175 | 2.0 | 2.0 | ----- | 173 | 1.9 | 1.9 | ----- |
| 25 | 169 | 1.9 | 1.9 | .35 | 800 | * | 800 | 0 | 2,400 | 3.00 | ** | 169 | 1.9 | 1.9 | 27.0 | 169 | 1.9 | 1.9 | 27.0 |
| 26 | 169 | 1.9 | 1.9 | .35 | 790 | * | 790 | 0 | 2,400 | 3.04 | ** | 169 | 2.0 | 2.0 | 27.0 | 169 | 1.9 | 1.9 | 27.0 |
| 27 | 168 | 1.9 | 1.9 | .35 | 890 | * | 890 | 0 | 2,400 | 2.70 | ** | 167 | 2.0 | 2.0 | 27.0 | 168 | 1.9 | 1.9 | 27.0 |
| 28 | 164 | 1.9 | 1.9 | 2.1 | 4,540 | 300 | 4,550 | 8,200 | 10,600 | 2.33 | ** | 165 | 2.0 | 1.9 | 26.9 | 162 | 1.9 | 1.9 | 27.0 |
| 29 | 168 | 1.8 | 1.8 | 3.9 | 7,640 | 400 | 7,650 | 19,700 | 21,900 | 2.86 | 11.9 | 168 | 1.9 | 1.8 | 26.9 | 168 | 1.7 | 1.7 | 27.0 |
| 30 | 168 | 1.9 | 2.0 | 7.4 | 11,030 | 1,500 | 11,130 | 20,700 | 23,300 | 2.09 | ** | 169 | 2.0 | 2.1 | 27.1 | 166 | 1.8 | 1.8 | 27.1 |
| 31 | 170 | 1.9 | 2.0 | 10.9 | 12,550 | 2,000 | 12,700 | 18,700 | 21,300 | 1.68 | ** | 173 | --- | --- | 26.7 | 168 | 1.9 | 2.0 | 27.0 |
| 32 | 164 | 1.9 | 1.7 | 14.4 | 12,010 | 2,900 | 12,350 | 7,400 | 9,300 | .75 | ** | 168 | 1.9 | 1.8 | 27.3 | 159 | 1.8 | 1.6 | 26.7 |

*Force too small to be measured accurately.
**Relaxation length not determined.

### TABLE II.- YAW TEST DATA - Continued

(b) SERIES B: $\bar{F}_z$ = 23,700 lb; $(F_z)_{\text{tire A}}$ = 23,700 lb; $(F_z)_{\text{tire B}}$ = 23,800 lb.

| Run | Average values | | | | | | | | | | | Tire A | | | | Tire B | | | |
|---|---|---|---|---|---|---|---|---|---|---|---|---|---|---|---|---|---|---|---|
| | $\bar{p}$, lb/sq in. | $\bar{\delta}_o$, in. | $\bar{\delta}$, in. | $\bar{\psi}$, deg | $\bar{F}_y$, lb | $\bar{F}_x$, lb | $\bar{F}_\psi$, lb | $\Delta\bar{M}_z$, lb-in. | $\bar{M}_z$, lb-in. | $\bar{q}$, in. | $\bar{l}_y$, in. | p, lb/sq in. | $\delta_o$, in. | $\delta$, in. | $r_e$, in. | p, lb/sq in. | $\delta_o$, in. | $\delta$, in. | $r_e$, in. |
| 33 | 79 | 3.8 | 3.8 | 0.35 | ------- | * | ------- | 0 | 5,300 | ----- | ** | 79 | 3.8 | 3.8 | 25.7 | 79 | 3.8 | 3.8 | 25.5 |
| 34 | 79 | 3.9 | 3.9 | .35 | 780 | * | 780 | 0 | 5,500 | 7.05 | ** | 79 | 3.8 | 3.8 | 25.6 | 78 | 3.9 | 3.9 | 25.5 |
| 35 | 80 | 3.8 | 3.8 | .35 | 830 | * | 830 | 0 | 5,400 | 6.51 | ** | 82 | 3.8 | 3.8 | 25.6 | 79 | 3.8 | 3.8 | 25.5 |
| 36 | 79 | 3.9 | 3.9 | .35 | 870 | * | 870 | 0 | 5,500 | 6.32 | ** | 80 | 3.8 | 3.8 | 25.6 | 79 | 3.9 | 3.9 | 25.4 |
| 37 | 83 | 3.9 | 3.9 | .35 | 950 | * | 950 | 0 | 5,600 | 6.02 | ** | 83 | 3.8 | 3.8 | 25.7 | 83 | 3.9 | 3.9 | 25.7 |
| 38 | 82 | 3.8 | 3.8 | .35 | 720 | * | 720 | 0 | 5,400 | 7.50 | ** | 82 | 3.8 | 3.8 | 25.6 | 82 | 3.8 | 3.8 | 25.6 |
| 39 | 79 | 3.9 | --- | 2.1 | 3,280 | 600 | 3,300 | 23,600 | ------ | ----- | ** | 79 | 4.0 | --- | ----- | 79 | 3.9 | --- | ----- |
| 40 | 79 | 3.9 | 3.9 | 2.1 | 3,060 | 300 | 3,070 | 30,400 | 35,900 | 11.69 | ** | 80 | 3.9 | 4.0 | 25.7 | 79 | 3.9 | 3.7 | 25.6 |
| 41 | 79 | 4.1 | 4.0 | 3.9 | 5,850 | 1,000 | 5,880 | 31,000 | 36,700 | 6.24 | ---- | 79 | 4.1 | 3.9 | 25.5 | 79 | 4.1 | 4.0 | 25.5 |
| 42 | 79 | 3.9 | 4.3 | 7.4 | 10,880 | 1,900 | 11,030 | 54,000 | 60,300 | 5.47 | ** | 79 | 3.9 | 4.4 | 25.7 | 78 | 4.0 | 4.2 | 25.8 |
| 43 | 80 | 4.0 | 4.5 | 10.9 | 14,390 | 3,100 | 14,720 | 36,400 | 43,200 | 2.93 | ** | 81 | 4.0 | 4.6 | 25.7 | 79 | 4.0 | 4.5 | 25.9 |
| 44 | 79 | 3.9 | 4.6 | 10.9 | 13,880 | 2,900 | 14,180 | 37,200 | 44,100 | 3.11 | ** | 79 | 3.9 | 4.6 | 25.7 | 79 | 3.8 | 4.6 | 26.0 |
| 45 | 79 | 3.9 | 4.7 | 14.4 | 16,400 | 4,200 | 16,930 | 27,300 | 34,400 | 2.03 | ** | 80 | 3.8 | 4.6 | 25.7 | 79 | 4.0 | 4.7 | 25.8 |
| 46 | 79 | --- | --- | 14.4 | ------- | --- | ------- | ------- | ------- | ----- | ** | 80 | --- | --- | 25.7 | 79 | --- | --- | 25.7 |
| 47 | 81 | 3.9 | 4.9 | 17.9 | 16,200 | 4,900 | 16,920 | 31,000 | 38,600 | 2.28 | ** | 81 | 3.8 | 4.9 | 26.2 | 81 | 4.0 | 4.9 | 25.3 |
| 48 | 127 | 2.8 | 2.8 | .35 | 1,010 | * | 1,010 | 0 | 4,100 | 4.06 | ** | 127 | 2.8 | 2.8 | 26.5 | 126 | 2.8 | 2.8 | 26.5 |
| 49 | 126 | 2.8 | 2.7 | 2.1 | 5,240 | 400 | 5,250 | 27,500 | 31,300 | 5.96 | ** | 126 | 2.9 | 2.7 | 26.5 | 126 | 2.8 | 2.6 | 26.5 |
| 50 | 128 | 2.8 | 2.8 | 2.1 | 4,860 | 400 | 4,870 | 25,300 | 29,400 | 6.04 | ** | 128 | 2.9 | 2.8 | 26.6 | 128 | 2.7 | 2.7 | 26.6 |
| 51 | 128 | 2.8 | 2.6 | 3.9 | 8,800 | 900 | 8,840 | 30,600 | 34,200 | 3.87 | 17.9 | 128 | 2.8 | 2.7 | 26.6 | 128 | 2.8 | 2.4 | 26.5 |
| 52 | 126 | 2.8 | 2.9 | 7.4 | 13,600 | 2,200 | 13,770 | 39,000 | 43,300 | 3.14 | ** | 126 | 2.8 | 3.0 | 26.5 | 126 | 2.7 | 2.8 | 26.7 |
| 53 | 126 | 2.8 | 2.9 | 10.9 | 15,350 | 2,900 | 15,620 | 23,900 | 28,200 | 1.81 | ** | 126 | 2.8 | 2.9 | 26.1 | 126 | 2.8 | 2.9 | 26.5 |
| 54 | 127 | 2.8 | 2.9 | 10.9 | 15,490 | 3,000 | 15,780 | 22,200 | 26,500 | 1.68 | ** | 128 | 2.8 | 3.0 | 26.4 | 126 | 2.8 | 2.9 | 26.5 |
| 55 | 127 | 2.7 | 3.0 | 14.4 | 16,330 | 3,800 | 16,760 | 23,400 | 27,900 | 1.66 | ** | 126 | 2.7 | 3.0 | 26.6 | 127 | 2.7 | 3.1 | 26.3 |
| 56 | 128 | 2.7 | 2.9 | 17.9 | 15,690 | 4,300 | 16,250 | 21,400 | 25,700 | 1.58 | ** | 130 | 2.7 | 2.9 | 27.5 | 127 | 2.7 | 2.8 | 25.7 |
| 57 | 202 | 2.1 | 2.1 | .35 | 1,050 | * | 1,050 | 0 | 3,200 | 3.05 | ** | 202 | 2.3 | 2.3 | 27.1 | 202 | 2.0 | 2.0 | 27.1 |
| 58 | 203 | 2.1 | 2.1 | .35 | 1,050 | * | 1,050 | 0 | 3,200 | 3.05 | ** | 203 | 2.2 | 2.2 | 27.1 | 203 | 2.1 | 2.1 | 27.3 |
| 59 | 202 | 2.1 | 2.1 | .35 | 1,210 | * | 1,210 | 0 | 3,200 | 2.64 | ** | 202 | 2.1 | 2.1 | 27.3 | 202 | 2.0 | 2.0 | 27.2 |
| 60 | 203 | 2.0 | 2.0 | .35 | 1,070 | * | 1,070 | 0 | 2,900 | 2.71 | ** | 206 | 2.1 | 2.1 | 27.1 | 204 | 1.9 | 1.9 | 27.2 |
| 61 | 203 | 2.1 | 2.1 | .35 | 950 | * | 950 | 0 | 3,200 | 3.37 | ** | 203 | 2.1 | 2.1 | 27.2 | 203 | 2.1 | 2.1 | 27.2 |
| 62 | 202 | 2.1 | 2.1 | .35 | 990 | * | 990 | 0 | 3,200 | 3.23 | ** | 202 | 2.1 | 2.1 | 27.2 | 203 | 2.1 | 2.1 | 27.1 |
| 63 | 203 | 2.1 | 2.1 | .35 | 980 | * | 980 | 0 | 3,200 | 3.27 | ** | 203 | 2.1 | 2.1 | 27.2 | 202 | 2.1 | 2.1 | 27.1 |
| 64 | 200 | 2.1 | 2.2 | 2.1 | 5,070 | 300 | 5,080 | 20,300 | 23,700 | 4.67 | ** | 200 | 2.1 | 2.2 | 27.2 | 203 | 2.0 | 2.0 | 27.3 |
| 65 | 203 | 2.1 | 2.0 | 2.1 | 5,210 | 300 | 5,220 | 22,000 | 24,900 | 4.77 | ** | 203 | 2.1 | 1.8 | 27.2 | 200 | 2.1 | 2.3 | 27.2 |
| 66 | 202 | 2.1 | 2.1 | 3.9 | 9,400 | 700 | 9,430 | 20,400 | 23,600 | 2.50 | ---- | 202 | 2.2 | 2.0 | 27.1 | 203 | 2.1 | 2.1 | 27.3 |
| 67 | 202 | 2.0 | 2.1 | 7.4 | 13,700 | 1,500 | 13,780 | 25,100 | 28,300 | 2.05 | ** | 202 | --- | 2.1 | 27.1 | 202 | 2.1 | 2.2 | 27.2 |
| 68 | 202 | 2.0 | 2.1 | 10.9 | 14,980 | 2,500 | 15,180 | 17,900 | 21,100 | 1.39 | ** | 202 | 2.0 | 2.1 | 27.2 | 202 | 2.0 | 2.1 | 27.1 |
| 69 | 202 | 2.1 | 2.2 | 10.9 | 14,790 | 2,500 | 15,000 | 16,300 | 19,700 | 1.31 | ** | 202 | 2.1 | 2.1 | 27.3 | 202 | 2.0 | 2.0 | 27.0 |
| 70 | 202 | 2.0 | 1.9 | 14.4 | 15,510 | 3,500 | 15,890 | 14,100 | 16,800 | 1.06 | ** | 202 | 2.0 | 2.0 | 27.2 | 203 | 2.0 | 2.3 | 27.2 |
| 71 | 202 | 2.1 | 2.1 | 17.9 | 14,960 | 4,100 | 15,500 | 18,100 | 21,300 | 1.37 | ** | 202 | 2.1 | 2.1 | 28.0 | 202 | --- | 2.1 | 26.4 |

*Force too small to be measured accurately.
**Relaxation length not determined.

TABLE II.- YAW TEST DATA - Continued

(c) SERIES C: $\bar{F}_z$ = 32,700 lb; $(F_z)_{tire\ A}$ = 32,900 lb; $(F_z)_{tire\ B}$ = 32,500 lb.

| Run | Average values | | | | | | | | | | | Tire A | | | | Tire B | | | |
| | $p$, lb/sq in. | $\delta_0$, in. | $\delta$, in. | $\bar{\psi}$, deg | $\bar{F}_y$, lb | $F_x$, lb | $\bar{F}_\psi$, lb | $\Delta\bar{M}_z$, lb-in. | $\bar{M}_z$, lb-in. | $\bar{q}$, in. | $\ell_y$, in. | $p$, lb/sq in. | $\delta_0$, in. | $\delta$, in. | $r_e$, in. | $p$, lb/sq in. | $\delta_0$, in. | $\delta$, in. | $r_e$, in. |
|---|---|---|---|---|---|---|---|---|---|---|---|---|---|---|---|---|---|---|---|
| 72 | 130 | 3.7 | 3.4 | 2.1 | 4,650 | 500 | 4,670 | 25,100 | 30,600 | 6.55 | ** | 130 | 3.8 | 3.4 | 26.3 | 130 | 3.7 | 3.4 | 26.3 |
| 73 | 130 | 3.7 | 3.6 | 2.1 | 4,520 | 300 | 4,530 | 24,400 | 30,400 | 6.71 | ** | 130 | 3.7 | 3.5 | 26.3 | 131 | 3.7 | 3.6 | 26.2 |
| 74 | 130 | 3.6 | 3.7 | 3.9 | 8,410 | 500 | 8,420 | 56,200 | 62,500 | 7.42 | ---- | 131 | 3.7 | 3.7 | 26.2 | 130 | 3.5 | 3.7 | 26.2 |
| 75 | 131 | 3.5 | 3.6 | 7.4 | 14,380 | 2,300 | 14,560 | 59,500 | 65,500 | 4.50 | ** | 131 | 3.4 | 3.4 | 26.3 | 131 | 3.5 | 3.7 | 26.4 |
| 76 | 135 | 3.6 | 3.9 | 10.9 | 18,360 | 3,800 | 18,750 | 52,800 | 59,700 | 3.18 | ** | 135 | 3.5 | 3.9 | ---- | 135 | 3.6 | 3.9 | ---- |
| 77 | 155 | 3.1 | 3.1 | .35 | 1,190 | * | 1,190 | 0 | 5,300 | 4.45 | ** | 155 | 3.1 | 3.1 | ---- | 155 | 3.1 | 3.1 | ---- |
| 78 | 147 | 3.2 | 3.2 | .35 | 1,140 | * | 1,140 | 0 | 5,400 | 4.74 | ** | 148 | 3.1 | 3.1 | 26.6 | 146 | 3.3 | 3.3 | 26.4 |
| 79 | 148 | 3.2 | 3.2 | .35 | 1,230 | * | 1,230 | 0 | 5,400 | 4.39 | ** | 148 | 3.1 | 3.1 | 26.5 | 148 | 3.3 | 3.3 | 26.4 |
| 80 | 147 | --- | --- | .35 | 1,080 | * | 1,080 | 0 | | | ** | 149 | --- | --- | 26.5 | 145 | --- | --- | 26.4 |
| 81 | 155 | 3.1 | 3.5 | 14.4 | 20,810 | 5,000 | 21,400 | 35,200 | 41,500 | 1.94 | ** | 155 | 3.1 | 3.6 | 26.7 | 155 | 3.1 | 3.5 | 26.4 |
| 82 | 144 | 3.2 | 3.6 | 17.9 | 21,760 | 6,200 | 22,610 | 32,000 | 38,400 | 1.70 | ** | 144 | 3.2 | 3.5 | ---- | 144 | 3.3 | 3.6 | 26.4 |
| 83 | 147 | 3.3 | 3.6 | 17.9 | 20,870 | 6,000 | 21,700 | 30,600 | 37,000 | 1.71 | ** | 148 | 3.3 | 3.5 | 27.2 | 146 | 3.3 | 3.6 | 25.8 |
| 84 | 174 | 2.9 | 2.7 | 2.1 | 6,070 | 600 | 6,090 | 25,100 | 29,600 | 4.86 | ** | 174 | 3.0 | 2.6 | 26.9 | 174 | 2.8 | 2.7 | 26.9 |
| 85 | 173 | 3.1 | 2.9 | 3.9 | 9,770 | 700 | 9,800 | 42,500 | 47,600 | 4.86 | ---- | 173 | 3.2 | 2.9 | 26.6 | 173 | 3.1 | 2.9 | 26.6 |
| 86 | 174 | 2.9 | 3.0 | 3.9 | 10,390 | 700 | 10,410 | 38,800 | 44,100 | 4.24 | 17.8 | 174 | 3.0 | 3.1 | 26.8 | 174 | 2.9 | 2.9 | 26.7 |
| 87 | 174 | 2.9 | 3.0 | 7.4 | 15,690 | 2,100 | 15,830 | 48,200 | 53,500 | 3.38 | ** | 174 | 2.8 | 3.1 | 27.0 | 174 | 2.9 | 3.0 | ---- |
| 88 | 173 | 2.9 | 3.0 | 10.9 | 19,050 | 3,500 | 19,370 | 43,000 | 48,300 | 2.49 | ** | 173 | 2.9 | 3.0 | 26.9 | 173 | 2.9 | 3.0 | 26.6 |
| 89 | 178 | 2.9 | 3.1 | 14.4 | 20,150 | 4,800 | 20,710 | 32,700 | 38,400 | 1.85 | ** | 178 | 2.8 | 3.1 | 26.9 | 178 | 2.9 | 3.1 | 26.6 |
| 90 | 175 | 2.9 | 3.1 | 17.9 | 21,160 | 5,900 | 21,950 | 28,700 | 34,400 | 1.57 | ** | 175 | 3.0 | 2.9 | 26.8 | 175 | 2.9 | 3.3 | 26.4 |
| 91 | 232 | 2.2 | 2.2 | .35 | 1,220 | * | 1,220 | 0 | 3,700 | 3.03 | ** | 232 | 2.2 | 2.2 | 27.2 | 232 | 2.2 | 2.2 | 27.2 |
| 92 | 232 | 2.3 | 2.3 | .35 | 1,320 | * | 1,320 | 0 | 4,000 | 3.03 | ** | 232 | 2.4 | 2.4 | 27.1 | 232 | 2.3 | 2.3 | 27.3 |
| 93 | 232 | 2.3 | 2.3 | .35 | 1,270 | * | 1,270 | 0 | 4,000 | 3.15 | ** | 232 | 2.3 | 2.3 | 27.3 | 232 | 2.3 | 2.3 | 27.3 |
| 94 | 232 | --- | --- | .35 | 1,170 | * | 1,170 | 0 | ---- | | ** | 232 | --- | --- | 27.3 | 232 | --- | --- | 27.2 |
| 95 | 227 | 2.3 | 2.3 | .35 | 1,300 | * | 1,300 | 0 | 4,000 | 3.08 | ** | 226 | 2.3 | 2.3 | 26.8 | 228 | 2.3 | 2.3 | 27.2 |
| 96 | 232 | 2.4 | 2.4 | .35 | 1,040 | * | 1,040 | 0 | 4,300 | 4.13 | ** | 232 | 2.5 | 2.5 | 27.2 | 232 | 2.3 | 2.3 | 27.3 |
| 97 | 233 | 2.3 | 2.4 | 2.1 | 5,840 | 300 | 5,850 | 13,900 | 18,300 | 3.13 | ** | 233 | 2.3 | 2.5 | 27.1 | 233 | 2.4 | 2.3 | 27.3 |
| 98 | 232 | 2.3 | 2.1 | 2.1 | 5,790 | 400 | 5,800 | 12,500 | 16,200 | 2.79 | ** | 232 | 2.3 | 2.1 | 27.3 | 232 | 2.3 | 2.3 | 27.3 |
| 99 | 233 | 2.4 | 2.4 | 3.9 | 10,460 | 700 | 10,480 | 41,700 | 46,100 | 4.40 | ---- | 233 | 2.4 | 2.3 | 27.2 | 233 | 2.4 | 2.5 | 27.2 |
| 100 | 229 | 2.4 | 2.3 | 3.9 | 10,890 | 600 | 10,910 | 32,600 | 36,600 | 3.35 | 11.5 | 228 | 2.4 | 2.2 | 27.2 | 229 | 2.4 | 2.4 | 27.2 |
| 101 | 231 | 2.3 | 2.3 | 7.4 | 16,350 | 2,000 | 16,470 | 41,300 | 45,300 | 2.79 | ** | 230 | 2.3 | 2.3 | 27.3 | 231 | 2.3 | 2.4 | 27.2 |
| 102 | 232 | 2.4 | 2.5 | 10.9 | 19,050 | 3,100 | 19,270 | 30,900 | 33,600 | 1.85 | ** | 232 | 2.4 | 2.6 | 27.4 | 232 | 2.5 | 2.5 | 27.0 |
| 103 | 231 | 2.5 | 2.5 | 14.4 | 19,900 | 4,500 | 20,390 | 31,700 | 36,400 | 1.79 | ** | 231 | 2.5 | 2.5 | 27.2 | 231 | 2.5 | 2.4 | 27.2 |
| 104 | 230 | 2.4 | 2.5 | 17.9 | 19,570 | 5,300 | 20,250 | 27,200 | 31,900 | 1.58 | ** | 230 | 2.4 | 2.6 | 26.6 | 230 | 2.5 | 2.4 | 25.9 |

*Force too small to be measured accurately.

**Relaxation length not determined.

TABLE II.- YAW TEST DATA - Continued

(d) SERIES D: $\bar{F}_z$ = 39,800 lb; $(F_z)_{tire\ A}$ = 39,900 lb; $(F_z)_{tire\ B}$ = 39,700 lb.

| Run | Average values | | | | | | | | | | | Tire A | | | | Tire B | | | |
|---|---|---|---|---|---|---|---|---|---|---|---|---|---|---|---|---|---|---|---|
| | $\bar{p}$, lb/sq in. | $\bar{\delta}_o$, in. | $\bar{\delta}$, in. | $\bar{\psi}$, deg | $\bar{F}_y$, lb | $\bar{F}_x$, lb | $\bar{F}_\psi$, lb | $\Delta\bar{M}_z$, lb-in. | $\bar{N}_z$, lb-in. | $\bar{q}$, in. | $\bar{L}_y$, in. | $p$, lb/sq in. | $\delta_o$, in. | $\delta$, in. | $r_e$, in. | $p$, lb/sq in. | $\delta_o$, in. | $\delta$, in. | $r_e$, in. |
| 105 | 128 | 4.0 | 3.8 | 2.1 | 3,780 | 600 | 3,800 | 38,700 | 45,100 | 11.87 | ** | 128 | 4.0 | 3.6 | 26.1 | 128 | 4.1 | 4.0 | 26.0 |
| 106 | 130 | 4.0 | 3.8 | 2.1 | 3,580 | 700 | 3,600 | 38,100 | 44,600 | 12.39 | ** | 131 | 4.0 | 3.9 | 26.1 | 129 | 4.1 | 3.7 | 26.0 |
| 107 | 127 | 4.1 | 4.2 | 3.9 | 6,980 | 800 | 7,020 | 70,200 | 77,500 | 11.04 | -- | 127 | 4.1 | 4.2 | 26.1 | 127 | 4.2 | 4.2 | 25.9 |
| 108 | 128 | 4.2 | 4.1 | 3.9 | 6,800 | 1,200 | 6,870 | 65,100 | 72,200 | 10.51 | -- | 128 | 4.3 | 4.3 | 26.0 | 128 | 4.1 | 3.9 | 25.9 |
| 109 | 126 | 4.2 | 4.3 | 7.4 | 13,510 | 2,900 | 13,770 | 78,000 | 85,500 | 6.21 | ** | 126 | 4.3 | 4.3 | 26.1 | 126 | 4.2 | 4.4 | 26.0 |
| 110 | 126 | 4.1 | 4.5 | 10.9 | 17,910 | 5,100 | 18,550 | 67,000 | 75,000 | 4.04 | ** | 126 | 4.0 | 4.5 | 26.1 | 127 | 4.2 | 4.5 | 26.1 |
| 111 | 151 | 3.5 | 3.3 | 2.1 | 4,790 | 600 | 4,810 | 32,100 | 37,800 | 7.86 | ** | 151 | 3.5 | 3.4 | 26.4 | 150 | 3.5 | 3.2 | 26.4 |
| 112 | 153 | 3.5 | 3.3 | 2.1 | 4,810 | 600 | 4,830 | 34,200 | 39,900 | 8.26 | ** | 153 | 3.5 | 3.4 | 26.4 | 153 | 3.5 | 3.2 | 26.4 |
| 113 | 150 | 3.7 | 3.5 | 3.9 | 8,310 | 1,100 | 8,370 | 60,600 | 66,800 | 7.98 | -- | 150 | 3.7 | 3.6 | 26.2 | 150 | 3.7 | 3.5 | 26.2 |
| 114 | 150 | 3.7 | 3.8 | 7.4 | 15,350 | 2,900 | 15,600 | 70,800 | 77,800 | 4.99 | ** | 150 | 3.8 | 3.8 | 26.5 | 150 | 3.7 | 3.5 | 26.4 |
| 115 | 152 | 3.6 | 4.1 | 10.9 | 20,220 | 4,900 | 20,780 | 63,800 | 71,600 | 3.45 | ** | 152 | 3.6 | 4.2 | 26.5 | 151 | 3.7 | 4.0 | 26.5 |
| 116 | 232 | 2.7 | 2.7 | .35 | 1,190 | * | 1,190 | 0 | 5,300 | 4.45 | ** | 232 | 2.7 | 2.7 | 27.2 | 231 | 2.6 | 2.6 | 27.1 |
| 117 | 230 | 2.7 | 2.7 | .35 | 1,320 | * | 1,320 | 0 | 5,300 | 4.02 | ** | 229 | 2.8 | 2.8 | 27.1 | 230 | 2.7 | 2.7 | 27.0 |
| 118 | 232 | 2.7 | 2.7 | .35 | 1,220 | * | 1,220 | 0 | 5,300 | 4.34 | ** | 232 | 2.6 | 2.6 | ---- | 232 | 2.7 | 2.7 | ---- |
| 119 | 230 | 2.7 | 2.7 | .35 | 1,210 | * | 1,210 | 0 | 5,300 | 4.38 | ** | 229 | 2.7 | 2.7 | 27.1 | 230 | 2.8 | 2.8 | 27.0 |
| 120 | 232 | 2.6 | 2.6 | .35 | 1,220 | * | 1,220 | 0 | 5,000 | 4.10 | ** | 232 | 2.6 | 2.6 | 27.2 | 232 | 2.6 | 2.6 | 27.0 |
| 121 | 231 | 2.6 | 2.6 | .35 | 1,280 | * | 1,280 | 0 | 5,000 | 3.91 | ** | 231 | 2.6 | 2.6 | 27.0 | 231 | 2.6 | 2.6 | 27.0 |
| 122 | 231 | 2.7 | 2.6 | 2.1 | 6,830 | 300 | 6,840 | 24,200 | 29,200 | 4.27 | ** | 231 | 2.7 | 2.6 | 27.1 | 231 | 2.7 | 2.5 | 27.0 |
| 123 | 230 | 2.6 | 2.6 | 2.1 | 6,790 | 500 | 6,800 | 24,400 | 29,400 | 4.32 | ** | 230 | 2.5 | 2.4 | 27.2 | 230 | 2.7 | 2.8 | 27.1 |
| 124 | 231 | 2.8 | 2.6 | 3.9 | 11,100 | 700 | 11,120 | 52,300 | 57,300 | 5.15 | -- | 232 | 2.9 | 2.5 | 26.9 | 231 | 2.8 | 2.6 | 27.0 |
| 125 | 230 | 2.7 | 2.6 | 3.9 | 10,990 | 700 | 11,010 | 50,100 | 55,300 | 5.00 | -- | 229 | 2.6 | 2.6 | 27.0 | 230 | 2.8 | 2.6 | 27.0 |
| 126 | 231 | 2.7 | 2.7 | 7.4 | 18,570 | 2,800 | 18,780 | 50,400 | 55,700 | 2.97 | ** | 231 | 2.7 | 2.6 | 27.2 | 231 | 2.7 | 2.9 | 27.0 |
| 127 | 231 | 2.7 | 2.8 | 10.9 | 22,020 | 4,800 | 22,530 | 43,900 | 49,600 | 2.20 | ** | 231 | 2.6 | 2.7 | 27.1 | 231 | 2.7 | 2.9 | 27.0 |
| 128 | 232 | 2.7 | 2.8 | 14.4 | 22,810 | 6,400 | 23,680 | 26,500 | 32,200 | 1.36 | ** | 232 | 2.8 | 2.8 | 27.3 | 232 | 2.7 | 2.8 | 27.6 |
| 129 | 231 | 2.7 | 2.7 | 17.9 | 21,930 | 7,600 | 23,200 | 24,700 | 30,000 | 1.29 | ** | 231 | 2.7 | 2.7 | 28.2 | 231 | 2.8 | 2.7 | 26.2 |

*Force too small to be measured accurately.
**Relaxation length not determined.

TABLE II.- YAW TEST DATA - Continued

(e) SERIES E: $\bar{F}_z = 45,200$ lb; $(F_z)_{tire\ A} = 45,400$ lb; $(F_z)_{tire\ B} = 45,000$ lb.

| Run | Average values | | | | | | | | | | | Tire A | | | | Tire B | | | |
|---|---|---|---|---|---|---|---|---|---|---|---|---|---|---|---|---|---|---|---|
| | $\bar{p}$, lb/sq in. | $\delta_o$, in. | $\bar{\delta}$, in. | $\bar{\psi}$, deg | $\bar{F}_y$, lb | $\bar{F}_x$, lb | $\bar{F}_\psi$, lb | $\Delta\bar{M}_z$, lb-in. | $\bar{M}_z$, lb-in. | $\bar{q}$, in. | $L_y$, in. | $p$, lb/sq in. | $\delta_o$, in. | $\delta$, in. | $r_e$, in. | $p$, lb/sq in. | $\delta_o$, in. | $\delta$, in. | $r_e$, in. |
| 130 | 151 | 4.0 | 3.8 | 2.1 | 4,900 | 900 | 4,930 | 40,400 | 47,400 | 9.61 | ** | 151 | 3.9 | 3.7 | 26.1 | 151 | 4.0 | 3.9 | 26.1 |
| 131 | 152 | 4.0 | 3.8 | 2.1 | 4,730 | 800 | 4,760 | 40,900 | 47,900 | 10.06 | ** | 150 | 3.9 | 3.7 | 26.2 | 154 | 4.0 | 3.9 | 26.1 |
| 132 | 152 | 4.1 | 4.0 | 3.9 | 8,460 | 1,000 | 8,510 | 74,700 | 82,200 | 9.66 | 20.0 | 153 | 4.1 | 4.0 | 26.1 | 150 | 4.2 | 4.0 | 26.1 |
| 133 | 151 | 4.1 | 3.9 | 3.9 | 8,420 | 1,400 | 8,500 | 74,400 | 81,700 | 9.61 | ---- | 151 | 4.0 | 3.8 | 26.1 | 151 | 4.1 | 4.0 | 26.2 |
| 134 | 150 | --- | 4.0 | 7.4 | 14,860 | 3,100 | 15,140 | 86,300 | 93,700 | 6.19 | ** | 150 | --- | 3.9 | 26.3 | 150 | --- | 4.1 | ---- |
| 135 | 152 | 4.2 | 4.7 | 10.9 | 19,990 | 4,900 | 20,560 | 84,100 | 93,400 | 4.54 | ** | 152 | 4.2 | 4.5 | 26.3 | 152 | --- | 4.9 | 26.2 |
| 136 | 183 | 3.6 | 3.6 | .35 | 1,090 | * | 1,090 | 0 | 7,200 | 6.61 | ** | 183 | 3.6 | 3.6 | 26.7 | 183 | 3.6 | 3.6 | 26.6 |
| 137 | 180 | 3.7 | 3.5 | 2.1 | 5,510 | 800 | 5,540 | 39,300 | 46,100 | 8.32 | ** | 180 | 3.7 | 3.5 | 26.6 | 180 | 3.7 | 3.5 | 26.5 |
| 138 | 183 | 3.4 | 3.2 | 2.1 | 5,850 | 700 | 5,850 | 41,100 | 47,100 | 8.05 | ** | 183 | 3.4 | 3.1 | 26.5 | 183 | 3.4 | 3.2 | 26.4 |
| 139 | 181 | 3.6 | 3.4 | 3.9 | 9,880 | 600 | 9,900 | 57,600 | 64,200 | 6.48 | ---- | 181 | 3.6 | 3.4 | 26.6 | 180 | --- | --- | 26.5 |
| 140 | 182 | 3.6 | 3.4 | 3.9 | 9,850 | 1,000 | 9,900 | 60,900 | 67,900 | 6.82 | ---- | 180 | 3.6 | 3.4 | 26.6 | 184 | 3.5 | 3.3 | 26.5 |
| 141 | 181 | 3.5 | 3.4 | 3.9 | 9,510 | 1,000 | 9,560 | 49,900 | 56,500 | 5.91 | ---- | 181 | 3.4 | 3.3 | 26.6 | 181 | 3.5 | 3.5 | 25.9 |
| 142 | 180 | 3.6 | 3.7 | 7.4 | 17,280 | 3,700 | 17,610 | 79,800 | 87,200 | 4.95 | ** | 180 | 3.6 | 3.8 | 26.6 | 179 | --- | 3.7 | ---- |
| 143 | 180 | 3.5 | 3.6 | 10.9 | 22,290 | 5,400 | 22,910 | 65,600 | 72,700 | 3.17 | ** | 180 | 3.5 | 3.8 | 26.7 | 180 | 3.4 | 3.3 | 26.5 |
| 144 | 233 | 2.9 | 2.9 | .35 | 1,260 | * | 1,260 | 0 | 6,000 | 4.76 | ** | 232 | 2.9 | 2.9 | ---- | 235 | 2.9 | 2.9 | ---- |
| 145 | 232 | 3.0 | 3.0 | .35 | 1,310 | * | 1,310 | 0 | 6,300 | 4.81 | ** | 232 | 3.0 | 3.0 | ---- | 232 | 3.1 | 3.1 | ---- |
| 146 | 232 | 2.9 | 2.9 | .35 | 1,350 | * | 1,350 | 0 | 6,000 | 4.44 | ** | 232 | 2.8 | 2.8 | 27.0 | 232 | 2.9 | 2.9 | 27.0 |
| 147 | 232 | 3.0 | 3.0 | .35 | 1,210 | * | 1,210 | 0 | 6,300 | 5.21 | ** | 231 | 3.0 | 3.0 | ---- | 232 | 3.0 | 3.0 | ---- |
| 148 | 232 | 2.9 | 2.9 | .35 | 1,410 | * | 1,410 | 0 | 6,000 | 4.26 | ** | 232 | 2.9 | 2.9 | 27.0 | 232 | 2.9 | 2.9 | 27.0 |
| 149 | 232 | 2.9 | 2.9 | .35 | ----- | * | ----- | 0 | 6,000 | ---- | ** | 232 | 2.9 | 2.9 | 27.0 | 232 | 3.0 | 3.0 | 26.9 |
| 150 | 232 | 2.9 | 2.9 | .35 | 1,210 | * | 1,210 | 0 | 6,000 | 4.96 | ** | 232 | 2.9 | 2.9 | 27.0 | 233 | 2.9 | 2.9 | 26.9 |
| 151 | 230 | 3.0 | 3.0 | .35 | 1,120 | * | 1,120 | 0 | 6,200 | 5.54 | ** | 230 | 3.0 | 3.0 | 27.0 | 230 | 3.0 | 3.0 | ---- |
| 152 | 232 | 2.8 | 2.8 | .35 | 1,320 | * | 1,320 | 0 | 5,700 | 4.32 | ** | 232 | 2.8 | 2.8 | 27.1 | 232 | 2.8 | 2.8 | 27.0 |
| 153 | 232 | 3.0 | 2.7 | 2.1 | 6,490 | 600 | 6,510 | 32,000 | 37,300 | 5.73 | ** | 232 | 3.0 | 2.5 | 27.1 | 232 | 3.1 | 2.8 | 27.0 |
| 154 | 233 | 2.9 | 2.8 | 2.1 | 6,160 | 400 | 6,170 | 28,700 | 34,400 | 5.58 | ** | 233 | 2.8 | 2.9 | 27.1 | 234 | 2.9 | 2.7 | 27.0 |
| 155 | 232 | 3.2 | 3.0 | 3.9 | 11,350 | 1,000 | 11,390 | 49,200 | 55,500 | 4.87 | ---- | 232 | 3.3 | 2.9 | 26.8 | 232 | 3.1 | 3.1 | 27.0 |
| 156 | 232 | 2.8 | 3.1 | 3.9 | 11,540 | 1,200 | 11,590 | 48,200 | 54,800 | 4.73 | 16.5 | 232 | 2.8 | 3.1 | 27.0 | 232 | --- | --- | ---- |
| 157 | 232 | 2.9 | 2.8 | 7.4 | 19,860 | 3,200 | 20,110 | 65,300 | 71,000 | 3.53 | ** | 232 | 2.8 | 2.7 | ---- | 232 | 3.0 | 2.9 | ---- |
| 158 | 232 | 2.9 | 3.0 | 7.4 | 19,570 | 3,300 | 19,830 | 61,800 | 68,100 | 3.43 | ** | 232 | 2.9 | 2.9 | 27.2 | 232 | 2.8 | 3.0 | ---- |
| 159 | 233 | 3.0 | 3.0 | 10.9 | 23,340 | 5,000 | 23,860 | 53,900 | 60,200 | 2.52 | ** | 233 | 2.9 | 2.9 | ---- | 232 | 3.0 | 3.1 | ---- |
| 160 | 232 | 2.9 | 3.0 | 10.9 | 22,710 | 5,000 | 23,230 | 53,400 | 59,400 | 2.55 | ** | 232 | 2.9 | 3.0 | ---- | 232 | 2.9 | 3.1 | ---- |
| 161 | 232 | --- | 3.2 | 14.4 | 24,660 | 6,600 | 25,530 | 37,900 | 44,900 | 1.76 | ** | 231 | --- | 3.2 | 27.2 | 232 | --- | --- | 26.7 |
| 162 | 232 | 2.9 | 3.2 | 17.9 | 24,250 | 8,300 | 25,630 | 32,300 | 39,300 | 1.53 | ** | 232 | 2.9 | 2.9 | 27.8 | 232 | --- | 3.3 | 26.3 |

*Force too small to be measured accurately.
**Relaxation length not determined.

TABLE II.- YAW TEST DATA --Continued

(f) SERIES F: $\bar{F}_z$ = 17,400 lb; $(F_z)_{tire\ A}$ = 17,300 lb; $(F_z)_{tire\ B}$ = 17,400 lb.

| Run | Average values | | | | | | | | | | | Tire A | | | | Tire B | | | |
|---|---|---|---|---|---|---|---|---|---|---|---|---|---|---|---|---|---|---|---|
| | $\bar{p}$, lb/sq in. | $\bar{\delta}_0$, in. | $\bar{\delta}$, in. | $\bar{\psi}$, deg | $\bar{F}_y$, lb | $\bar{F}_x$, lb | $\bar{F}_\psi$, lb | $\Delta M_z$, lb-in. | $\bar{M}_z$, lb-in. | $q$, in. | $\bar{l}_y$, in. | $p$, lb/sq in. | $\delta_0$, in. | $\delta$, in. | $r_e$, in. | $p$, lb/sq in. | $\delta_0$, in. | $\delta$, in. | $r_e$, in. |
| 163 | 61 | 3.4 | 3.4 | 0.35 | 530 | * | 530 | 0 | 4,100 | 7.74 | ** | 61 | 3.3 | 3.3 | 25.8 | 62 | 3.4 | 3.4 | 25.8 |
| 164 | 60 | 3.5 | 3.3 | 2.1 | 2,680 | 300 | 2,690 | 18,000 | 22,000 | 8.18 | ** | 60 | 3.5 | 3.3 | 25.9 | 60 | 3.5 | 3.3 | 25.8 |
| 165 | 59 | 3.6 | 3.5 | 3.9 | 4,690 | 800 | 4,730 | 32,900 | 37,200 | 7.86 | ---- | 59 | 3.6 | 3.6 | 25.7 | 59 | 3.6 | 3.4 | 25.8 |
| 166 | 60 | 3.4 | 3.6 | 7.4 | 8,760 | 1,700 | 8,910 | 34,300 | 38,800 | 4.35 | ** | 60 | 3.3 | 3.8 | 26.1 | 60 | 3.5 | 3.4 | 25.9 |
| 167 | 59 | 3.5 | 3.9 | 10.9 | 11,070 | 2,700 | 11,380 | 32,700 | 37,700 | 3.31 | ** | 59 | 3.5 | 3.8 | 25.9 | 60 | --- | 4.0 | 25.8 |
| 168 | 60 | 3.4 | 4.1 | 14.4 | 12,850 | 4,000 | 13,440 | 29,000 | 34,400 | 2.56 | ** | 59 | 3.4 | 4.2 | 25.9 | 59 | --- | 4.1 | 25.8 |
| 169 | 60 | 3.4 | 4.3 | 17.9 | 13,060 | 4,800 | 13,900 | 23,500 | 29,200 | 2.10 | ** | 59 | --- | 4.5 | 26.2 | 60 | 3.4 | 4.2 | 25.4 |
| 170 | 84 | 2.6 | 2.5 | 2.1 | 3,470 | 300 | 3,480 | 17,100 | 19,900 | 5.72 | ** | 84 | 2.6 | 2.6 | 26.5 | 84 | 2.6 | 2.4 | 26.4 |
| 171 | 84 | 2.7 | 2.7 | 3.9 | 6,070 | 600 | 6,100 | 29,500 | 32,700 | 5.36 | ---- | 84 | 2.7 | 2.7 | 26.4 | 84 | 2.8 | 2.7 | 26.3 |
| 172 | 85 | 2.6 | 2.8 | 7.4 | 9,980 | 1,700 | 10,120 | 28,000 | 31,500 | 3.11 | ** | 85 | 2.4 | 2.5 | 26.6 | 85 | 2.7 | 3.0 | 26.4 |
| 173 | 84 | 2.7 | 3.0 | 10.9 | 11,740 | 2,800 | 12,060 | 24,100 | 27,900 | 2.31 | ** | 84 | --- | 3.1 | 26.4 | 84 | 2.7 | 2.8 | 26.2 |
| 174 | 84 | 2.8 | 3.1 | 14.4 | 13,010 | 3,300 | 13,420 | 22,300 | 26,300 | 1.96 | ** | 84 | --- | 3.1 | 26.6 | 85 | 2.8 | 3.1 | 26.2 |
| 175 | 84 | 2.8 | 3.2 | 17.9 | 13,310 | 4,200 | 13,960 | 18,400 | 26,600 | 1.62 | ** | 84 | --- | 3.2 | 26.9 | 84 | 2.8 | 3.2 | 25.8 |
| 176 | 170 | 1.7 | 1.7 | .35 | 830 | * | 830 | 0 | 2,000 | 2.41 | ** | 170 | 1.6 | 1.6 | 27.3 | 170 | 1.7 | 1.7 | 27.4 |
| 177 | 167 | 1.8 | 1.8 | .35 | 760 | * | 760 | 0 | 2,200 | 2.89 | ** | 167 | 1.9 | 1.9 | 27.3 | 166 | 1.7 | 1.7 | 27.4 |
| 178 | 169 | 1.7 | 1.7 | .35 | 880 | * | 880 | 0 | 2,000 | 2.27 | ** | 169 | 1.6 | 1.6 | ---- | 169 | 1.8 | 1.8 | ---- |
| 179 | 168 | 1.8 | 1.8 | .35 | 740 | * | 740 | 0 | 2,200 | 2.97 | ** | 168 | 1.8 | 1.8 | 27.3 | 168 | 1.8 | 1.8 | 27.1 |
| 180 | 169 | 1.8 | 1.8 | .35 | 810 | * | 810 | 0 | 2,200 | 2.72 | ** | 169 | 1.9 | 1.9 | 27.3 | 168 | 1.7 | 1.7 | 27.3 |
| 181 | 169 | 1.7 | 1.7 | .35 | 850 | * | 850 | 0 | 2,000 | 2.35 | ** | 169 | --- | --- | 27.2 | 169 | 1.7 | 1.7 | 27.3 |
| 182 | 169 | 1.7 | 1.6 | 2.1 | 4,050 | 100 | 4,050 | 8,700 | 10,500 | 2.59 | ** | 169 | 1.7 | 1.5 | 27.4 | 169 | 1.8 | 1.6 | 27.5 |
| 183 | 168 | 1.8 | 1.8 | 3.9 | 6,810 | 500 | 6,830 | 12,200 | 14,400 | 2.11 | 11.7 | 168 | 1.9 | 1.9 | 27.2 | 167 | 1.7 | 1.8 | 27.4 |
| 184 | 169 | 1.7 | 1.6 | 3.9 | 7,350 | 500 | 7,370 | 16,700 | 18,500 | 2.51 | 11.4 | 169 | 1.8 | 1.5 | 27.4 | 169 | 1.6 | 1.7 | 27.3 |
| 185 | 169 | 1.7 | 1.5 | 3.9 | 6,150 | ---- | | 20,800 | 22,400 | ---- | ** | 169 | 1.7 | 1.4 | ---- | 169 | 1.6 | 1.5 | ---- |
| 186 | 168 | 1.7 | 1.5 | 7.4 | 10,450 | 1,500 | 10,560 | 19,200 | 20,800 | 1.97 | ** | 169 | 1.7 | 1.5 | 27.3 | 168 | 1.8 | 1.4 | 27.3 |
| 187 | 168 | 1.7 | 1.7 | 10.9 | 11,520 | 2,300 | 11,750 | 15,200 | 17,200 | 1.46 | ** | 169 | 1.8 | 1.6 | 27.4 | 168 | 1.7 | 1.7 | 27.1 |
| 188 | 169 | 1.8 | 1.7 | 14.4 | 12,120 | 3,100 | 12,510 | 11,300 | 13,300 | 1.06 | ** | 169 | 1.8 | 1.5 | 27.7 | 169 | 1.8 | 1.8 | 26.9 |
| 189 | 167 | 1.9 | 1.8 | 17.9 | 12,170 | 3,700 | 12,720 | 10,100 | 12,300 | .97 | ** | 168 | --- | 1.7 | 27.0 | 166 | 1.9 | 1.8 | 26.7 |

*Force too small to be measured accurately.

**Relaxation length not determined.

TABLE II.- YAW TEST DATA - Continued

(g) SERIES G: $F_z = 9,600$ lb; $(F_z)_{tire\ A} = 9,700$ lb; $(F_z)_{tire\ B} = 9,600$ lb.

| Run | Average values | | | | | | | | | | | Tire A | | | | Tire B | | | |
|---|---|---|---|---|---|---|---|---|---|---|---|---|---|---|---|---|---|---|---|
| | $p$, lb/sq in. | $\bar{\delta}_o$, in. | $\bar{\delta}$, in. | $\bar{\psi}$, deg | $\bar{F}_y$, lb | $\bar{F}_x$, lb | $\bar{F}_\psi$, lb | $\Delta\bar{N}_z$, lb-in. | $R_z$, lb-in. | $\bar{q}$, in. | $L_y$, in. | $p$, lb/sq in. | $\delta_o$, in. | $\delta$, in. | $r_e$, in. | $p$, lb/sq in. | $\delta_o$, in. | $\delta$, in. | $r_e$, in. |
| 190 | 29 | 3.6 | 3.6 | 0.35 | 450 | * | 450 | 0 | 3,800 | 8.44 | ** | 29 | 3.6 | 3.6 | 25.6 | 29 | 3.7 | 3.7 | 25.3 |
| 191 | 29 | 3.4 | 3.2 | 2.1 | 1,710 | 200 | 1,720 | 6,500 | 9,700 | 5.64 | ** | 29 | 3.3 | 3.1 | 25.7 | 29 | 3.4 | 3.2 | 25.5 |
| 192 | 29 | 3.5 | 3.3 | 3.9 | 3,100 | 300 | 3,110 | 20,100 | 23,500 | 7.56 | -- | 29 | 3.4 | 3.3 | 25.5 | 29 | 3.6 | 3.3 | 25.4 |
| 193 | 29 | 3.5 | 3.6 | 7.4 | 6,310 | 1,000 | 6,390 | 25,700 | 29,500 | 4.62 | ** | 29 | 3.5 | 3.7 | 25.7 | 29 | 3.6 | 3.5 | 25.7 |
| 194 | 29 | 3.5 | 3.7 | 10.9 | 7,590 | 1,400 | 7,720 | 21,700 | 25,700 | 3.33 | ** | 29 | 3.5 | 3.5 | 25.5 | 29 | 3.5 | 3.8 | 25.7 |
| 195 | 29 | 3.2 | 3.9 | 14.4 | 8,690 | 2,100 | 8,940 | 6,900 | 11,200 | 1.25 | ** | 29 | 3.1 | 4.0 | 26.0 | 29 | 3.2 | 3.7 | 25.7 |
| 196 | 29 | 3.4 | 3.9 | 17.9 | 8,560 | 2,600 | 8,940 | 7,400 | 11,700 | 1.31 | ** | 29 | 3.4 | 3.9 | 26.2 | 29 | 3.5 | 4.0 | 24.9 |
| 197 | 39 | 2.6 | 2.6 | .35 | 480 | * | 480 | 0 | 2,400 | 5.00 | ** | 39 | 2.6 | 2.6 | 26.0 | 39 | 2.7 | 2.7 | 25.9 |
| 198 | 39 | 2.6 | 2.5 | 2.1 | 1,860 | 200 | 1,870 | 8,500 | 10,800 | 5.78 | ** | 39 | 2.6 | 2.3 | 26.2 | 39 | 2.7 | 2.6 | 26.0 |
| 199 | 39 | 3.0 | 2.9 | 3.9 | 3,640 | 400 | 3,660 | 17,500 | 20,400 | 5.57 | -- | 39 | 3.1 | 3.0 | 25.9 | 39 | 3.0 | 2.9 | 25.9 |
| 200 | 39 | 2.6 | 2.8 | 7.4 | 6,670 | 900 | 6,730 | 19,100 | 21,900 | 3.25 | ** | 39 | 2.6 | 2.7 | 26.2 | 39 | 2.7 | 2.8 | 26.1 |
| 201 | 39 | --- | 3.3 | 10.9 | 8,100 | 1,400 | 8,220 | 18,400 | 22,000 | 2.68 | ** | 39 | --- | 3.3 | 25.9 | 39 | --- | 3.3 | 25.9 |
| 202 | 39 | 2.5 | 3.0 | 14.4 | 8,860 | 1,900 | 9,050 | 9,400 | 12,500 | 1.38 | ** | 39 | 2.5 | 3.0 | 26.3 | 39 | 2.6 | 3.0 | 25.9 |
| 203 | 39 | 2.8 | 3.2 | 17.9 | 8,530 | 2,500 | 8,890 | 8,600 | 12,000 | 1.35 | ** | 39 | 2.8 | 3.2 | 26.7 | 39 | 2.8 | 3.2 | 25.3 |
| 204 | 59 | 2.0 | 2.0 | .35 | 630 | * | 630 | 0 | 1,700 | 2.70 | ** | 59 | 2.0 | 2.0 | 26.3 | 58 | 2.1 | 2.1 | 26.4 |
| 205 | 59 | 1.9 | 1.8 | 2.1 | 2,480 | 200 | 2,490 | 5,300 | 6,700 | 2.69 | ** | 59 | 1.9 | 1.8 | 26.6 | 59 | 1.9 | 1.7 | 26.7 |
| 206 | 59 | 2.4 | 2.2 | 3.9 | 4,690 | 400 | 4,710 | 14,600 | 16,600 | 3.52 | -- | 59 | 2.3 | 2.1 | 26.3 | 59 | 2.3 | 2.2 | 26.4 |
| 207 | 59 | 1.9 | 2.1 | 7.4 | 7,270 | 1,000 | 7,340 | 16,000 | 17,800 | 2.43 | ** | 59 | 1.8 | 2.3 | 26.7 | 59 | 1.9 | 1.8 | 26.6 |
| 208 | 59 | 2.1 | 2.3 | 10.9 | 8,110 | 1,500 | 8,250 | 15,100 | 17,300 | 2.10 | ** | 58 | --- | 2.4 | 26.6 | 59 | 2.1 | 2.1 | 26.3 |
| 209 | 84 | 1.7 | 1.7 | .35 | 630 | * | 630 | 0 | 1,400 | 2.22 | ** | 84 | 1.7 | 1.7 | 26.7 | 84 | 1.6 | 1.6 | 26.8 |
| 210 | 84 | 1.6 | 1.6 | .35 | 640 | * | 640 | 0 | 1,300 | 2.03 | ** | 84 | 1.7 | 1.7 | 26.9 | 84 | 1.6 | 1.6 | 26.9 |
| 211 | 84 | 1.6 | 1.6 | .35 | 640 | * | 640 | 0 | 1,300 | 2.03 | ** | 84 | 1.6 | 1.6 | ---- | 83 | 1.6 | 1.6 | ---- |
| 212 | 84 | 1.6 | 1.4 | 2.1 | 2,700 | 200 | 2,710 | ------- | ------- | ---- | ** | 84 | 1.6 | 1.3 | 27.1 | 83 | 1.7 | 1.4 | 27.0 |
| 213 | 84 | 1.7 | 1.7 | 3.9 | 4,890 | 300 | 4,900 | 14,300 | 15,700 | 3.20 | - | 84 | 1.8 | 1.6 | 26.7 | 84 | 1.6 | 1.7 | 26.8 |
| 214 | 84 | 1.6 | 1.5 | 7.4 | 7,540 | 800 | 7,580 | 13,700 | 14,800 | 1.95 | ** | 84 | 1.7 | 1.4 | 27.0 | 84 | 1.6 | 1.6 | 27.0 |
| 215 | 127 | 1.3 | 1.3 | .35 | 550 | * | 550 | 0 | 1,100 | 2.00 | ** | 127 | 1.3 | 1.3 | 27.0 | 127 | 1.3 | 1.3 | 27.2 |
| 216 | 126 | 1.2 | 1.2 | 2.1 | 2,460 | 200 | 2,470 | ------- | ------- | ---- | ** | 127 | 1.2 | 1.1 | 27.5 | 125 | 1.3 | 1.3 | 27.3 |
| 217 | 126 | 1.5 | 1.4 | 3.9 | 4,910 | 300 | 4,920 | 16,100 | 17,300 | 3.52 | - | 126 | 1.5 | 1.3 | 27.1 | 126 | 1.5 | 1.5 | 27.2 |
| 218 | 126 | 1.3 | 1.3 | 7.4 | 6,700 | 700 | 6,730 | 11,800 | 12,900 | 1.92 | ** | 126 | 1.4 | 1.4 | 27.2 | 126 | 1.3 | 1.2 | 27.4 |
| 219 | 168 | 1.0 | 1.0 | .35 | 500 | * | 500 | 0 | 800 | 1.60 | ** | 168 | 1.0 | 1.0 | 27.5 | 168 | 1.0 | 1.0 | 27.0 |
| 220 | 168 | 1.0 | 1.0 | 2.1 | 2,440 | 100 | 2,440 | ------- | ------- | ---- | ** | 168 | 1.0 | .9 | 27.6 | 168 | 1.0 | 1.0 | 27.3 |
| 221 | 166 | 1.2 | 1.2 | 3.9 | 4,250 | 300 | 4,260 | 9,700 | 10,800 | 2.54 | - | 166 | 1.3 | 1.5 | 27.3 | 165 | 1.2 | 1.0 | 27.5 |
| 222 | 168 | 1.1 | 1.0 | 7.4 | 6,310 | 600 | 6,330 | 11,000 | 11,800 | 1.86 | ** | 167 | --- | --- | 27.4 | 168 | 1.1 | 1.0 | 27.6 |

*Force too small to be measured accurately.

**Relaxation length not determined.

TABLE II.- YAW TEST DATA - Continued

(h) SERIES H: $F_z$ = 9,600 lb; $(F_z)_{tire\ A}$ = 9,700 lb; $(F_z)_{tire\ B}$ = 9,600 lb.

| Run | $\bar{p}$, lb/sq in. | $\bar{\delta}_0$, in. | $\bar{\delta}$, in. | $\bar{\psi}$, deg | $\bar{F}_y$, lb | $\bar{F}_x$, lb | $\bar{F}_\psi$, lb | $\Delta\bar{M}_z$, lb-in. | $\bar{M}_z$, lb-in. | $\bar{q}$, in. |
|---|---|---|---|---|---|---|---|---|---|---|
| | | | | | Average values | | | | | |
| 223 | 30 | 3.4 | 3.4 | 0.35 | 480 | * | 480 | 0 | 3,500 | 7.29 |
| 224 | 29 | 3.4 | 3.4 | .35 | 450 | * | 450 | 0 | 3,500 | 7.78 |
| 225 | 29 | 3.6 | 3.6 | .35 | 450 | * | 450 | 0 | 3,800 | 8.44 |
| 226 | 29 | 3.4 | 3.3 | 2.1 | 1,660 | 200 | 1,670 | 11,300 | 14,700 | 8.80 |
| 227 | 29 | 3.6 | 3.4 | 2.1 | 1,550 | 200 | 1,560 | 12,800 | 16,300 | 10.45 |
| 228 | 29 | 3.5 | 3.4 | 3.9 | 3,050 | 300 | 3,060 | 9,800 | 13,300 | 4.35 |
| 229 | 29 | 3.5 | 3.3 | 3.9 | 2,960 | 400 | 2,980 | 13,000 | 16,400 | 5.50 |
| 230 | 29 | 3.6 | 3.5 | 5.7 | 3,710 | 500 | 3,740 | 17,900 | 21,600 | 5.78 |
| 231 | 29 | 3.6 | 3.6 | 7.4 | 4,830 | 800 | 4,890 | 14,000 | 17,800 | 3.64 |
| 232 | 29 | 3.5 | 3.5 | 10.9 | 4,910 | 1,200 | 5,050 | 13,800 | 17,500 | 3.47 |
| 233 | 29 | 3.6 | 3.5 | 14.4 | 4,870 | 1,700 | 5,140 | 12,100 | 15,800 | 3.07 |
| 234 | 29 | 3.3 | 3.6 | 17.9 | 4,560 | 1,600 | 4,830 | 9,700 | 13,500 | 2.80 |
| 235 | 39 | 2.7 | 2.7 | .35 | 540 | * | 540 | 0 | 2,600 | 4.81 |
| 236 | 39 | 2.9 | 2.9 | .35 | 530 | * | 530 | 0 | 2,900 | 5.47 |
| 237 | 39 | 2.9 | 2.9 | .35 | 470 | * | 470 | 0 | 2,900 | 6.17 |
| 238 | 39 | 2.9 | 2.9 | .35 | 590 | * | 590 | 0 | 2,900 | 4.92 |
| 239 | 39 | 2.9 | 2.9 | .35 | 580 | * | 580 | 0 | 2,900 | 5.00 |
| 240 | 39 | 2.9 | 2.9 | .35 | 540 | * | 540 | 0 | 2,900 | 5.37 |
| 241 | 39 | 2.7 | 2.5 | 2.1 | 2,080 | 100 | 2,080 | 9,500 | 11,800 | 5.67 |
| 242 | 39 | 2.8 | 2.6 | 2.1 | 2,130 | 300 | 2,140 | 10,100 | 12,500 | 5.84 |
| 243 | 39 | 3.1 | 3.0 | 2.1 | 2,260 | 200 | 2,270 | 9,600 | 12,700 | 5.59 |
| 244 | 39 | 2.9 | 2.7 | 3.9 | 3,360 | 400 | 3,380 | 10,300 | 12,900 | 3.82 |
| 245 | 39 | 3.1 | 2.9 | 3.9 | 3,220 | 300 | 3,230 | 14,500 | 17,400 | 5.39 |
| 246 | 39 | 3.0 | 3.0 | 5.7 | 3,870 | 400 | 3,890 | 18,200 | 21,300 | 5.48 |
| 247 | 39 | 3.0 | 3.1 | 7.4 | 4,730 | 600 | 4,770 | 13,400 | 16,600 | 3.48 |
| 248 | 39 | 3.0 | 2.9 | 10.9 | 5,040 | 1,300 | 5,190 | 10,200 | 13,100 | 2.52 |
| 249 | 39 | 3.0 | 3.3 | 14.4 | 4,980 | 1,600 | 5,220 | 9,300 | 12,900 | 2.47 |
| 250 | 39 | 3.0 | 3.0 | 14.4 | 5,640 | 1,800 | 5,910 | ------ | ------ | ---- |
| 251 | 39 | 2.9 | 3.1 | 14.4 | 5,700 | 1,700 | 5,940 | 7,200 | 10,400 | 1.75 |
| 252 | 39 | 3.0 | 3.2 | 17.9 | 4,550 | 1,900 | 4,910 | 7,400 | 10,800 | 2.20 |

*Force too small to be measured accurately.

TABLE II.- YAW TEST DATA - Concluded

(i) SERIES I: $\bar{F}_z = 9{,}600$ lb.

| Run | Average values | | | | | | | | | |
|-----|-----------------|-----------|-----------|-----------------|----------------|----------------|----------------|------------------------|-----------------------|--------------|
|     | $\bar{p}$, lb/sq in. | $\bar{\delta}_0$, in. | $\bar{\delta}$, in. | $\bar{\psi}$, deg | $\bar{F}_y$, lb | $\bar{F}_x$, lb | $\bar{F}_\psi$, lb | $\Delta\bar{M}_z$, lb-in. | $\bar{M}_z$, lb-in. | $\bar{q}$, in. |
| 253 | 39 | 2.9 | 2.9 | 0.35 | 570 | * | 570 | 0 | 2,900 | 5.09 |
| 254 | 39 | --- | --- | .35 | 510 | * | 510 | 0 | ------- | ---- |
| 255 | 39 | 2.8 | 2.8 | .35 | 620 | * | 620 | 0 | 2,800 | 4.52 |
| 256 | 39 | 2.8 | 2.8 | .35 | 590 | * | 590 | 0 | 2,800 | 4.75 |
| 257 | 39 | 3.1 | 2.7 | 2.1 | ----- | 300 | ----- | 17,000 | 19,600 | ---- |
| 258 | 39 | 2.8 | 2.6 | 2.1 | 2,490 | 400 | 2,500 | 16,300 | 18,700 | 7.48 |
| 259 | 39 | 3.1 | 3.1 | 3.9 | 4,440 | 500 | 4,460 | 19,100 | 22,300 | 5.00 |
| 260 | 39 | 3.0 | 2.8 | 3.9 | 4,170 | 600 | 4,200 | 16,900 | 19,700 | 4.69 |
| 261 | 39 | 3.0 | 3.3 | 7.4 | 7,120 | 1,100 | 7,200 | 17,500 | 21,100 | 2.93 |
| 262 | 39 | 2.9 | 3.0 | 7.4 | 6,710 | 1,200 | 6,810 | 16,900 | 20,000 | 2.94 |
| 263 | 39 | 3.1 | 3.4 | 10.9 | 8,220 | 1,800 | 8,410 | 11,000 | 14,700 | 1.75 |
| 264 | 39 | 3.0 | 3.2 | 10.9 | 7,970 | 1,800 | 8,170 | 13,200 | 16,600 | 2.03 |
| 265 | 39 | 3.1 | 3.3 | 14.4 | 8,380 | 2,400 | 8,710 | 7,500 | 11,100 | 1.27 |
| 266 | 39 | 3.0 | 3.3 | 14.4 | 8,260 | 2,500 | 8,620 | 6,500 | 10,100 | 1.17 |
| 267 | 39 | 2.9 | 3.2 | 17.9 | 8,130 | 2,600 | 8,540 | 4,700 | 8,100 | .95 |

*Force too small to be measured accurately.

TABLE III.- STATIC-RELAXATION-LENGTH DATA

| Run | Test series | Tire A | | | | | | Tire B | | | | | |
|-----|-------------|--------|--|--|--|--|--|--------|--|--|--|--|--|
| | | $p_o$, lb/sq in. | $p$, lb/sq in. | $F_z$, lb | $r$, in. | $\delta_o$, in. | $L_s$, in. | $p_o$, lb/sq in. | $p$, lb/sq in. | $F_z$, lb | $r$, in. | $\delta_o$, in. | $L_s$, in. |
| 268 | A | 28 | 29 | 17,000 | 27.5 | 5.1 | 20.9 | 29 | 31 | 16,900 | 27.5 | 5.2 | 20.5 |
| 269 | A | 56 | 58 | 17,000 | 27.6 | 3.8 | 26.5 | 59 | 63 | 16,900 | 27.7 | 3.7 | 25.3 |
| 270 | A | --- | --- | 17,000 | ----- | --- | ----- | 95 | --- | 16,900 | 27.8 | 2.7 | 31.1 |
| 271 | A | 146 | 148 | 17,000 | 27.8 | 2.2 | 26.9 | 146 | 148 | 16,900 | 27.9 | 2.2 | 28.2 |
| 272 | B | 78 | 79 | 23,700 | 27.6 | 3.8 | 25.3 | 78 | 79 | 23,800 | 27.7 | 3.8 | 19.8 |
| 273 | B | 122 | 124 | 23,700 | 27.7 | 2.9 | 26.1 | 122 | 124 | 23,800 | 27.8 | 2.9 | 24.3 |
| 274 | B | 202 | 203 | 23,700 | 27.9 | 2.1 | 22.5 | 202 | 203 | 23,800 | 27.9 | 2.0 | 25.6 |
| 275 | C | 128 | --- | 32,900 | 27.9 | 3.5 | 20.3 | 128 | --- | 32,500 | 28.0 | 3.7 | 22.1 |
| 276 | C | 171 | 173 | 32,900 | 28.0 | 2.9 | 23.0 | 171 | 173 | 32,500 | 28.1 | 3.1 | 23.7 |
| 277 | C | 229 | --- | 32,900 | 28.1 | 2.5 | 28.0 | 230 | --- | 32,500 | 28.2 | 2.5 | 20.7 |
| 278 | D | 126 | --- | 39,900 | 27.9 | 4.1 | 18.7 | 125 | --- | 39,700 | 27.9 | 4.1 | 15.8 |
| 279 | D | 147 | --- | 39,900 | 28.0 | 3.8 | 22.8 | 148 | --- | 39,700 | 28.0 | 3.8 | 22.2 |
| 280 | D | 231 | --- | 39,900 | 28.1 | 2.7 | 20.9 | 231 | --- | 39,700 | 28.2 | 2.8 | 19.8 |
| 281 | E | 143 | 148 | 45,400 | 28.0 | 4.5 | 18.9 | 143 | 148 | 45,000 | 28.0 | 4.3 | 18.9 |
| 282 | E | 177 | 184 | 45,400 | 28.1 | 3.7 | 20.2 | 177 | 183 | 45,000 | 28.1 | 3.8 | 19.3 |
| 283 | E | 228 | 231 | 45,400 | 28.2 | 3.3 | 22.5 | 228 | 234 | 45,000 | 28.2 | 3.3 | 19.0 |
| 284 | F | 57 | 59 | 17,300 | 27.7 | 3.6 | 20.8 | 58 | 60 | 17,400 | 27.7 | 3.6 | 20.6 |
| 285 | F | 162 | 164 | 17,300 | 27.9 | 1.9 | 24.5 | 161 | 162 | 17,400 | 27.9 | 1.9 | 26.7 |
| 286 | H | 29 | 29 | 9,700 | 27.2 | 3.5 | 25.6 | 28 | 29 | 9,600 | 27.3 | 3.3 | 23.6 |
| 287 | H | 38 | 39 | 9,700 | 27.2 | 2.8 | 29.7 | 36 | 37 | 9,600 | 27.3 | 2.8 | 23.7 |

TABLE IV.- UNYAWED-ROLLING RELAXATION-LENGTH DATA

| Run | Test series | Average values | | | | |
|-----|-------------|----------------|---|---|---|---|
| | | $\bar{p}$, lb/sq in. | $\bar{F}_z$, lb | $\bar{\delta}_o$, in. | $\bar{L}_f$, in. | $\bar{L}_\lambda$, in. |
| 288 | A | 58 | 17,000 | 3.5 | 31.6 | 23.8 |
| 289 | A | 60 | 17,000 | 3.7 | 27.0 | ---- |
| 290 | A | 60 | 17,000 | 3.7 | 23.3 | 24.8 |
| 291 | A | 62 | 17,000 | 3.7 | 24.4 | 20.3 |
| 292 | A | 62 | 17,000 | 3.7 | 23.3 | ---- |
| 293 | A | 104 | 17,000 | 2.4 | ---- | ---- |
| 294 | A | 150 | 17,000 | 2.0 | ---- | ---- |
| 295 | A | 150 | 17,000 | 2.1 | ---- | ---- |
| 296 | B | 79 | 23,700 | 3.8 | ---- | ---- |
| 297 | B | 126 | 23,700 | 2.7 | 16.4 | 21.3 |
| 298 | B | 203 | 23,700 | 2.3 | 20.4 | ---- |
| 299 | C | 130 | 32,700 | 3.7 | 25.2 | ---- |
| 300 | C | 131 | 32,700 | 3.7 | 22.9 | ---- |
| 301 | C | 173 | 32,700 | 3.1 | 23.4 | ---- |
| 302 | C | 172 | 32,700 | 3.1 | 21.9 | ---- |
| 303 | C | 231 | 32,700 | 2.6 | 25.3 | ---- |
| 304 | C | 229 | 32,700 | 2.6 | 21.0 | ---- |
| 305 | D | 126 | 39,800 | 4.2 | 14.0 | ---- |
| 306 | D | 126 | 39,800 | 4.2 | 19.5 | ---- |
| 307 | D | 150 | 39,800 | 3.6 | 19.7 | ---- |
| 308 | D | 150 | 39,800 | 3.7 | 19.5 | ---- |
| 309 | D | 232 | 39,800 | 2.8 | 22.6 | ---- |
| 310 | D | 232 | 39,800 | 2.8 | 28.3 | ---- |
| 311 | D | 232 | 39,800 | 2.8 | 24.8 | ---- |
| 312 | E | 150 | 45,200 | 4.2 | 18.8 | ---- |
| 313 | E | 150 | 45,200 | 4.2 | 18.8 | ---- |
| 314 | E | 180 | 45,200 | 3.7 | 18.3 | ---- |
| 315 | E | 180 | 45,200 | 3.8 | 17.1 | ---- |
| 316 | E | 232 | 45,200 | 3.1 | 23.2 | ---- |
| 317 | E | 232 | 45,200 | 3.1 | 18.5 | ---- |

TABLE V.- LOCKED-WHEEL DRAG TEST DATA

$$\left[\bar{F}_z = 9{,}730 \text{ lb for } \bar{F}_x = 0\right]$$

| Run | Average values | | | | $(F_z)_{tire\ A} + (F_z)_{tire\ B'}$ lb | $(F_x)_{tire\ A} + (F_x)_{tire\ B'}$ lb | Tire A | | Tire B | | Remarks |
|---|---|---|---|---|---|---|---|---|---|---|---|
| | $\bar{p}$, lb/sq in. | $\delta_o$, in. | $\bar{\mu}_x$ | $\bar{E}_x$, lb/in. | | | p, lb/sq in. | $\delta_o$, in. | p, lb/sq in. | $\delta_o$, in. | |
| 318 | 19 | 4.6 | 0.81 | 7,800 | 18,450 | 14,870 | 19 | 4.6 | 19 | 4.6 | |
| 319 | 19 | 4.9 | .84 | 7,160 | 18,410 | 15,460 | 19 | 4.7 | 19 | 5.0 | |
| 320 | 29 | 3.9 | .88 | 8,640 | 18,360 | 16,190 | 29 | 3.8 | 29 | 4.0 | |
| 321 | 29 | 3.6 | .82 | 7,700 | 18,430 | 15,070 | 29 | 3.5 | 29 | 3.7 | |
| 322 | 30 | 3.4 | .88 | 6,750 | 18,360 | 16,200 | 30 | 3.4 | 30 | 3.5 | |
| 323 | 29 | 3.7 | .88 | 7,700 | 18,360 | 16,820 | 29 | 3.6 | 29 | 3.8 | Wet concrete |
| 324 | 29 | 3.6 | .74 | 6,900 | 18,530 | 13,700 | 29 | 3.6 | 29 | 3.6 | Wet concrete |
| 325 | 29 | 3.7 | .73 | 8,100 | 18,540 | 13,500 | 29 | 3.6 | 28 | 3.8 | |
| 326 | 39 | 2.8 | .81 | 8,300 | 18,440 | 14,950 | 39 | 2.8 | 39 | 2.7 | |
| 327 | 39 | 3.4 | .90 | 8,130 | 18,340 | 16,510 | 39 | 3.3 | 39 | 3.4 | |
| 328 | 59 | 2.2 | .79 | 8,900 | 18,470 | 14,590 | 59 | 2.2 | 59 | 2.2 | |
| 329 | 59 | 2.6 | .86 | 9,590 | 18,390 | 15,730 | 59 | 2.6 | 59 | 2.6 | |
| 330 | 84 | 1.7 | .80 | 8,310 | 18,460 | 14,700 | 84 | 1.7 | 84 | 1.6 | |
| 331 | 84 | 2.1 | .85 | 8,450 | 18,400 | 15,560 | 84 | 2.1 | 84 | 2.0 | Wet concrete |
| 332 | 85 | 1.6 | .74 | 7,600 | 18,530 | 13,680 | 85 | 1.6 | 85 | 1.6 | Wet concrete |
| 333 | 84 | 1.6 | .73 | 7,770 | 18,540 | 13,570 | 84 | 1.6 | 84 | 1.7 | |
| 334 | 84 | 1.6 | .84 | 6,510 | 18,410 | 15,420 | 84 | 1.6 | 84 | 1.7 | |
| 335 | 84 | 1.7 | .89 | 8,340 | 18,350 | 16,250 | 84 | 1.7 | 84 | 1.7 | |
| 336 | 126 | 1.3 | .74 | 9,400 | 18,530 | 13,780 | 126 | 1.3 | 126 | 1.3 | |
| 337 | 126 | 1.3 | .69 | 10,250 | 18,580 | 12,900 | 126 | 1.3 | 126 | 1.3 | |
| 338 | 126 | 1.4 | .79 | 8,250 | 18,470 | 14,600 | 126 | 1.4 | 126 | 1.4 | |
| 339 | 125 | 1.6 | .80 | 8,300 | 18,460 | 14,700 | 126 | 1.7 | 126 | 1.6 | |
| 340 | 150 | 1.2 | .71 | 9,780 | 18,570 | 13,160 | 150 | 1.2 | 150 | 1.1 | |
| 341 | 150 | 1.4 | .75 | 9,100 | 18,520 | 13,840 | 150 | 1.4 | 150 | 1.4 | |
| 342 | 168 | 1.1 | .72 | 9,370 | 18,550 | 13,590 | 168 | 1.1 | 168 | 1.1 | |
| 343 | 168 | 1.3 | .73 | 7,790 | 18,540 | 13,490 | 168 | 1.3 | 168 | 1.3 | |
| 344 | 180 | 1.0 | .81 | 8,050 | 18,450 | 14,880 | 180 | 1.0 | 180 | 1.0 | |
| 345 | 180 | 1.3 | .71 | 7,770 | 18,560 | 13,260 | 180 | 1.3 | 180 | 1.3 | |
| 346 | 180 | 1.1 | .76 | 7,320 | 18,500 | 14,140 | 180 | 1.1 | 180 | 1.1 | |
| 347 | 180 | 1.1 | .64 | 7,260 | 18,650 | 11,930 | 180 | 1.1 | 180 | 1.0 | Wet concrete |
| 348 | 180 | 1.1 | .69 | 6,990 | 18,590 | 12,800 | 180 | 1.1 | 180 | 1.0 | Wet concrete |
| 349 | 202 | 1.0 | .76 | ------- | 18,500 | 14,070 | 201 | 1.1 | 202 | 1.1 | |
| 350 | 202 | 1.2 | .71 | 7,450 | 18,570 | 13,160 | 202 | 1.2 | 201 | 1.1 | |

TABLE VI.- TIRE FOOTPRINT DATA

| Run | Test series | $p_o$, lb/sq in. | $p$, lb/sq in. | $F_z$, lb | $\delta_o$, in. | $A_g$, in.$^2$ | $A_n$, in.$^2$ | $b$, in. | $2h$, in. |
|-----|-------------|------------------|----------------|-----------|-----------------|----------------|----------------|----------|-----------|
| | | | | Tire A | | | | | |
| 351 | C | 152 | 152 | ------ | 0.7 | 47 | 33 | 5.4 | 10.5 |
| 352 | C | 152 | 153 | ------ | 1.7 | 106 | 85 | 8.9 | 16.3 |
| 353 | C | 152 | 156 | 32,900 | 3.4 | 240 | 173 | 12.9 | 22.3 |
| 354 | After I | 199 | 200 | 8,620 | 1.0 | 59 | 47 | 6.7 | 11.3 |
| 355 | After I | 179 | 180 | 8,620 | 1.1 | 64 | 50 | 6.9 | 11.8 |
| 356 | After I | 168 | 170 | 8,620 | 1.2 | 66 | 51 | 7.0 | 11.7 |
| 357 | After I | 150 | 151 | 8,620 | 1.3 | 74 | 61 | 7.8 | 12.4 |
| 358 | After I | 59 | 59 | 8,620 | 2.0 | 127 | 94 | 9.6 | 15.3 |
| 359 | After I | 18 | 19 | 8,620 | 3.7 | 274 | 190 | 13.2 | 23.4 |
| | | | | Tire B | | | | | |
| 360 | C | 180 | 180 | ------ | 1.1 | 81 | 53 | 7.2 | 13.0 |
| 361 | C | 180 | 180 | ------ | 1.8 | 130 | 84 | 9.2 | 16.5 |
| 362 | C | 180 | 182 | 32,500 | 2.8 | 207 | 135 | 11.9 | 20.4 |
| 363 | C | 135 | 135 | ------ | 1.0 | 50 | 29 | 5.6 | 10.1 |
| 364 | C | 135 | 136 | ------ | 1.9 | 116 | 73 | 8.7 | 15.5 |
| 365 | C | 135 | 137 | ------ | 2.8 | 186 | 120 | 11.6 | 19.1 |
| 366 | C | 135 | 138 | 32,500 | 3.8 | 248 | 166 | 12.8 | 22.2 |
| 367 | After I | 200 | 200 | 8,560 | 1.0 | 60 | 43 | 6.7 | 11.3 |
| 368 | After I | 200 | 200 | 8,560 | 1.0 | 58 | 42 | 6.6 | 11.4 |
| 369 | After I | 180 | 181 | 8,560 | 1.2 | 61 | 44 | 6.8 | 11.5 |
| 370 | After I | 166 | 167 | 8,560 | 1.1 | 65 | 48 | 6.9 | 12.0 |
| 371 | After I | 150 | 151 | 8,560 | 1.3 | 69 | 49 | 7.0 | 11.9 |
| 372 | After I | 150 | 151 | 8,560 | 1.3 | 69 | 48 | 6.9 | 12.1 |
| 373 | After I | 126 | 127 | 8,560 | 1.3 | 77 | 55 | 7.2 | 12.7 |
| 374 | After I | 83 | 84 | 8,560 | 1.6 | 104 | 70 | 8.9 | 14.4 |
| 375 | After I | 83 | 85 | 8,560 | 1.7 | 108 | 68 | 9.0 | 14.4 |
| 376 | After I | 83 | 85 | 8,560 | 1.7 | 111 | 75 | 9.1 | 14.9 |
| 377 | After I | 57 | 58 | 8,560 | 1.9 | 139 | 94 | 10.0 | 16.5 |
| 378 | After I | 37 | 39 | 8,560 | 2.6 | 190 | 119 | 11.6 | 18.7 |
| 379 | After I | 28 | 29 | 8,560 | 3.1 | 221 | 137 | 11.8 | 20.6 |
| 380 | After I | 17 | 19 | 8,560 | 4.0 | 304 | 193 | 13.7 | 24.3 |
| 381 | After I | --- | 19 | 8,560 | --- | 319 | 221 | 13.9 | 24.7 |
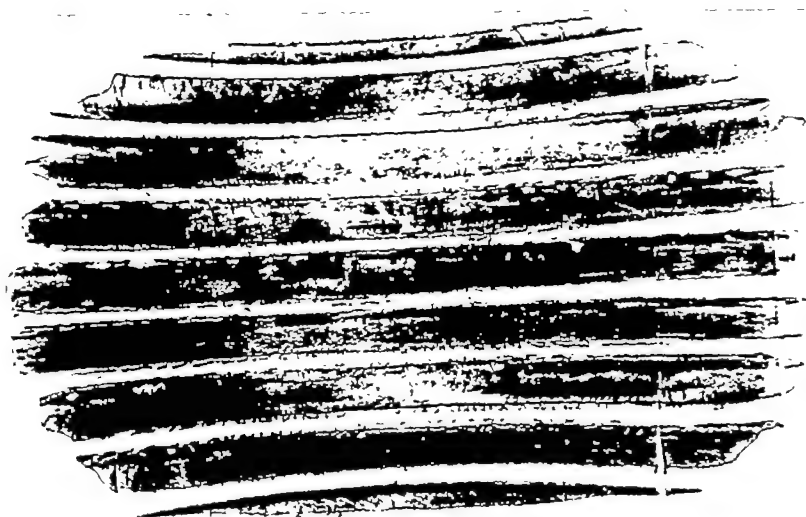
(a) Run 359; $\delta_0$ = 3.7 inches; p = 19 pounds per square inch.

(b) Run 358; $\delta_0$ = 2.0 inches; p = 59 pounds per square inch.
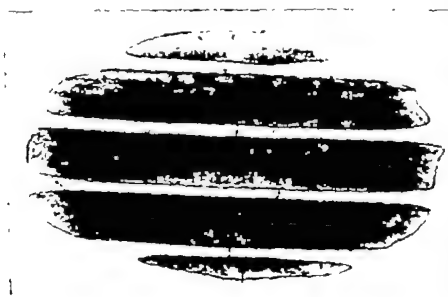
L-84904

(c) Run 356; $\delta_0$ = 1.2 inches; p = 170 pounds per square inch.

Figure 1.- Typical tire footprints for tire A at $F_Z$ = 8,620 pounds.
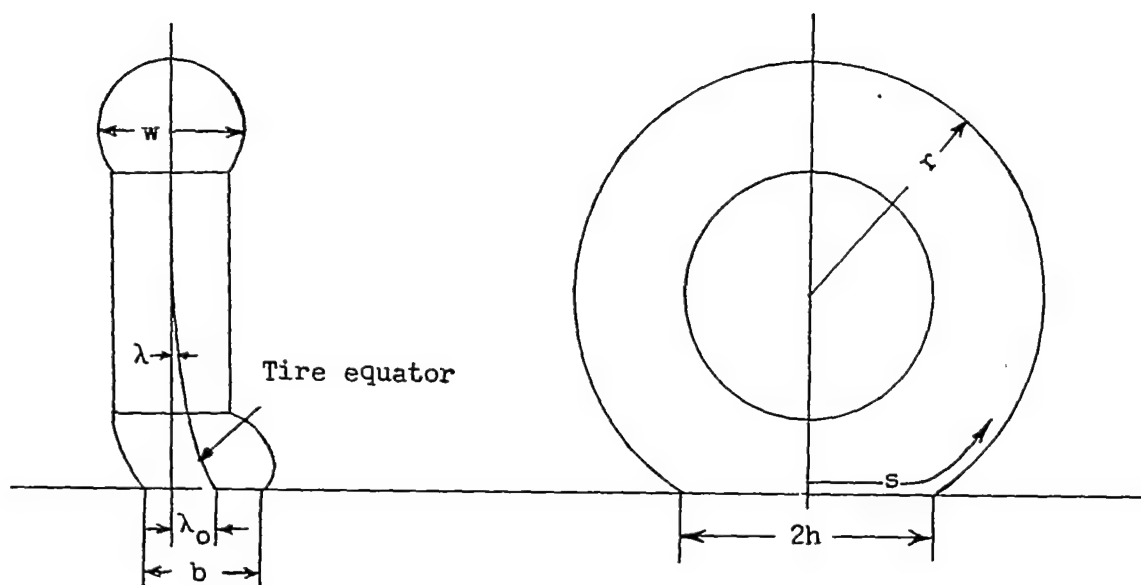
(a) Tire dimensions.
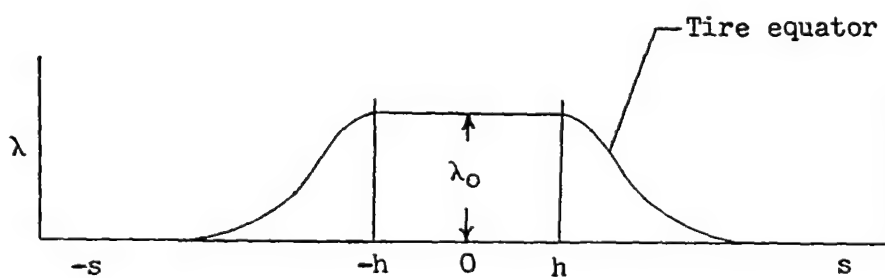


(b) Shape of distortion curve.

Figure 2.- Tire dimensions and tire distortion.

Concrete weight cans
Weight per can = 8,000 lb
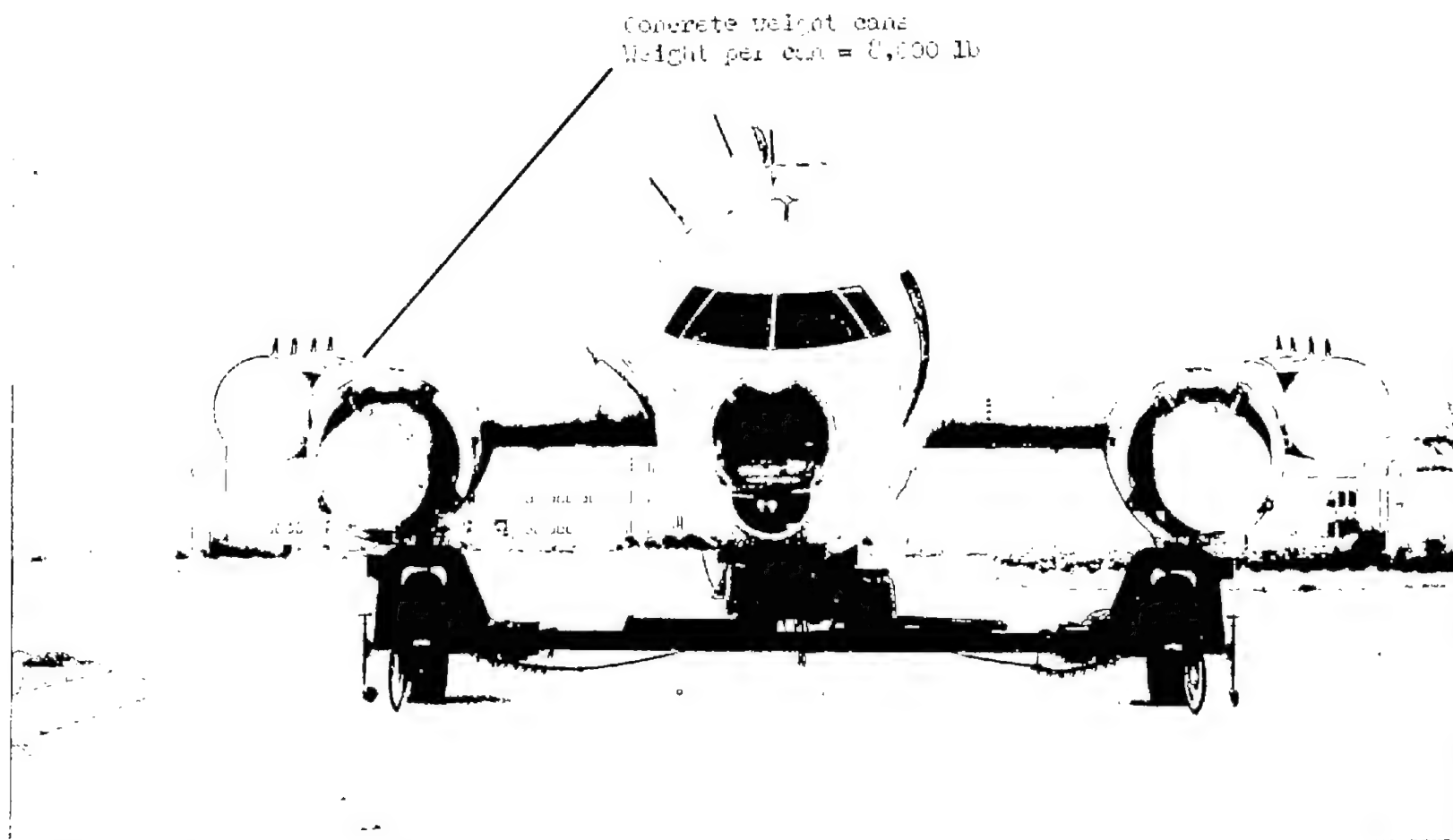
L-79570.1

(a) End view.

Figure 3.- Test vehicle.
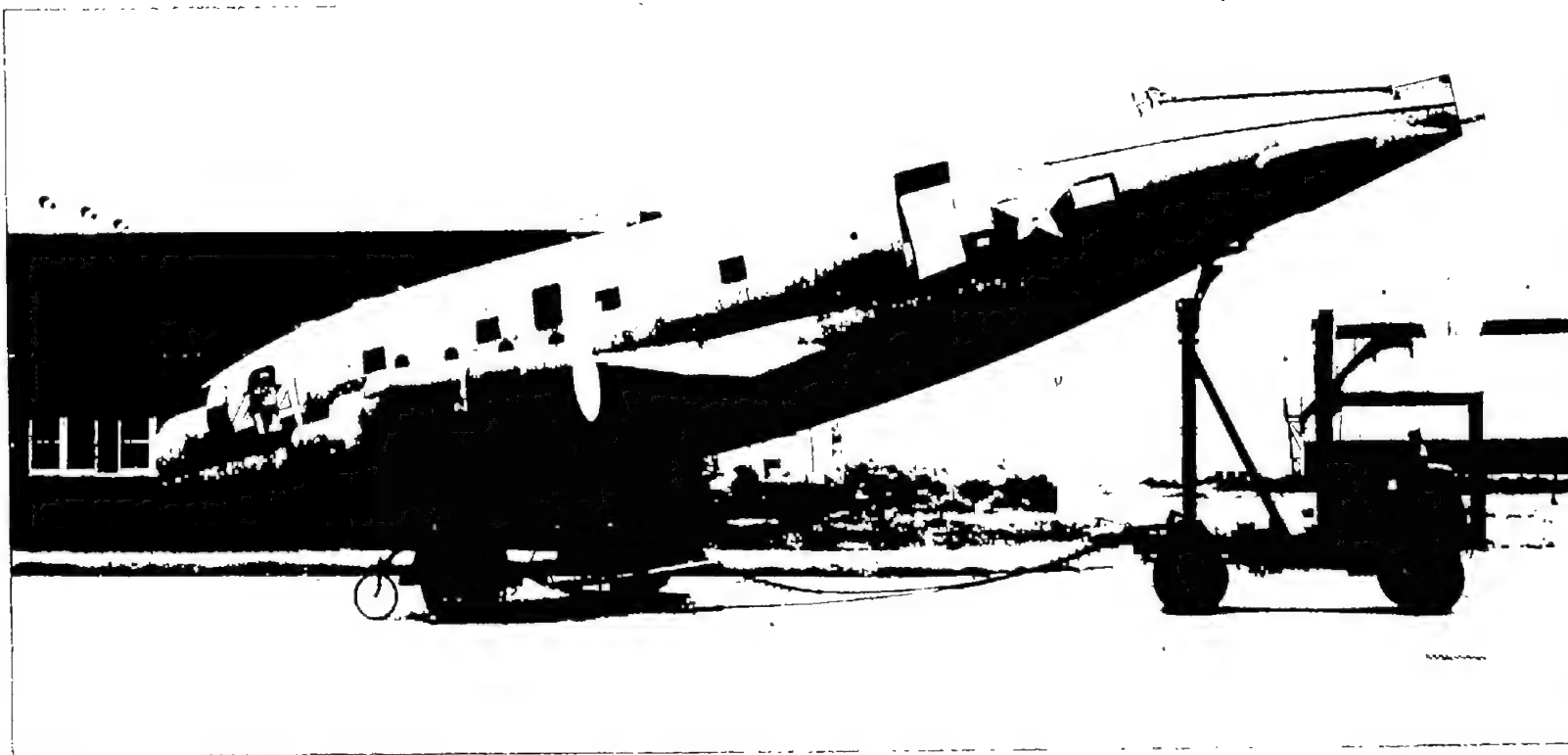
(b) Side view.

L-79571

Figure 3.- Concluded.

Slide wire

Wheel and strut assembly

Circular slide wire

Starting point
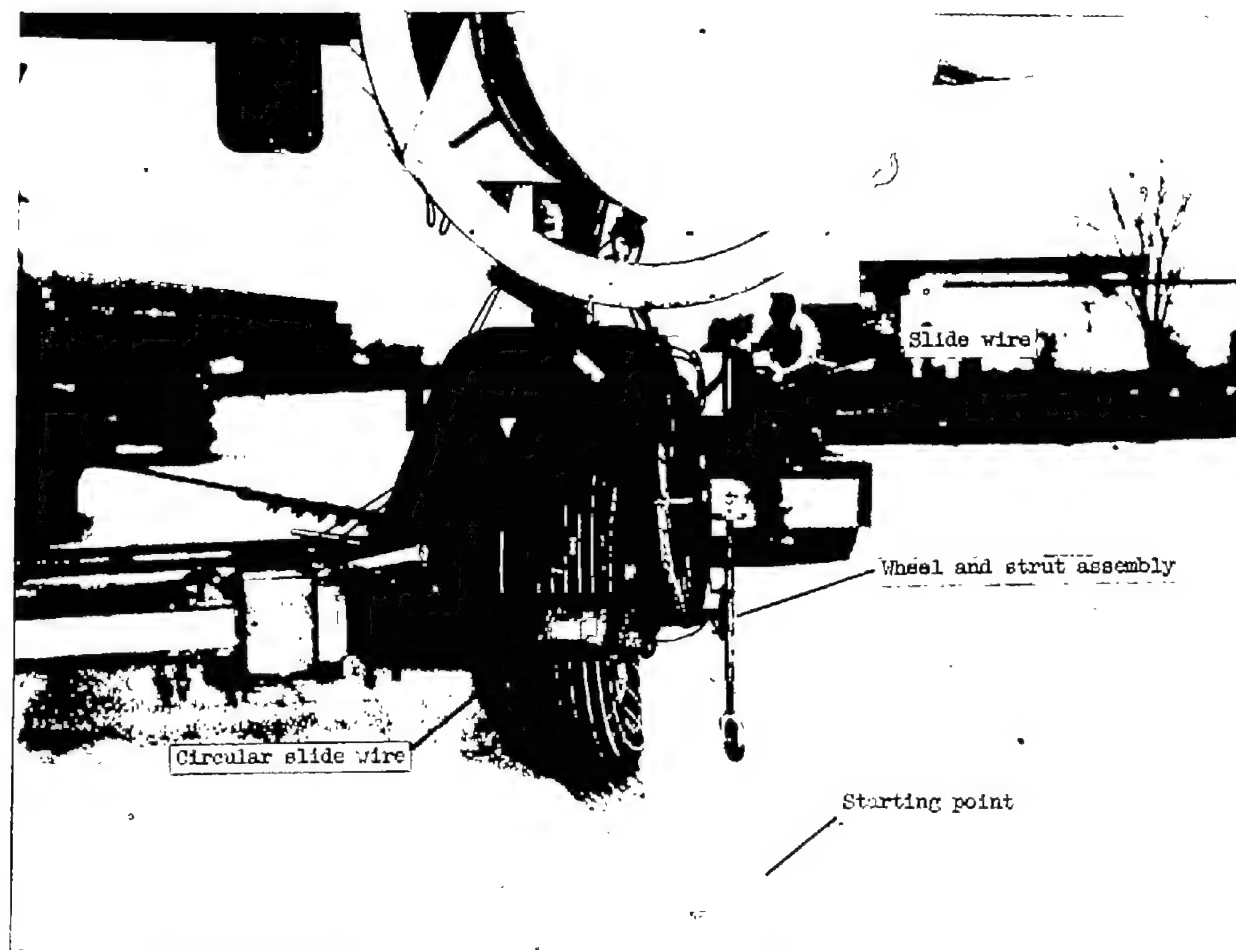
L-79491.1

(a) Rear view.

Figure 4.- Tire A under yawed rolling at $\psi = 17.9^\circ$.

Bicycle wheel

Starting point
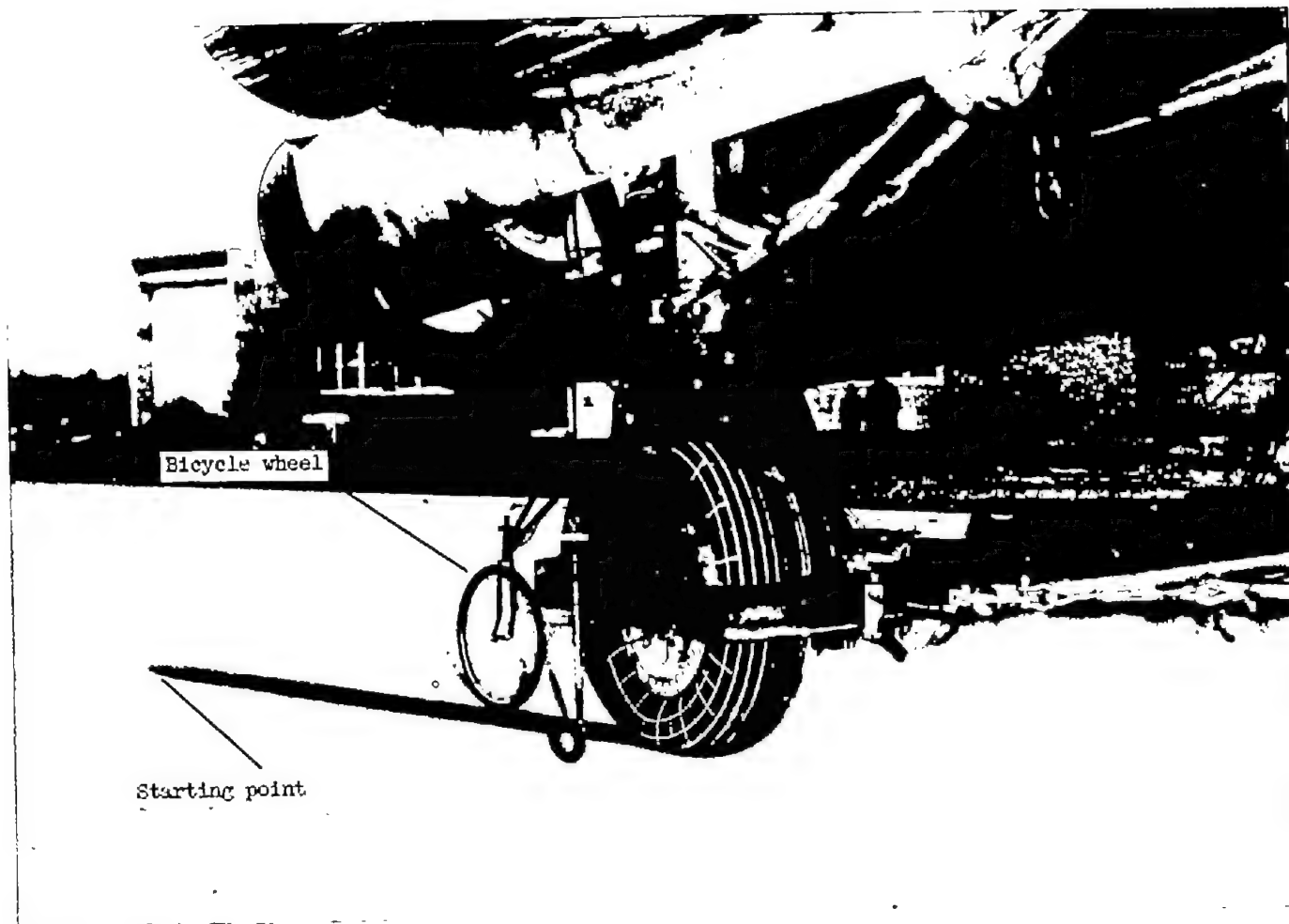
(b) Side view.

L-79492.1

Figure 4.- Continued.

Starting point
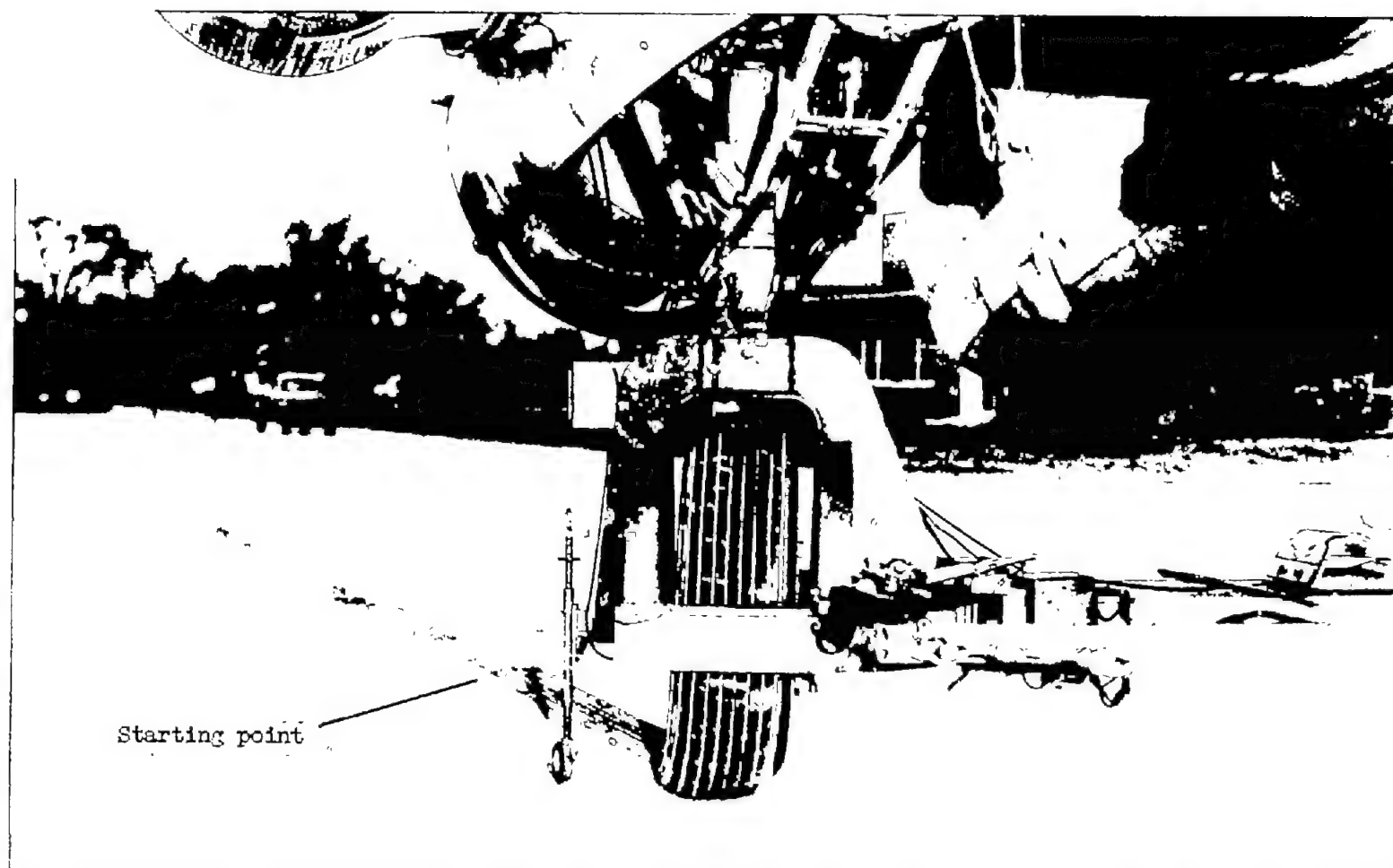
(c) Front view.

L-79493.1

Figure 4.- Concluded.
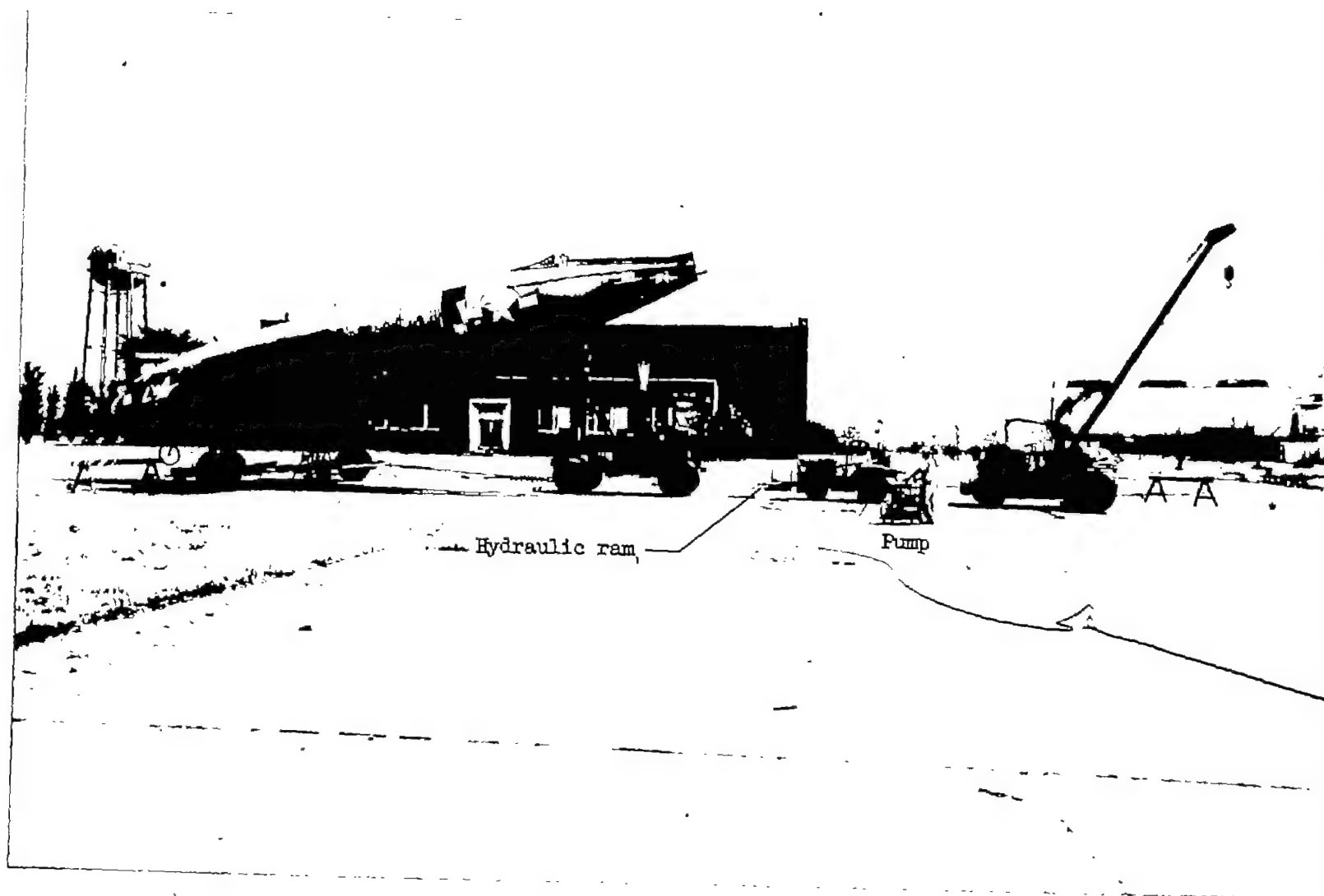
Figure 5.- Locked-wheel drag-test setup.

L-80727.1

(a) Initial-force-buildup
stage of run.

(b) Steady-state stage of run.
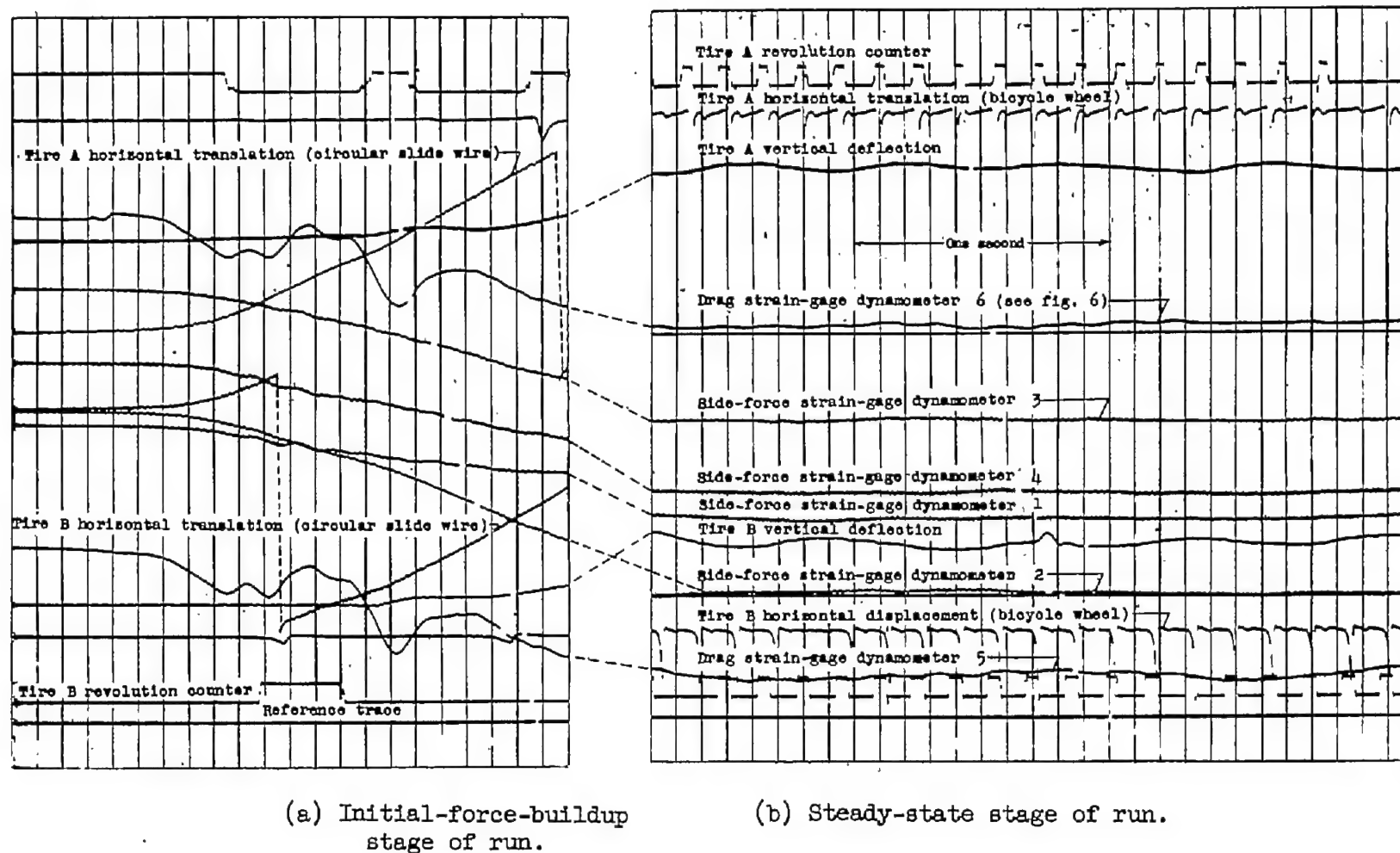
Figure 6.- Typical oscillograph record. Run 47; p = 81 pounds per square
inch; $\delta_0$ = 3.9 inches; $\psi$ = 17.9°.
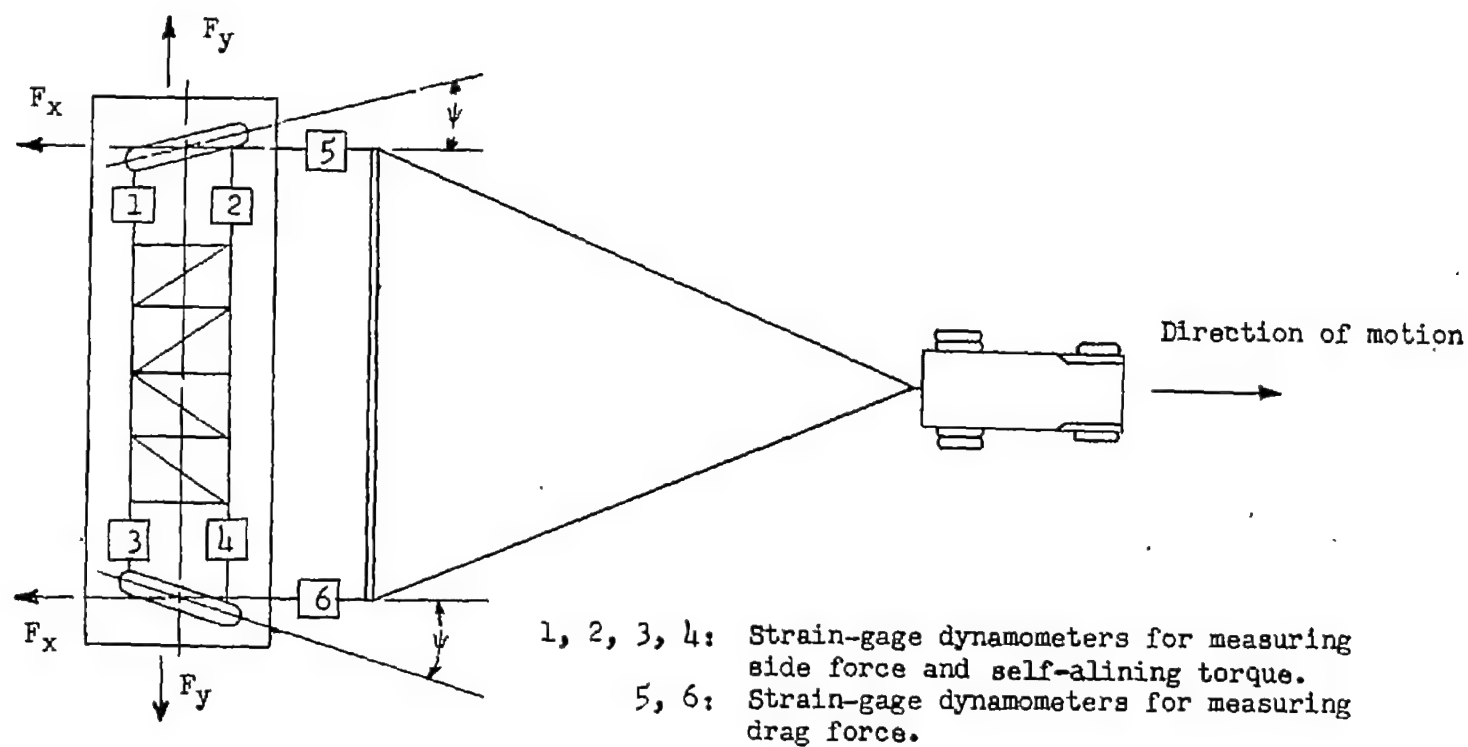
Figure 7.- Strain-gage dynamometer location.

1, 2, 3, 4:  Strain-gage dynamometers for measuring
            side force and self-alining torque.
5, 6:       Strain-gage dynamometers for measuring
            drag force.
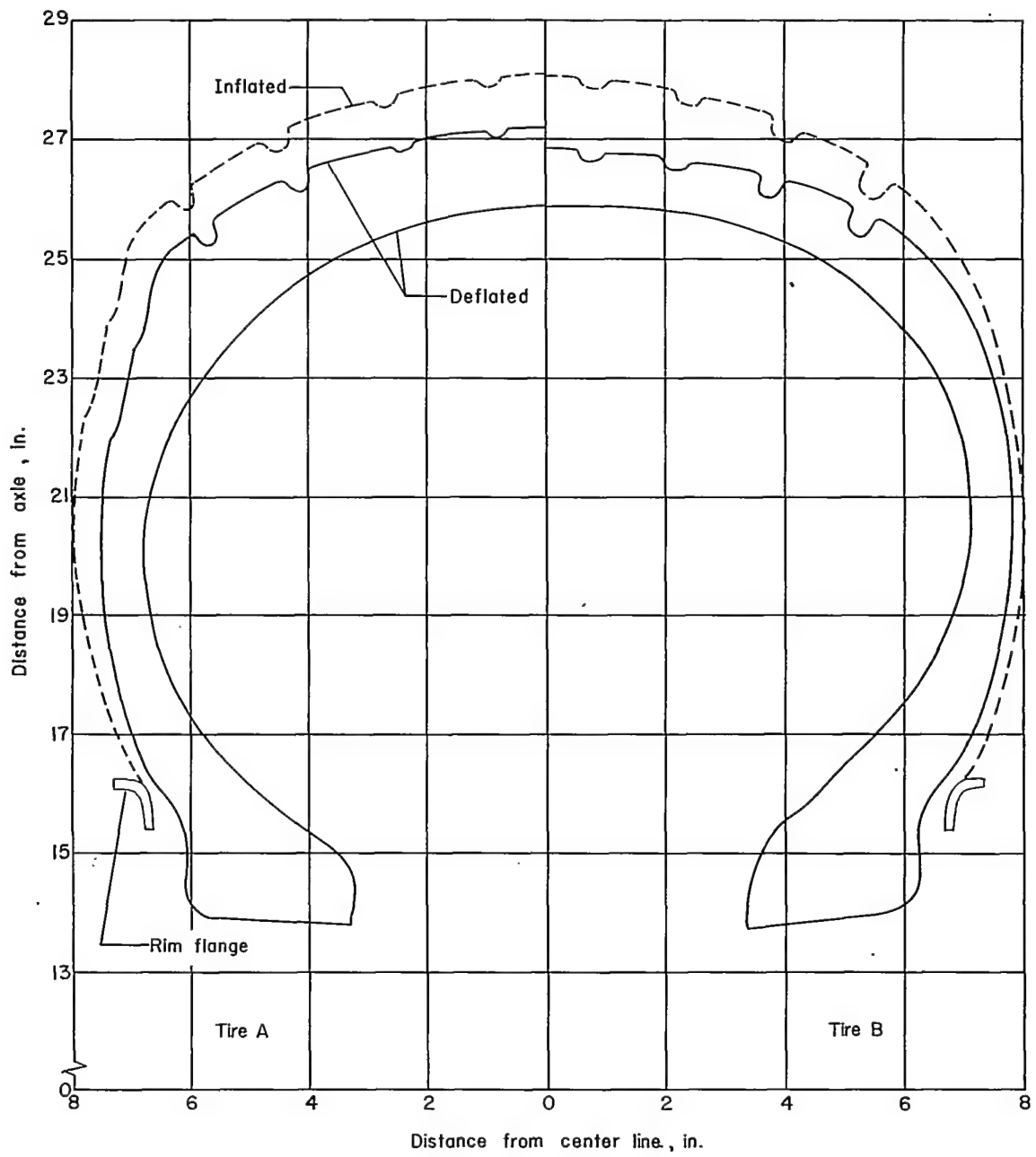
Figure 8.- Tire profiles.
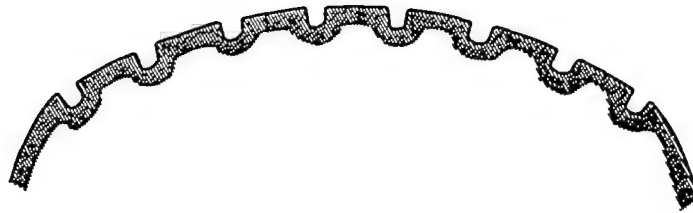
(a) Approximate tread shape of tires A and B
at beginning of test.
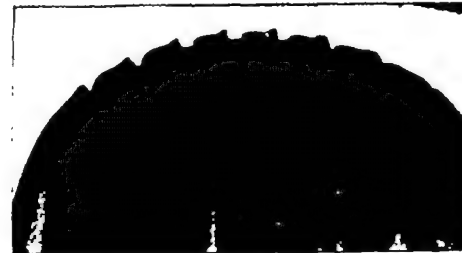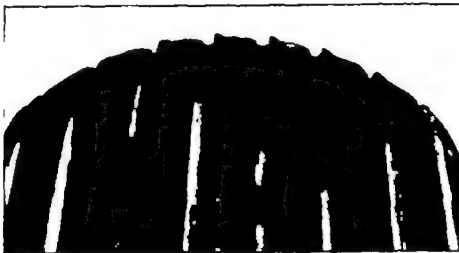


(b) At conclusion of test series C.
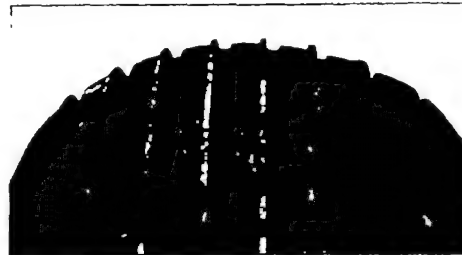


(c) At conclusion of test series F.



(d) At conclusion of test series I.

Tire A                                                    Tire B

L-84905

Figure 9.- Tire wear.
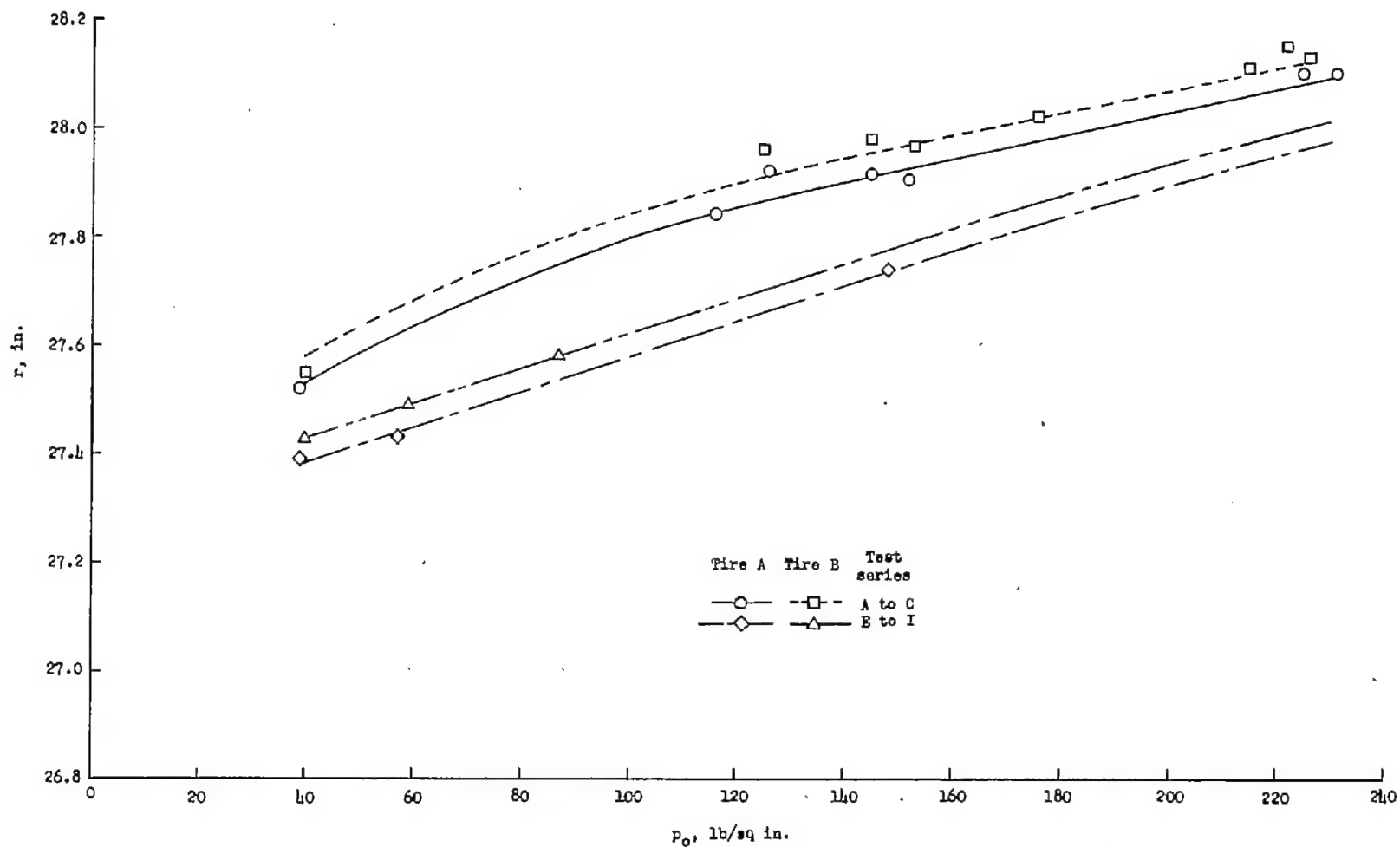
Figure 10.- Variation of unloaded tire radius with inflation pressure and tire wear. Data shown are at equilibrium and were measured after 24 hours at constant pressure.
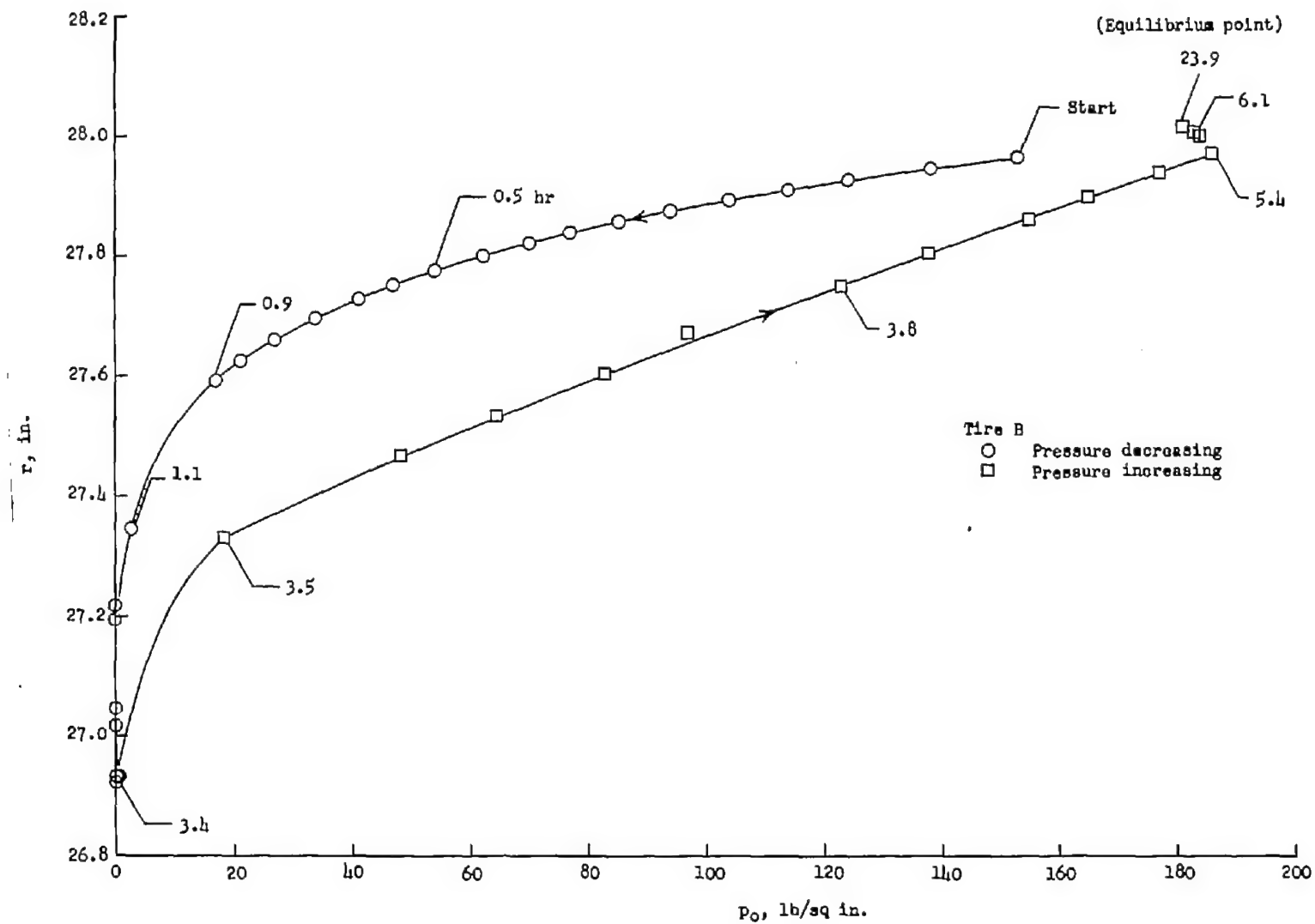
Figure 11.- Radius-pressure hysteresis loop for tire B (unloaded).
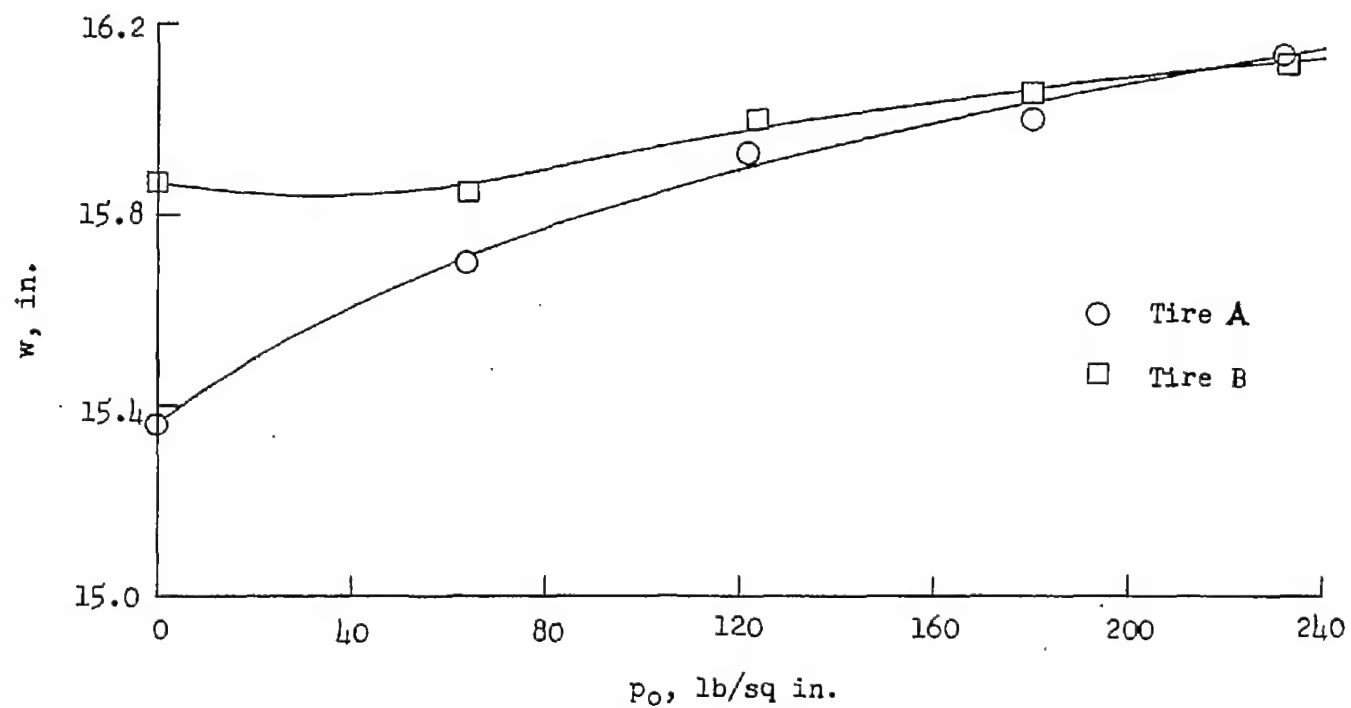
Figure 12.- Variation of maximum tire width with inflation pressure.
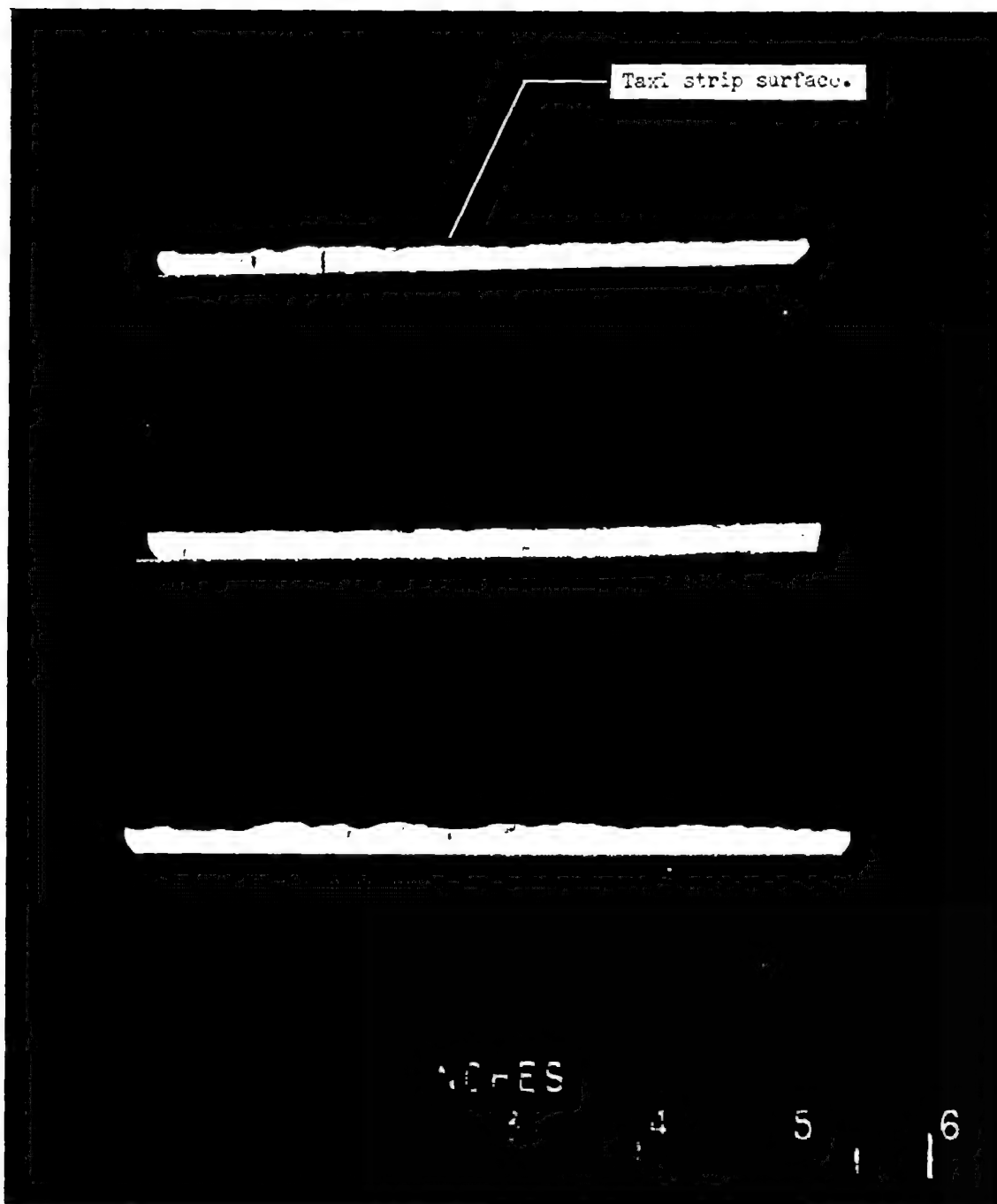
Taxi strip surface.

L-84422.1

Figure 13.- Representative samples of concrete-taxi-strip surface roughness.
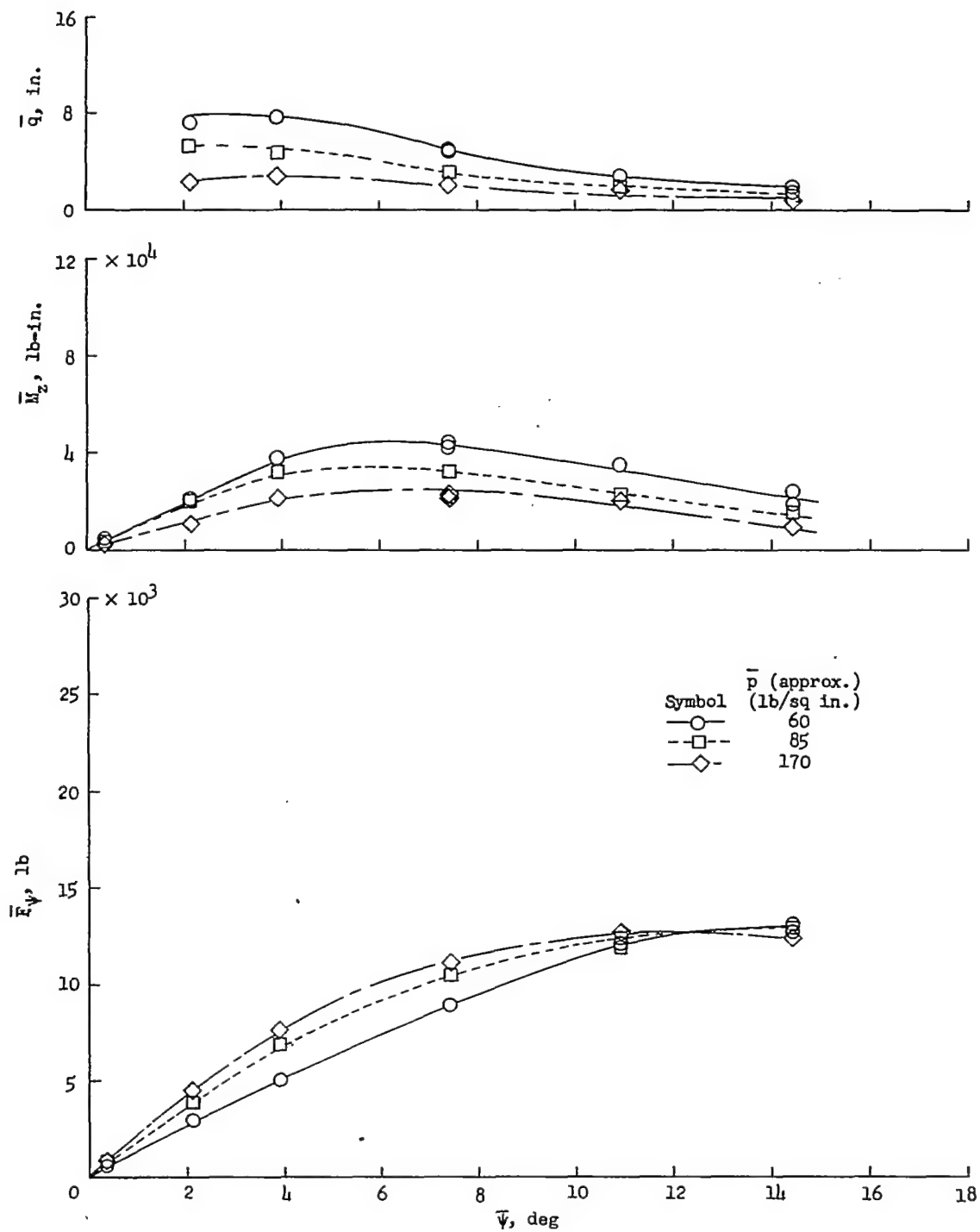
(a) Test series A; $\bar{F}_z$ = 17,000 pounds.

Figure 14.- Variation of normal force, self-alining torque, and pneumatic
caster with yaw angle for the different vertical loads and inflation
pressures investigated.
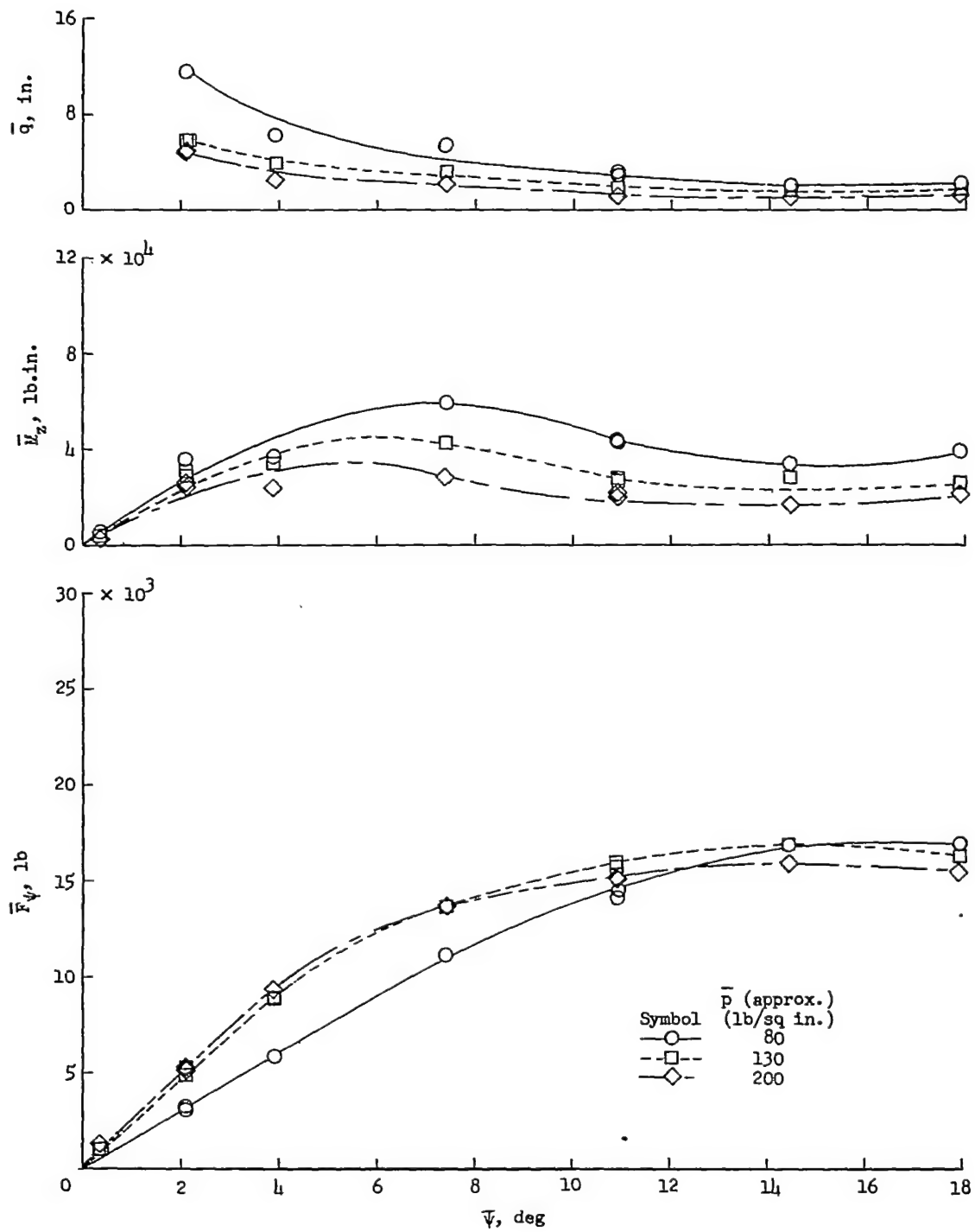
(b) Test series B; $\bar{F}_z = 23,700$ pounds.

Figure 14.- Continued.
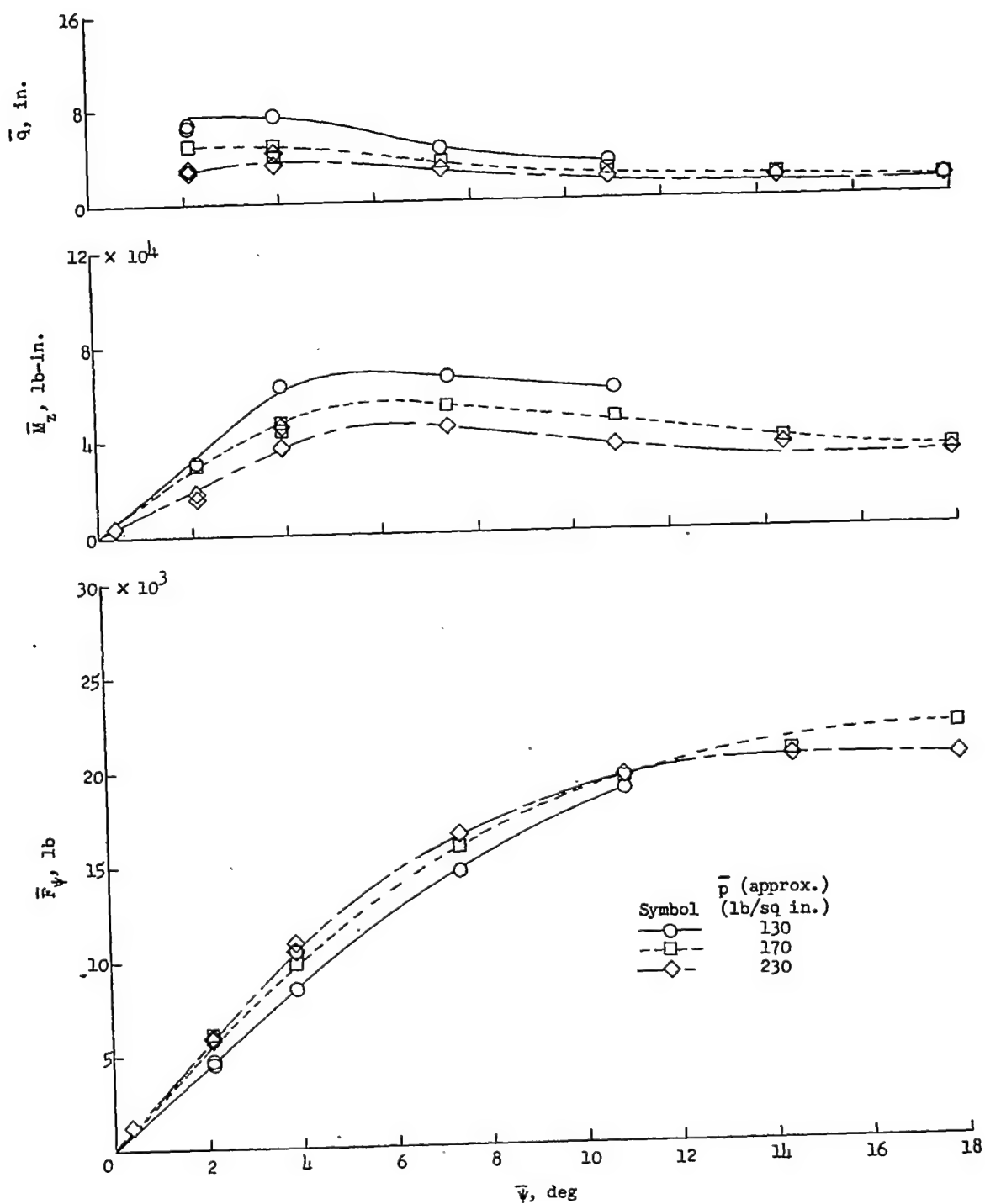
(c) Test series C; $\bar{F}_z = 32,700$ pounds.

Figure 14.- Continued.
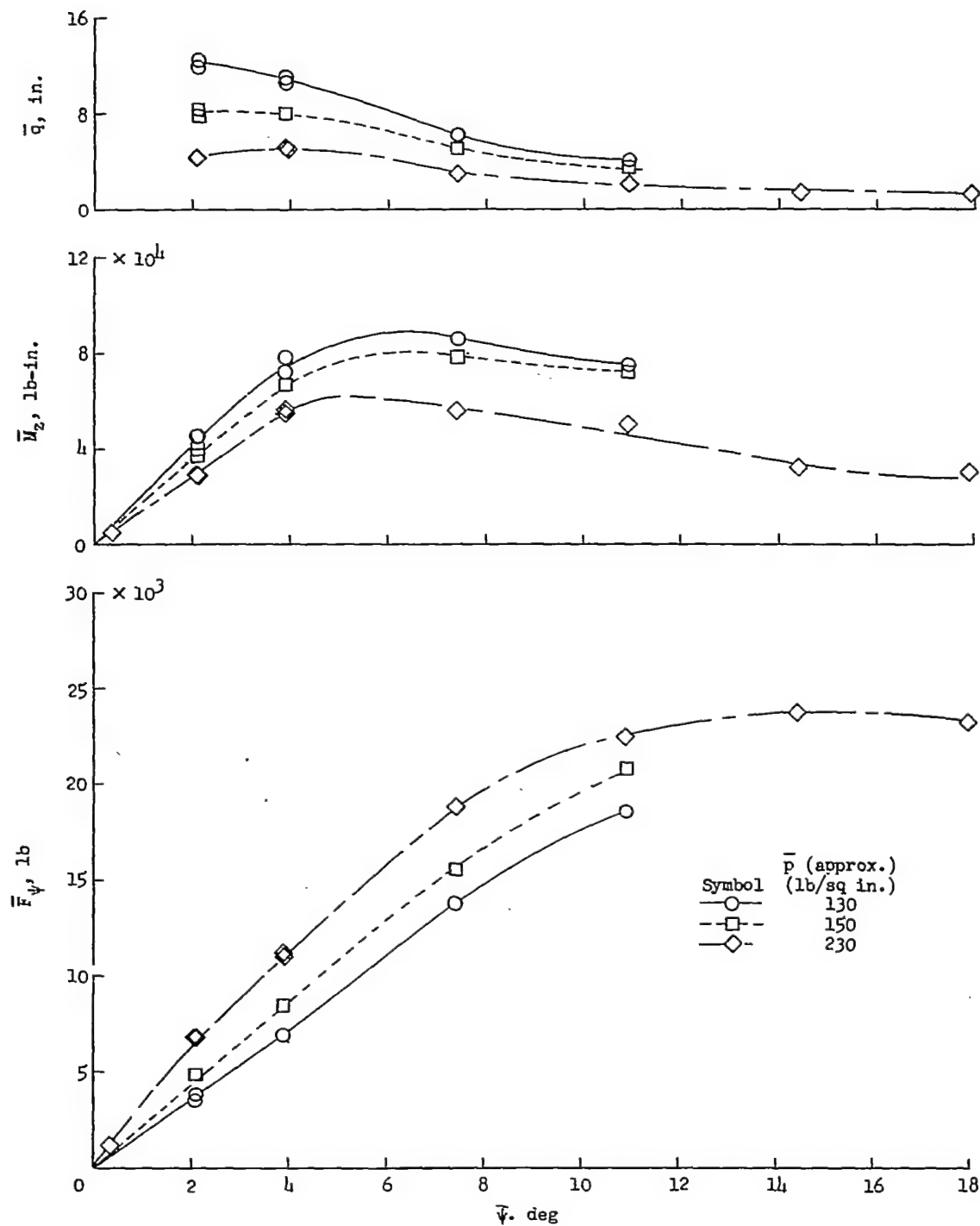
(d) Test series D; $\bar{F}_z = 39,800$ pounds.

Figure 14.- Continued.
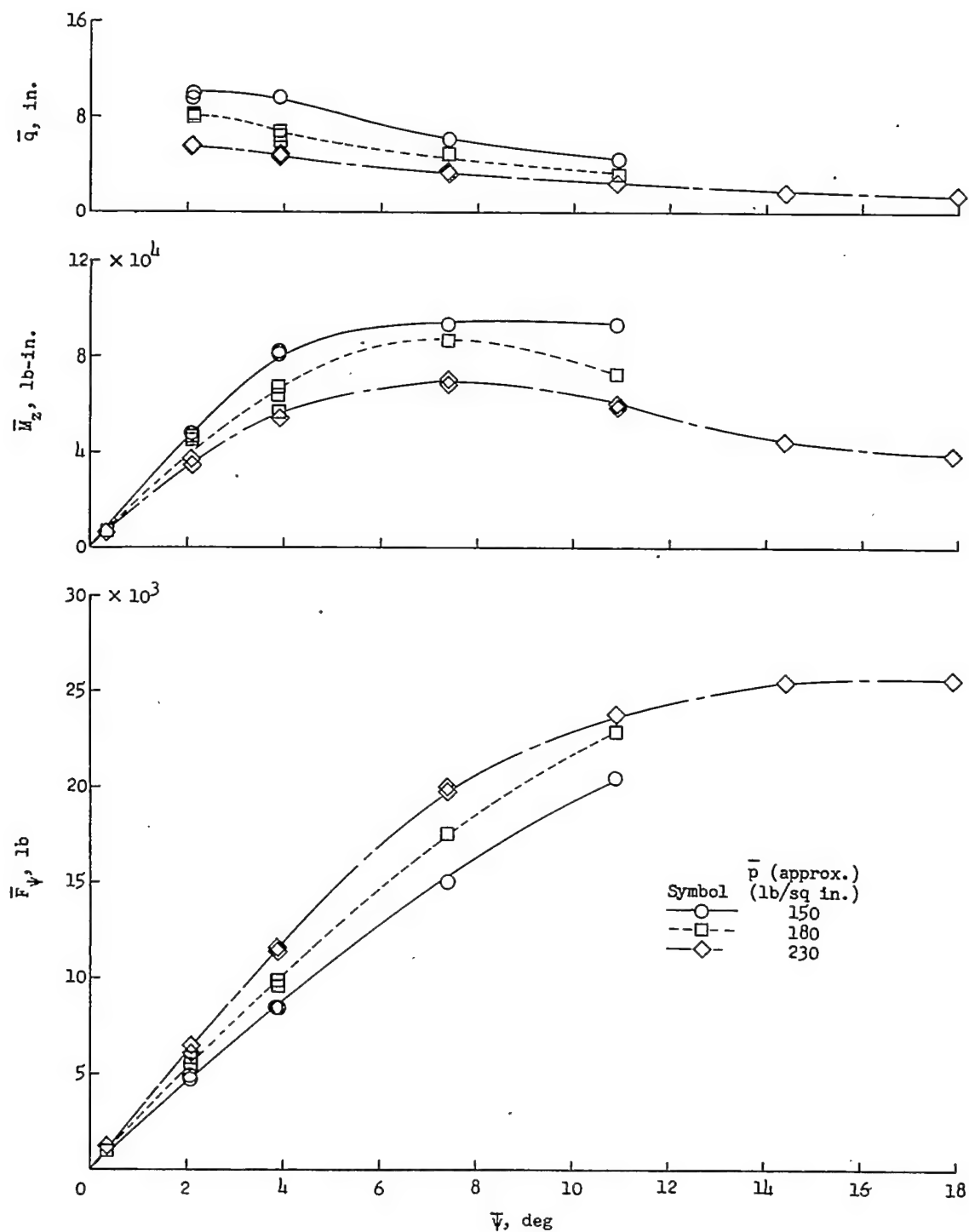
(e) Test series E; $\bar{F}_Z = 45,200$ pounds.

Figure 14.- Continued.
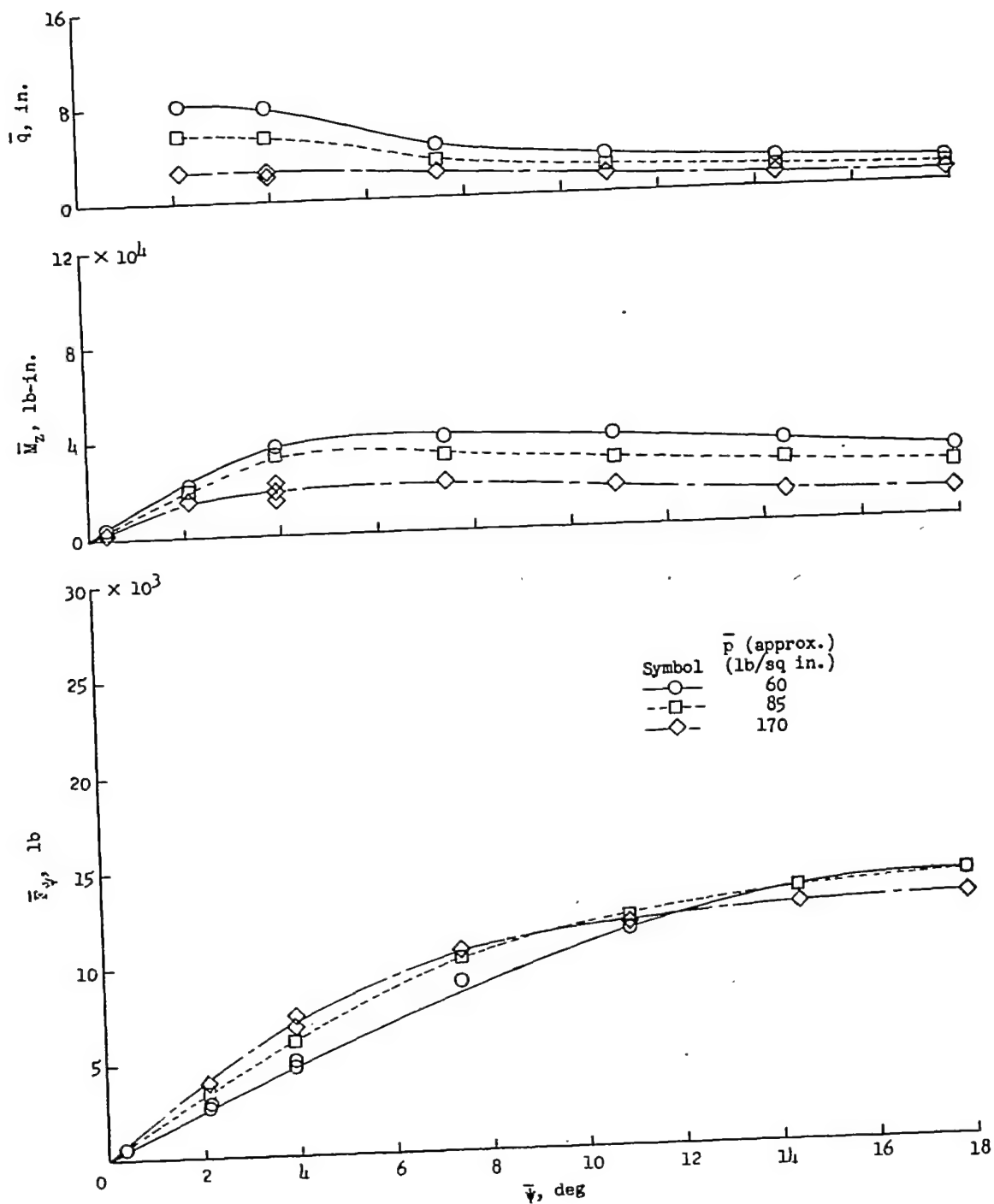
(f) Test series F; $\bar{F}_z = 17,400$ pounds.

Figure 14.- Continued.
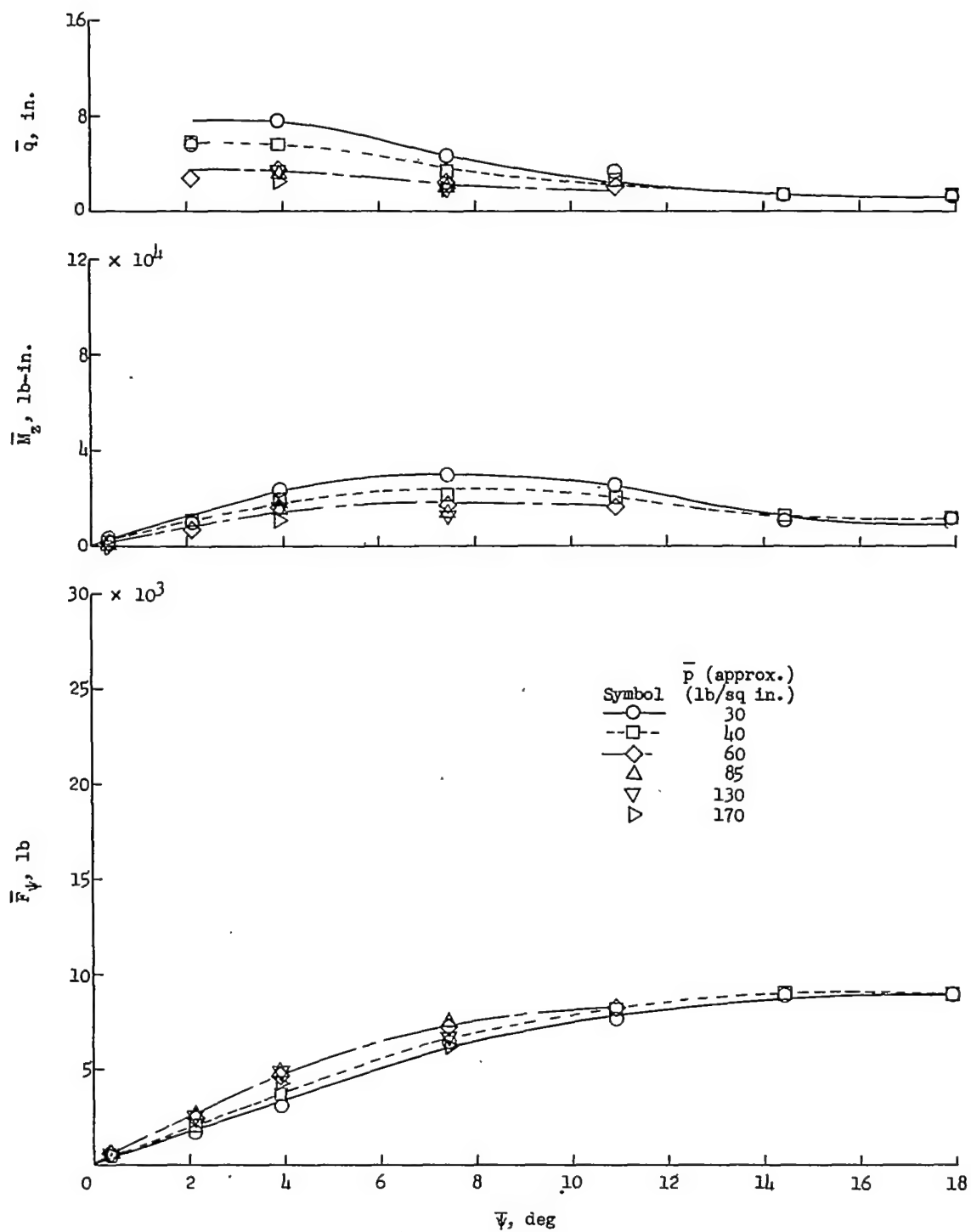
(g) Test series G; $\bar{F}_z = 9,600$ pounds.

Figure 14.- Continued.
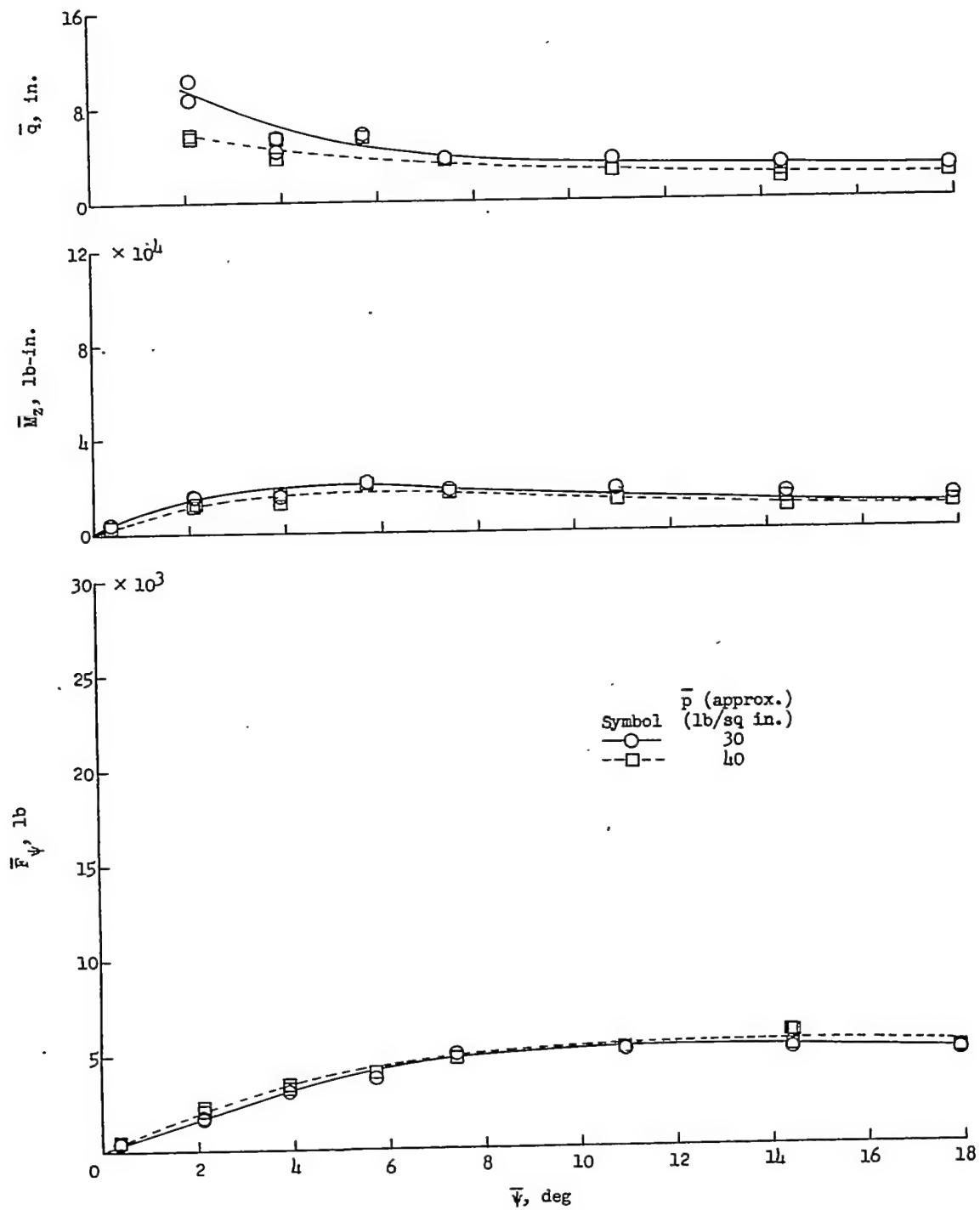
(h) Test series H; $\bar{F}_Z \doteq 9,600$ pounds.

Figure 14.- Continued.
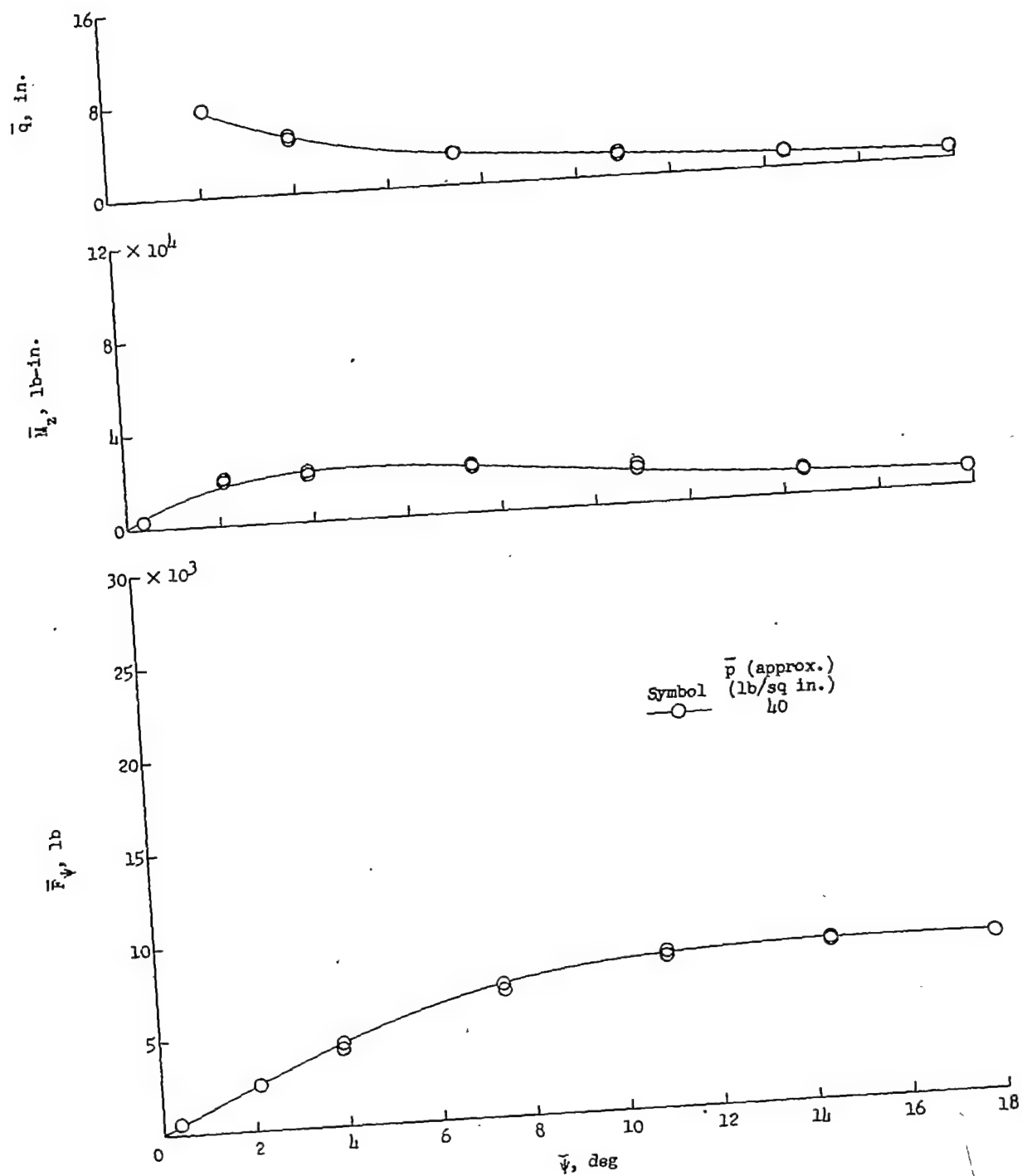
(i) Test series I; $\bar{F}_z = 9{,}600$ pounds.

Figure 14.- Concluded.
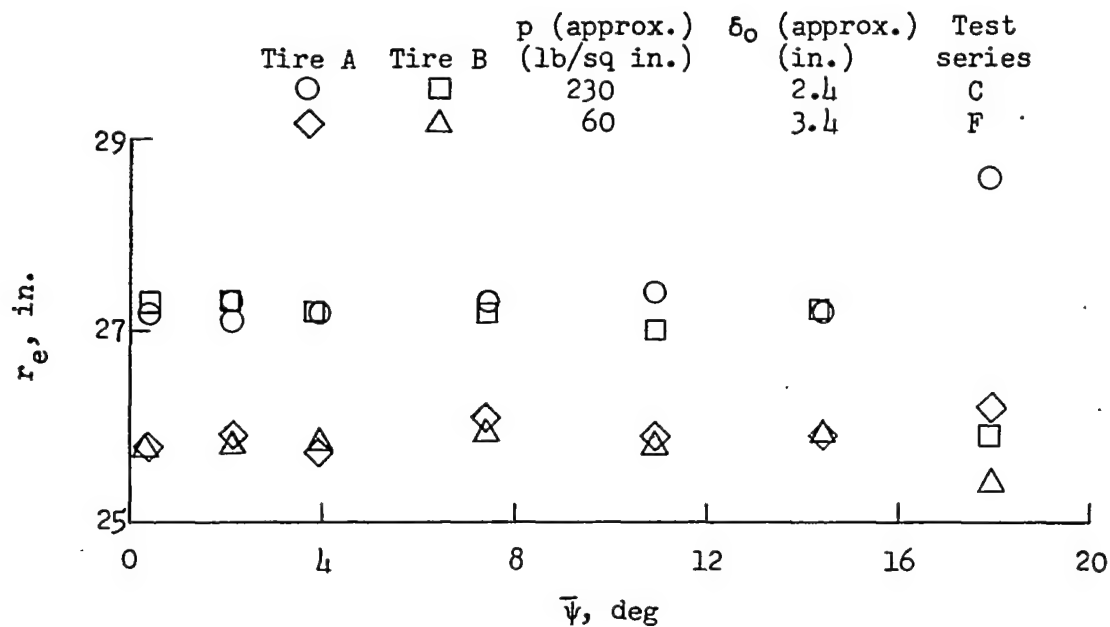
(a) Variation of rolling radius with yaw angle.
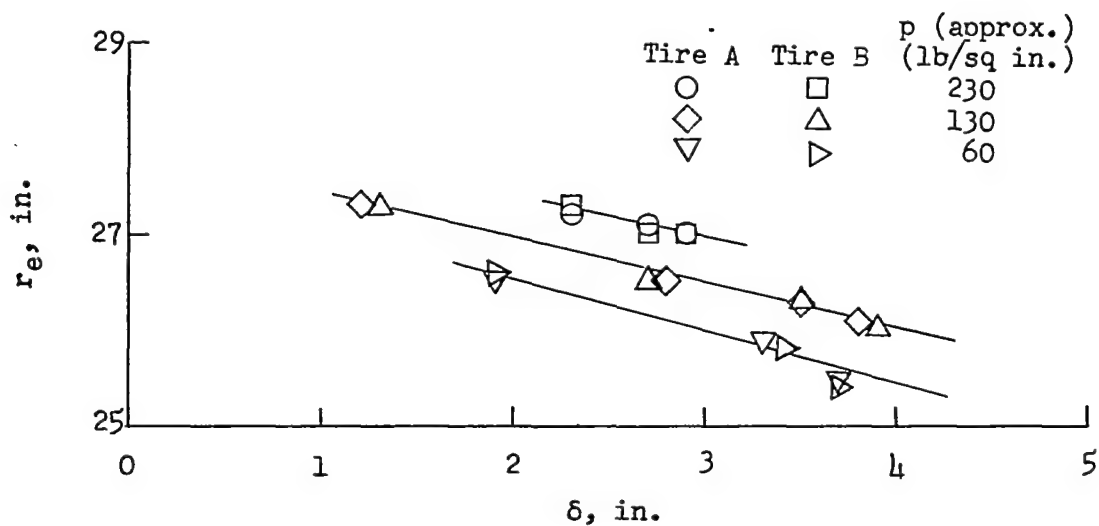


(b) Variation of rolling radius with vertical tire deflection
($\psi = 0.35°$ and $2.1°$).

Figure 15.- Variation of rolling radius with yaw angle and vertical
tire deflection.
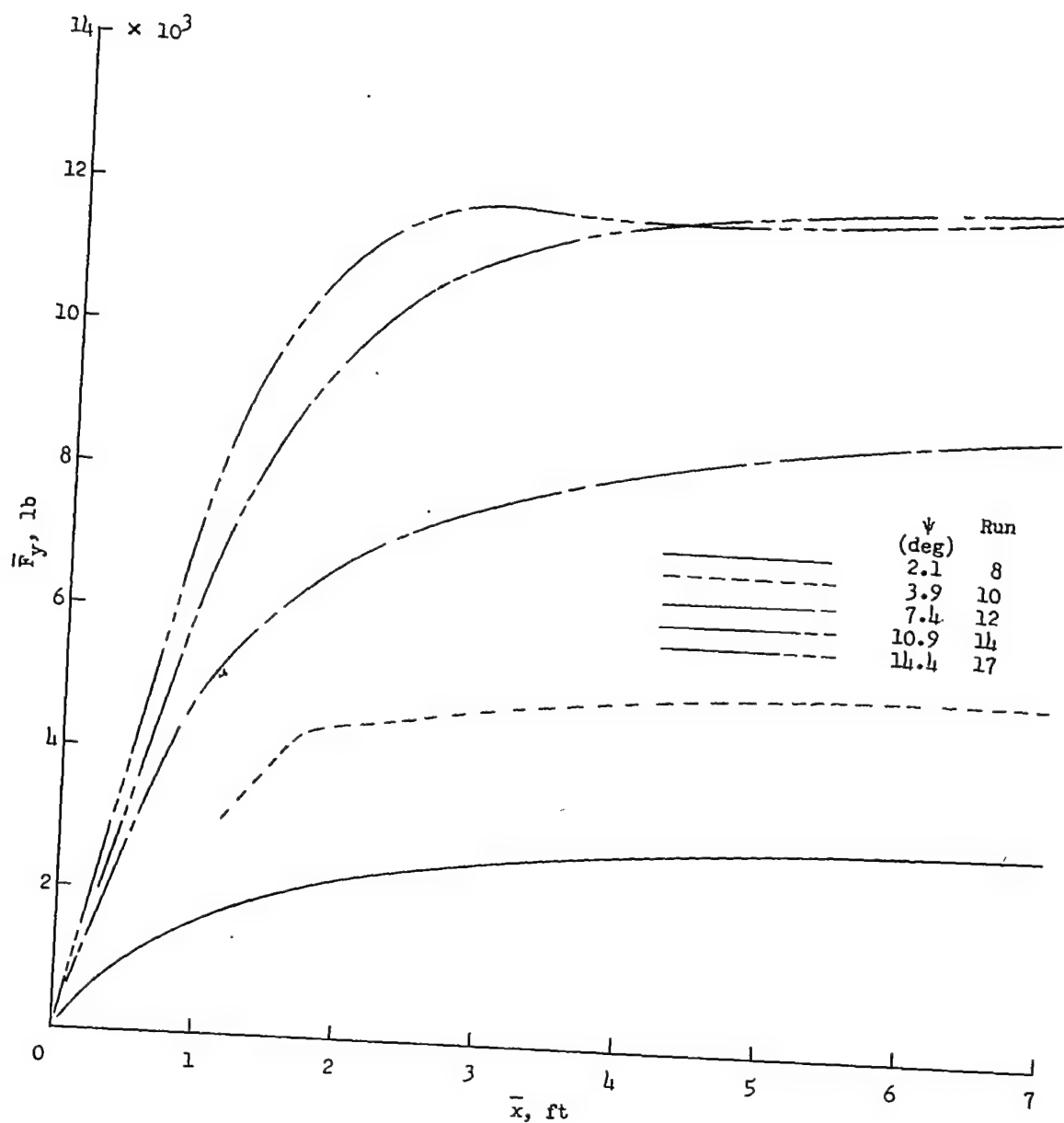
(a) Test series A: $\bar{F}_z = 17,000$ pounds; $\tilde{p} \approx 60$ pounds per square inch; $\delta_0 \approx 3.7$ inches.

Figure 16.- Buildup of cornering force with distance rolled for some typical runs at several pressures and for three test series.
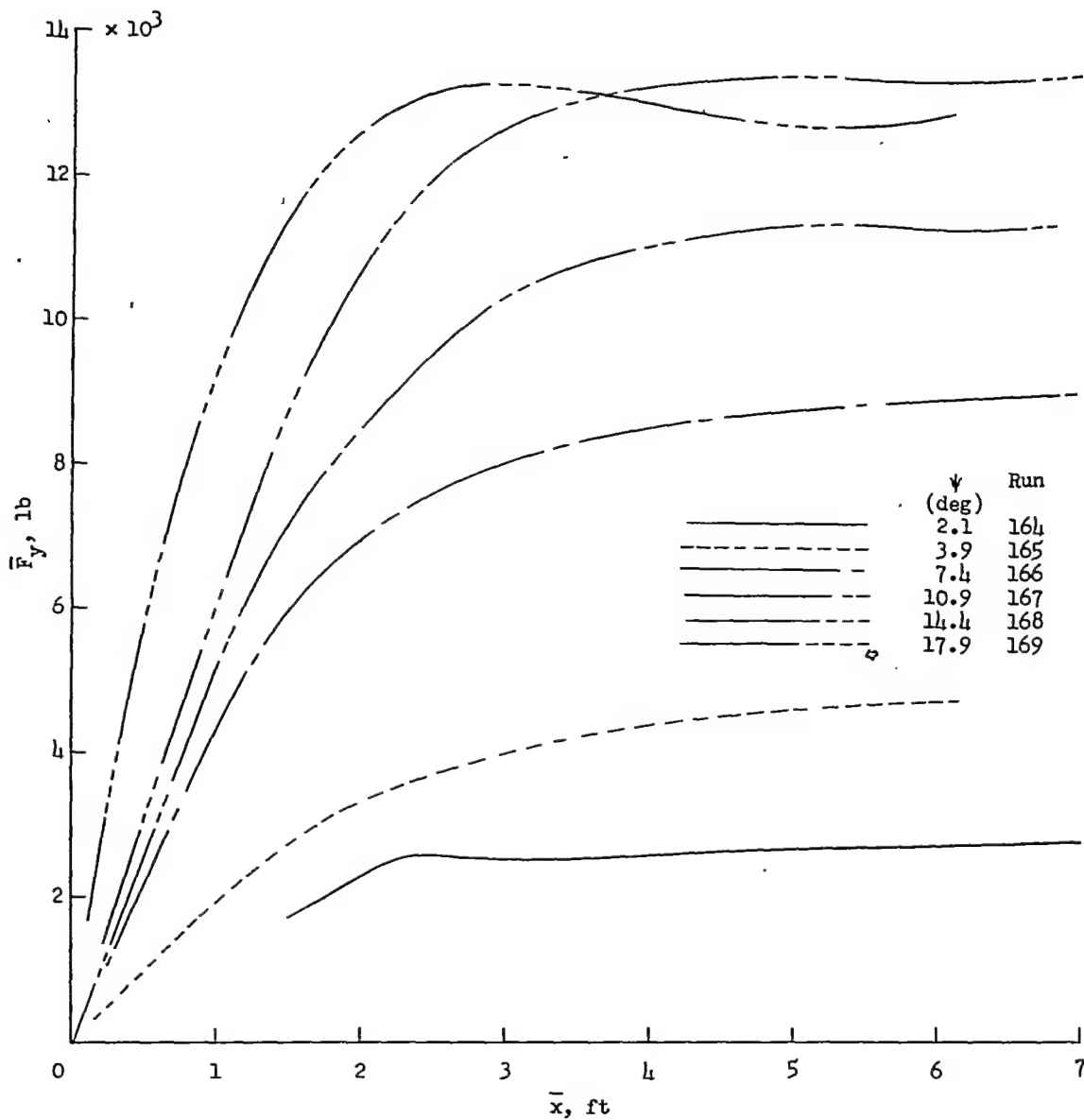
(b) Test series F:  $\bar{F}_z = 17,400$ pounds;  $\bar{p} \approx 60$ pounds per square inch;
$\bar{\delta}_o \approx 3.5$ inches.

Figure 16.- Continued.
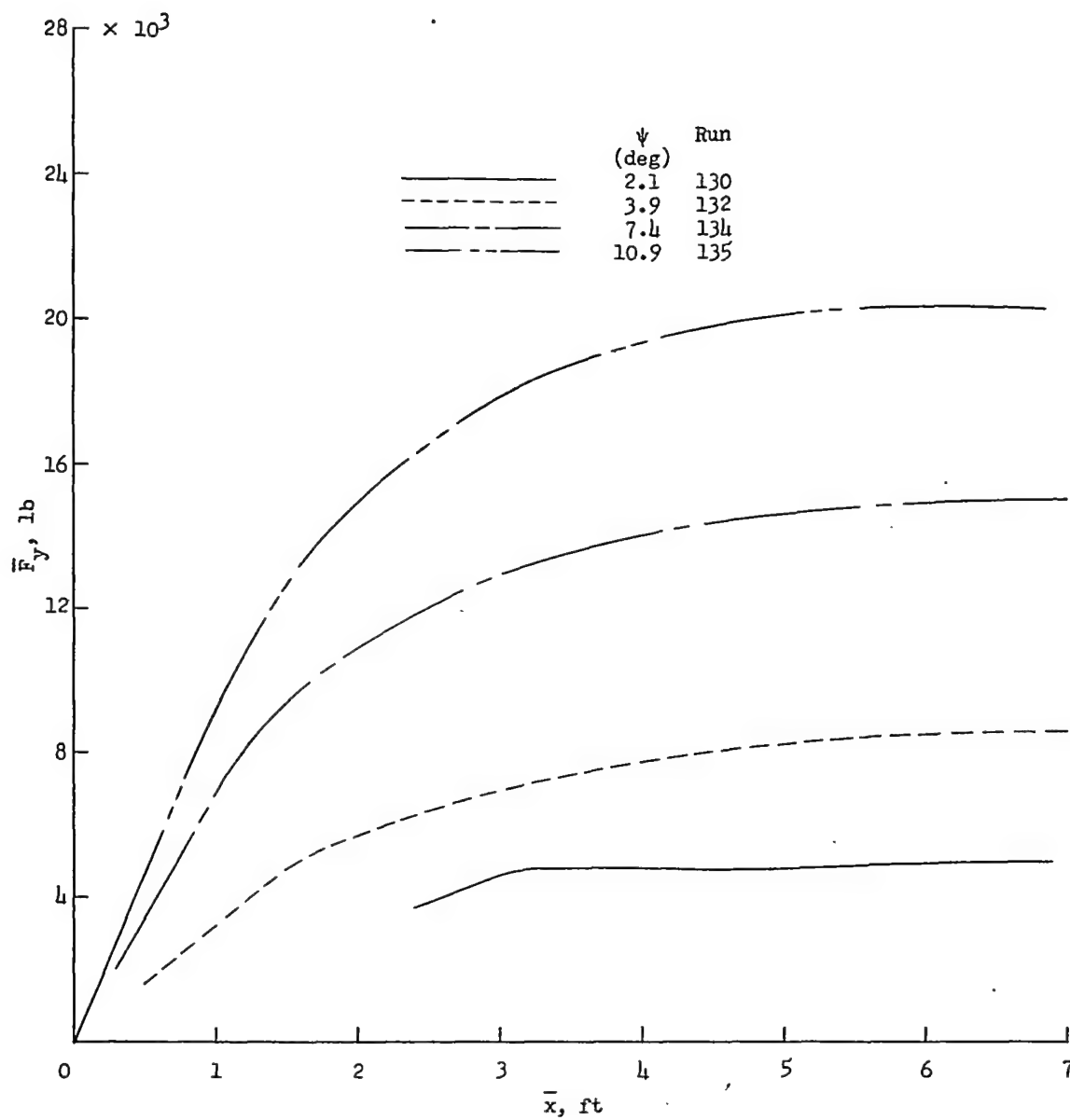
(c) Test series E: $\bar{F}_z = 45,200$ pounds; $\bar{p} \approx 150$ pounds per square inch; $\bar{\delta}_o \approx 4.1$ inches.

Figure 16.- Continued.
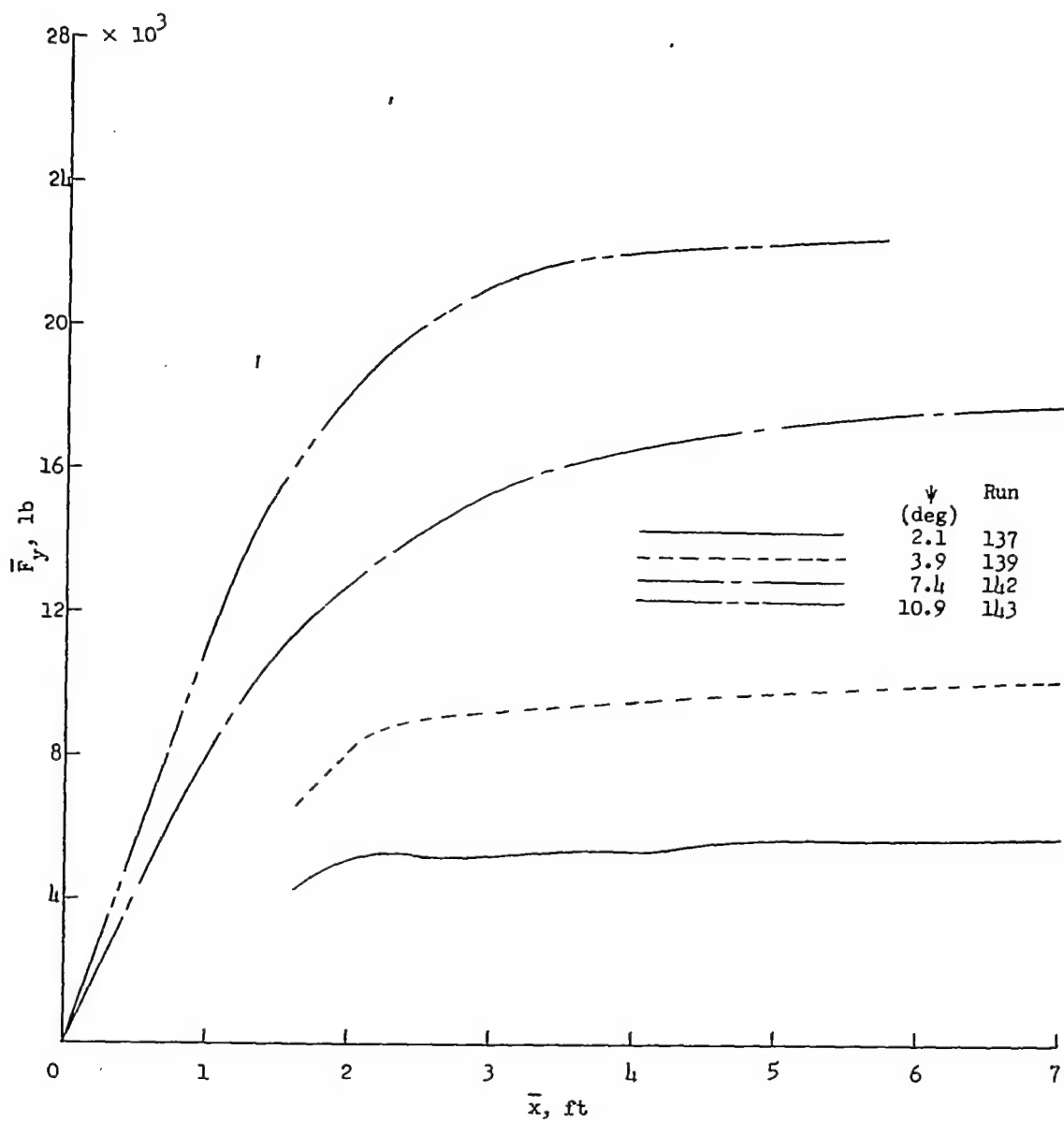
(d) Test series E: $\bar{F}_z = 45,200$ pounds; $\bar{p} \approx 180$ pounds per square inch; $\bar{\delta}_o \approx 3.6$ inches.

Figure 16.- Continued.
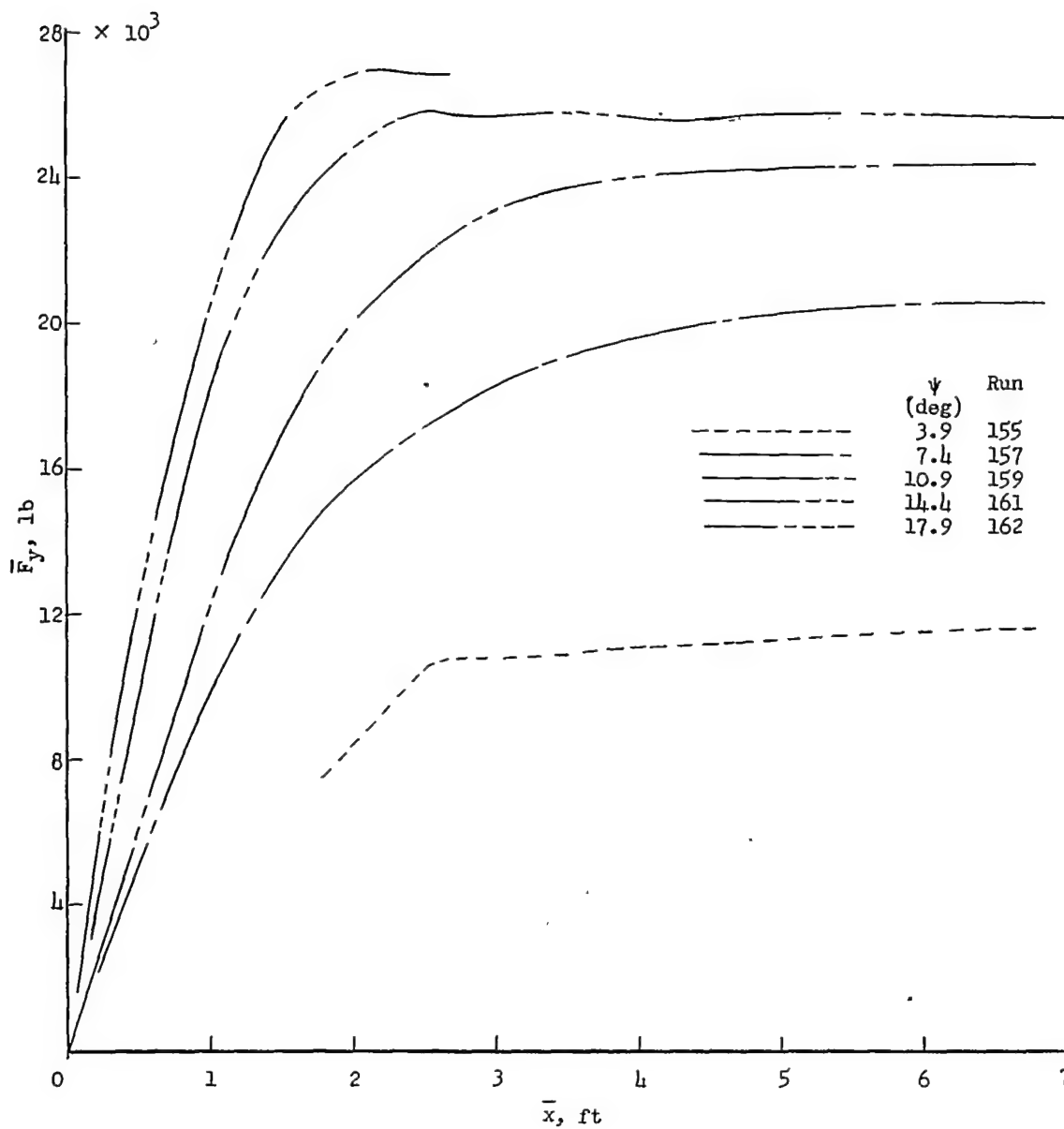
(e) Test series E: $\bar{F}_z$ = 45,200 pounds; $\bar{p}$ ≈ 230 pounds per square inch; $\bar{\delta}_o$ ≈ 3.0 inches.

Figure 16.- Concluded.
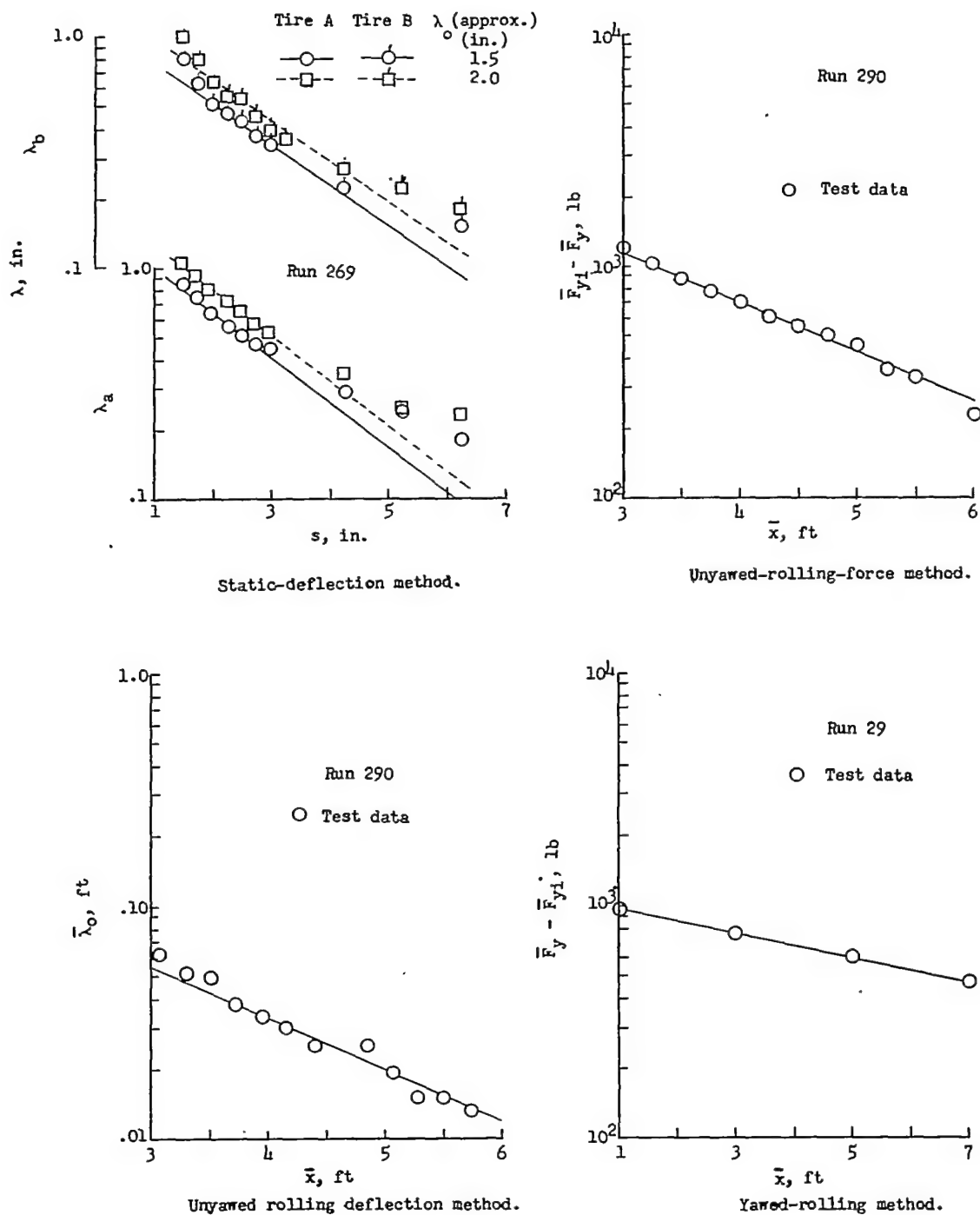
(a) Test series A: $\tilde{F}_Z = 17,000$ pounds; for runs 269 and 290, $\bar{p} \approx 60$ pounds per square inch and $\bar{\delta}_0 \approx 3.7$ inches; for run 29, $\bar{p} \approx 168$ pounds per square inch and $\bar{\delta}_0 \approx 1.8$ inches.

Figure 17.- Sample test data obtained from the four methods used to determine relaxation length.

Run 273

Static-deflection method.

Run 297

Unyawed-rolling-force method.

Run 297

Unyawed-rolling-deflection method.

Run 51

Yawed-rolling method.
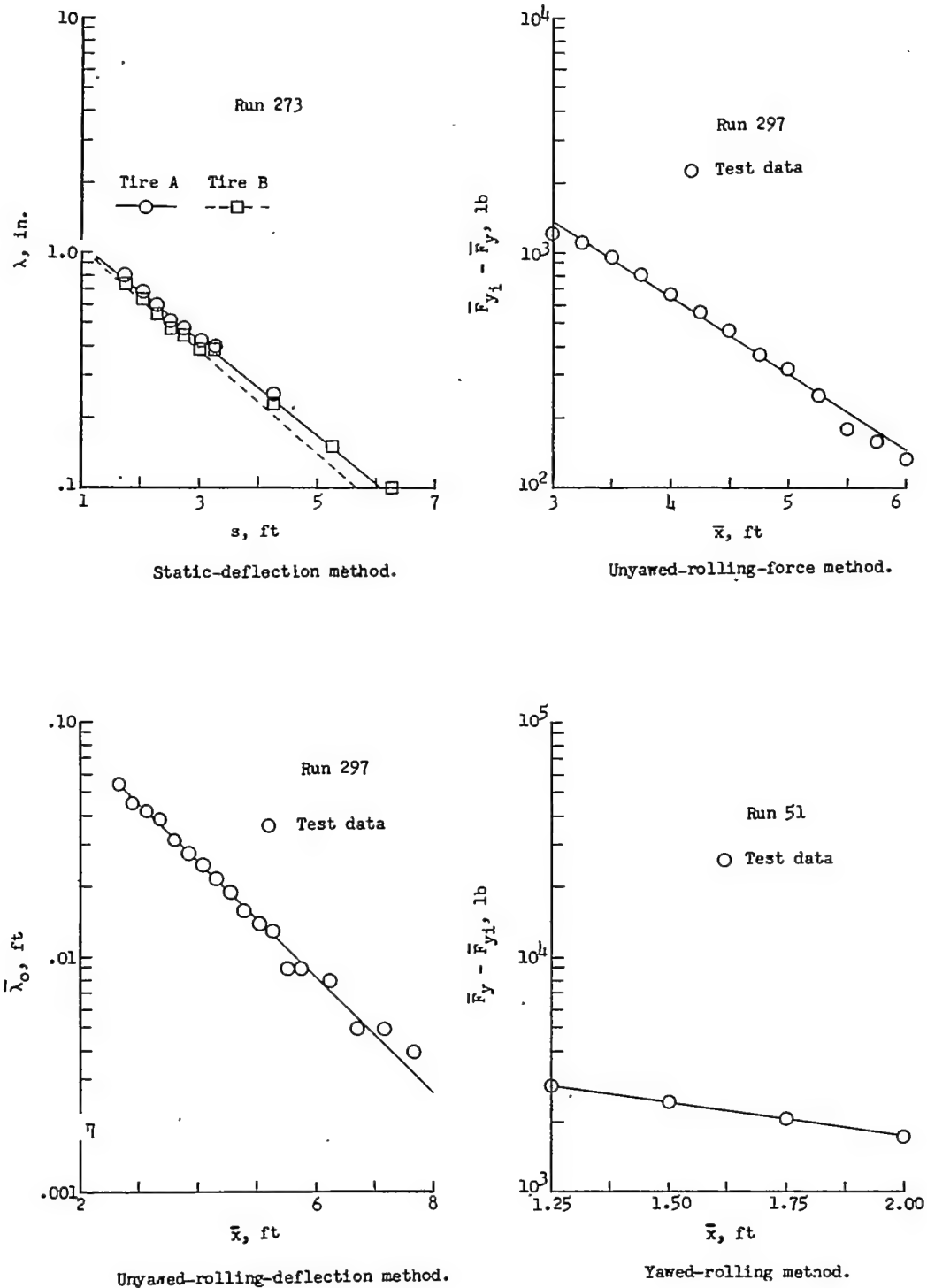
(b) Test series B:  $\bar{F}_z = 23,700$ pounds;  $\bar{p} \approx 130$ pounds per square inch;  $\delta_0 \approx 2.8$ inches.

Figure 17.- Continued.
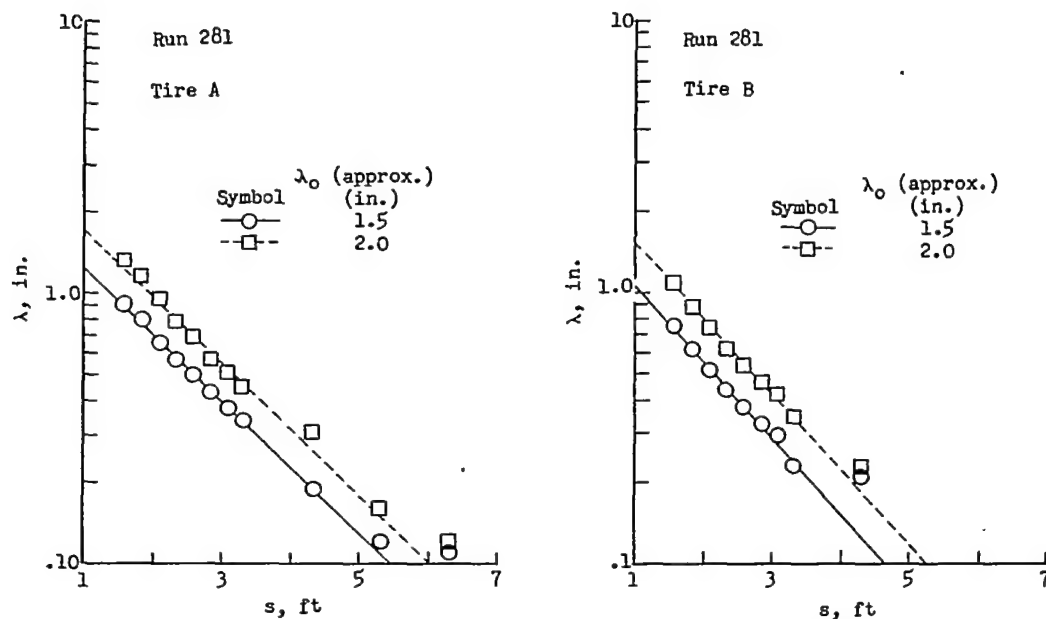
Static-deflection method.
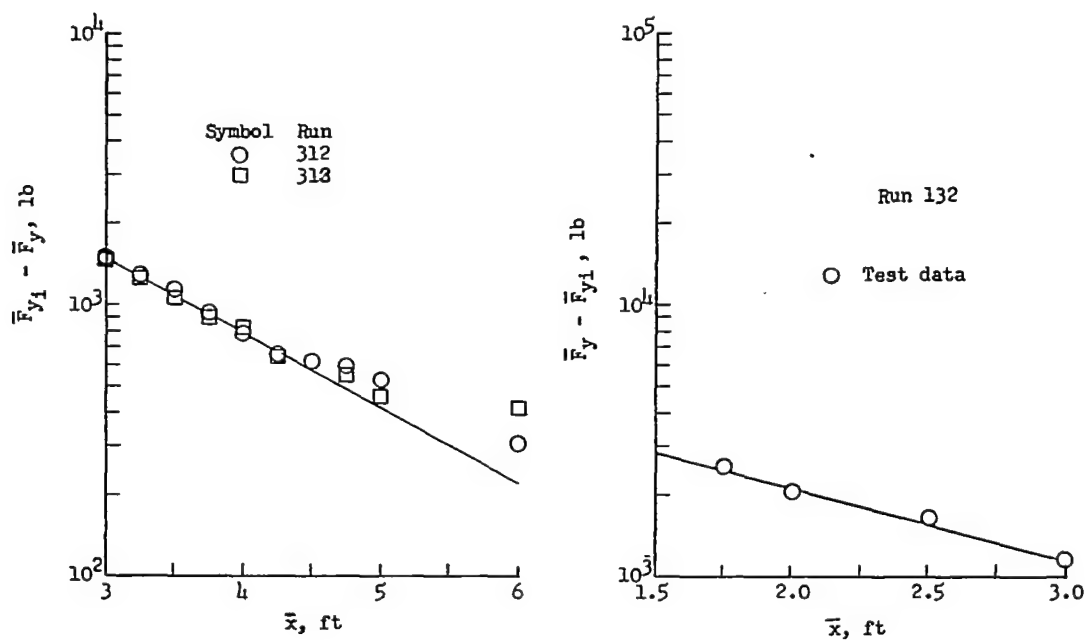


Unyawed-rolling-force method.



Yawed-rolling method.

(c) Test series E: $\bar{F}_z = 45,200$ pounds; $\bar{p} \approx 150$ pounds per square inch; $\bar{\delta}_o \approx 4.3$ inches.

Figure 17.- Continued.
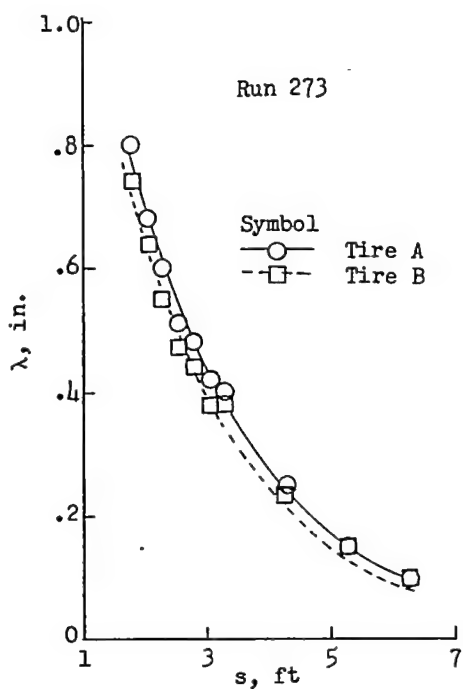
Static-deflection method.
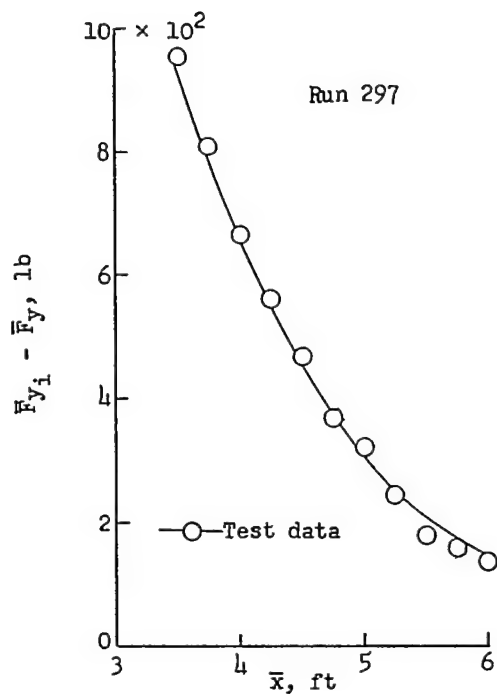
Unyawed-rolling-force method.
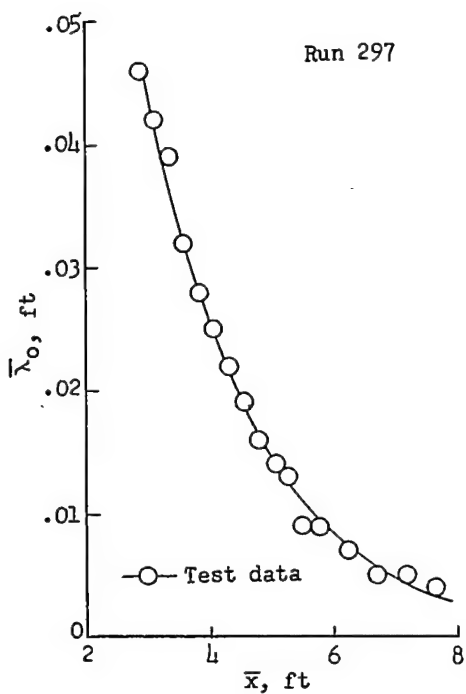
Unyawed-rolling-deflection method.
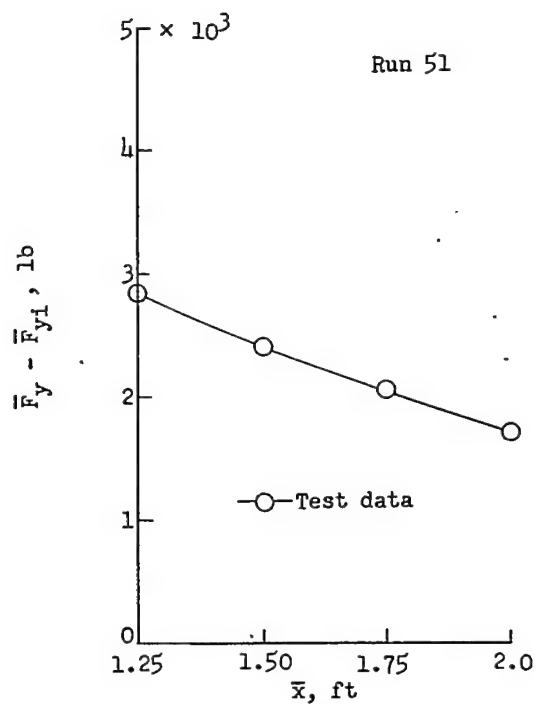
Yawed-rolling method.

(d) Data for test series B (see fig. 17(b)) replotted in linear coordinates.

Figure 17.- Concluded.
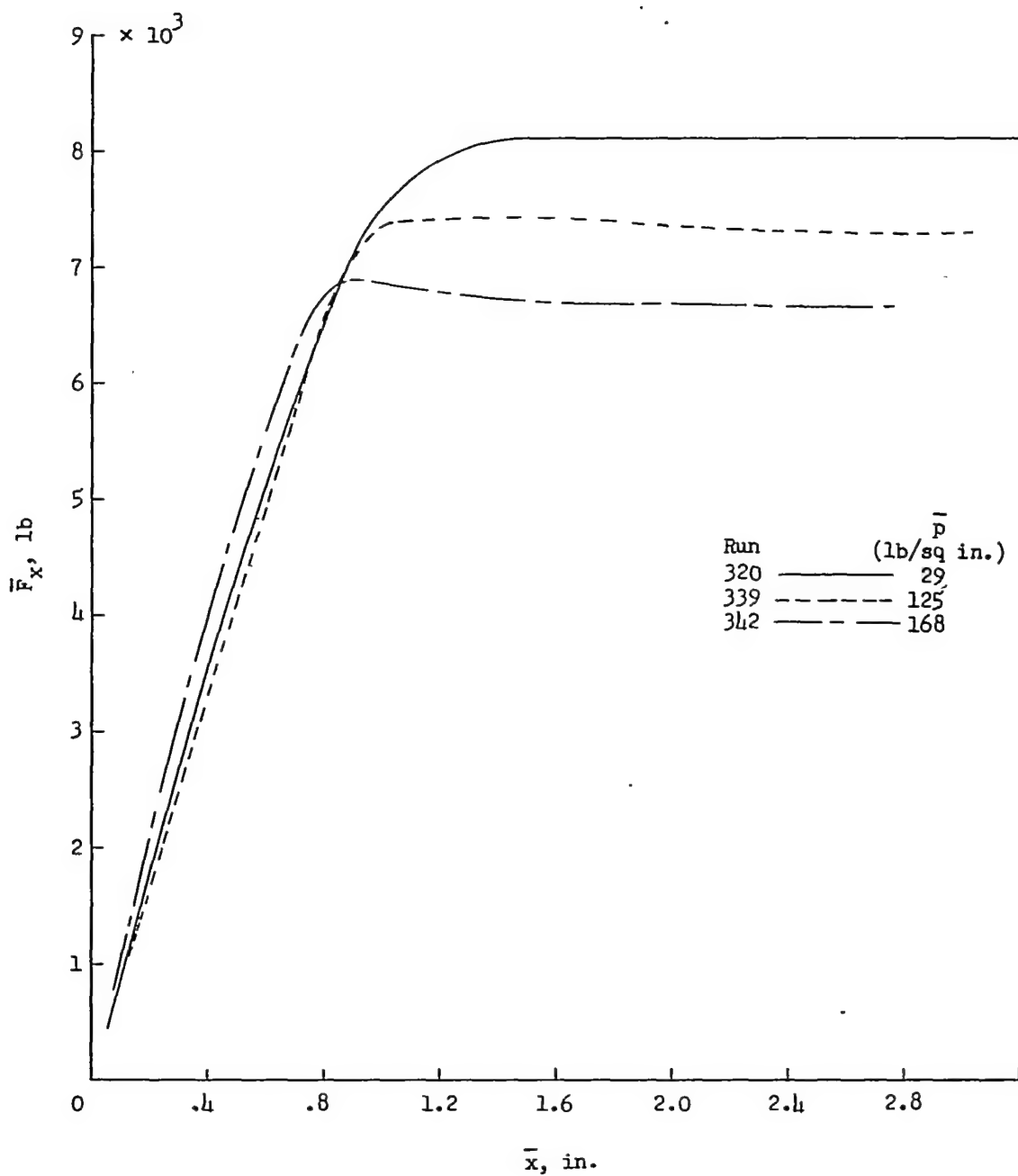
Figure 18.- Drag force buildup with horizontal distance pulled for several
typical runs.  Locked-wheel drag tests with  $\bar{F}_z$ = 9,730 pounds   for
$\bar{F}_x$ = 0.
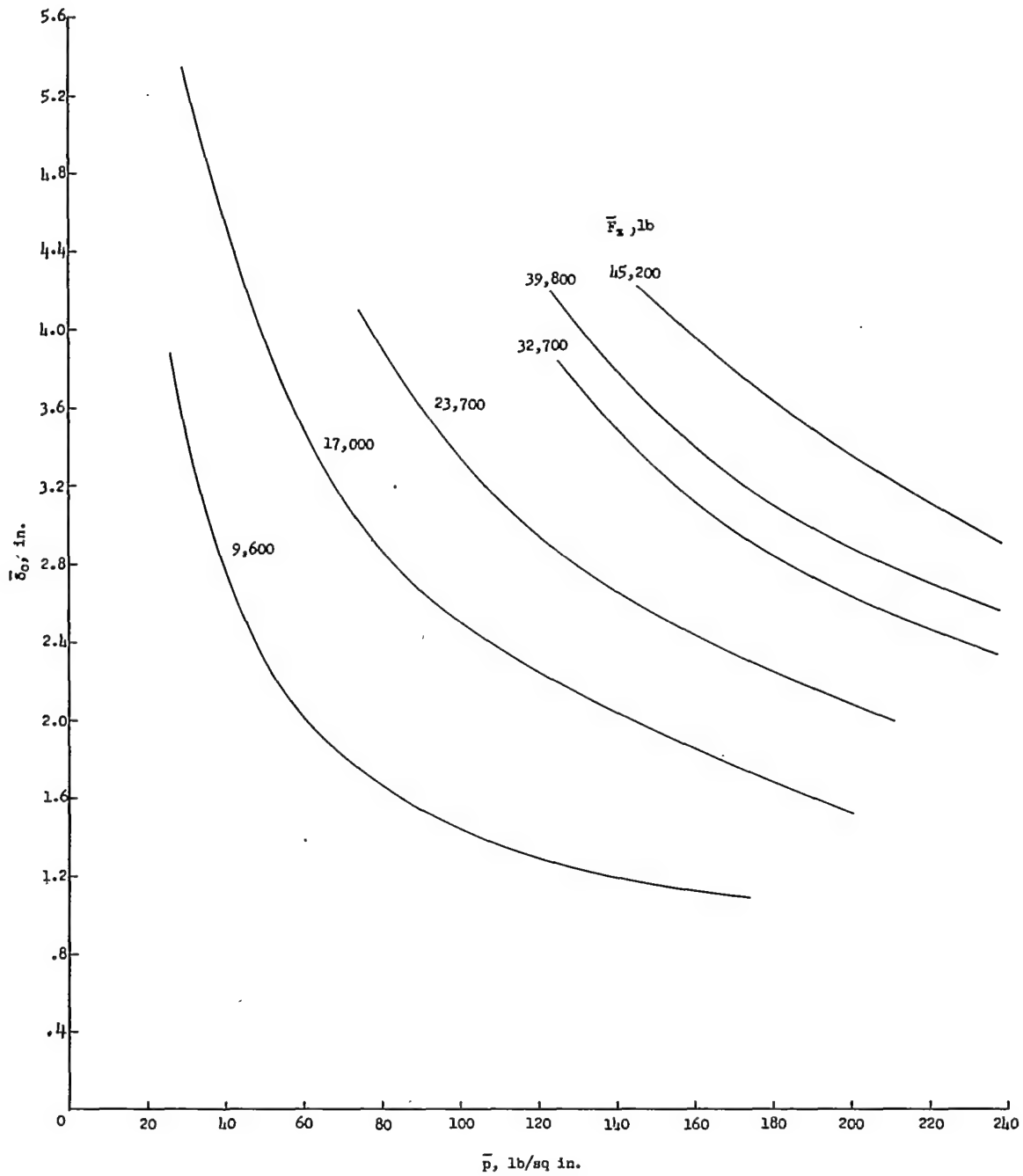
Figure 19.- Average vertical-load—vertical-tire-deflection characteristics
of tires A and B.
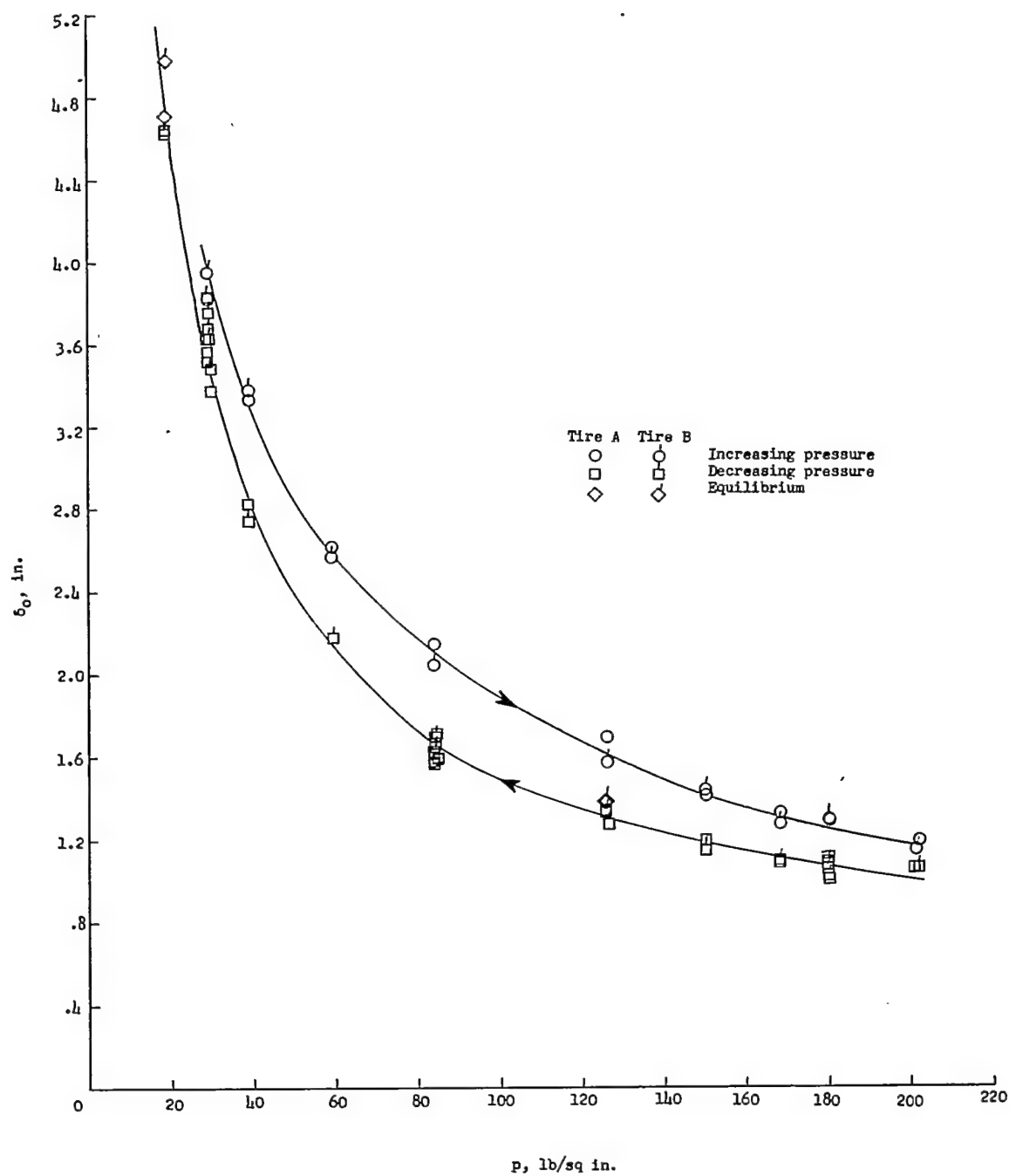
Figure 20.- Hysteresis effects on tire-pressure—vertical-deflection relationships (table V, locked-wheel drag tests) for $\bar{F}_z = 9,730$ pounds.
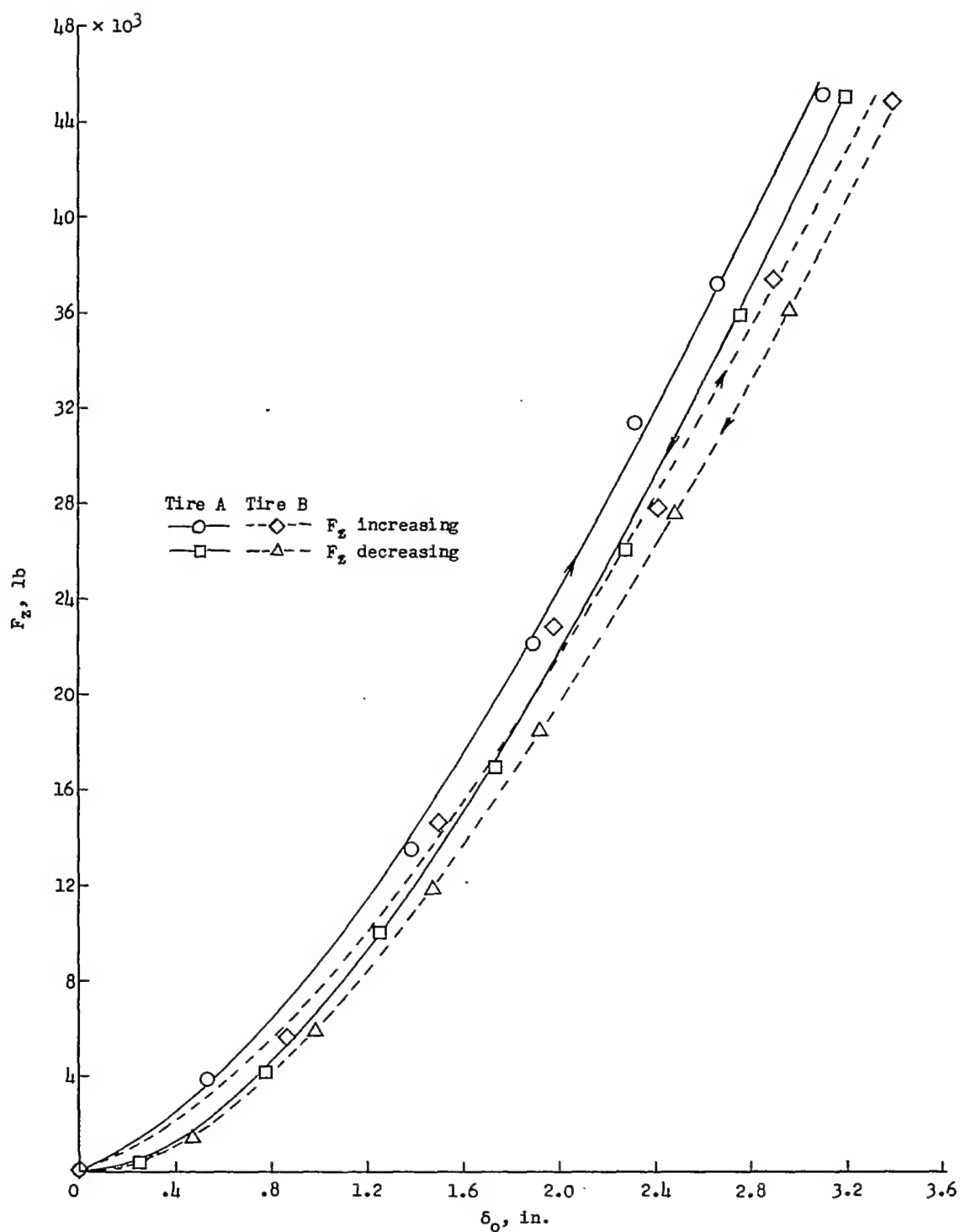
Figure 21.- Variation of vertical load with vertical tire deflection for $p_O = 219$ pounds per square inch. $p = 221$ pounds per square inch at $F_{z_{max}}$.
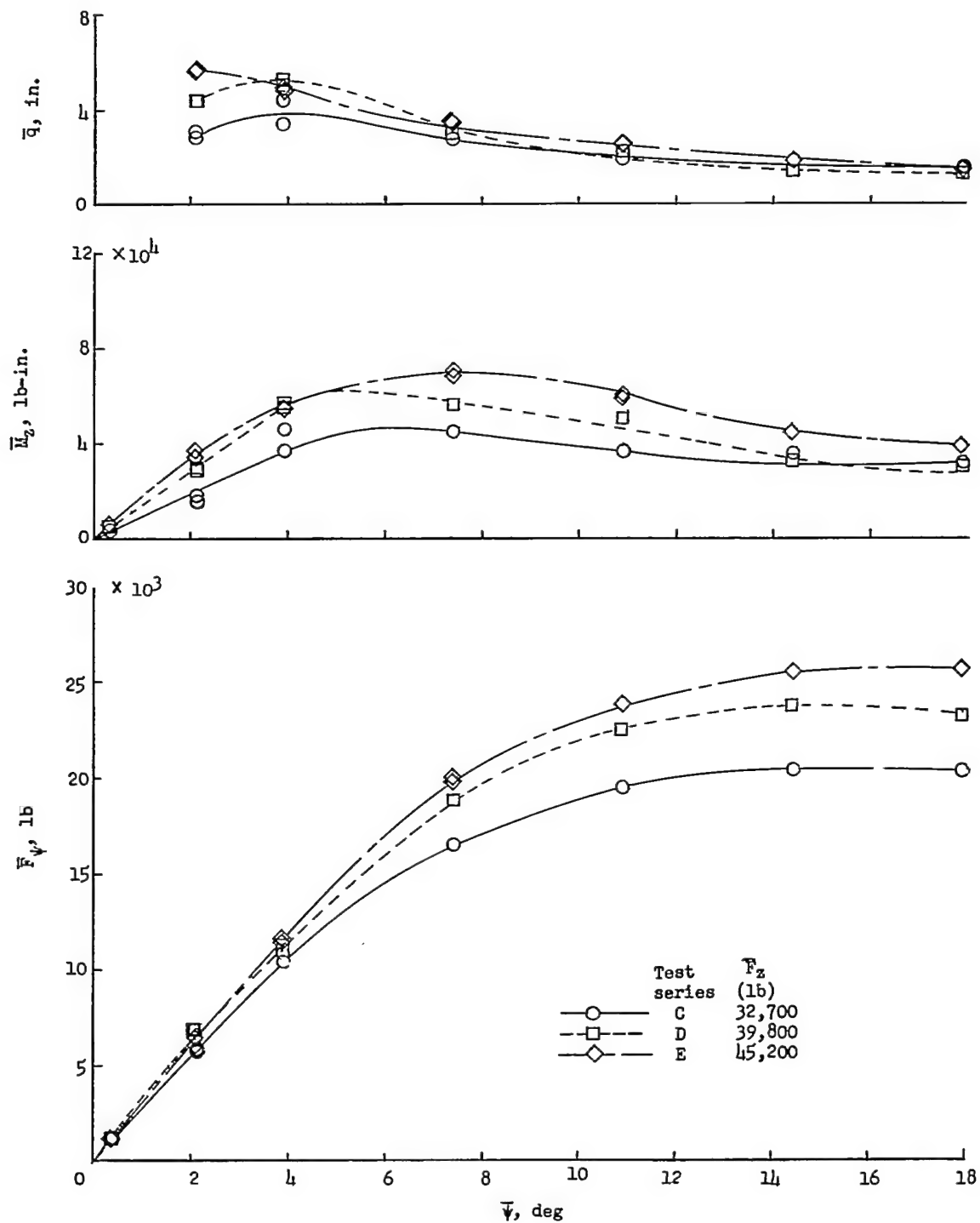
Figure 22.- Variation of normal force, self-alining torque, and pneumatic caster with yaw angle for constant inflation pressure. $\bar{p} \approx 230$ pounds per square inch.
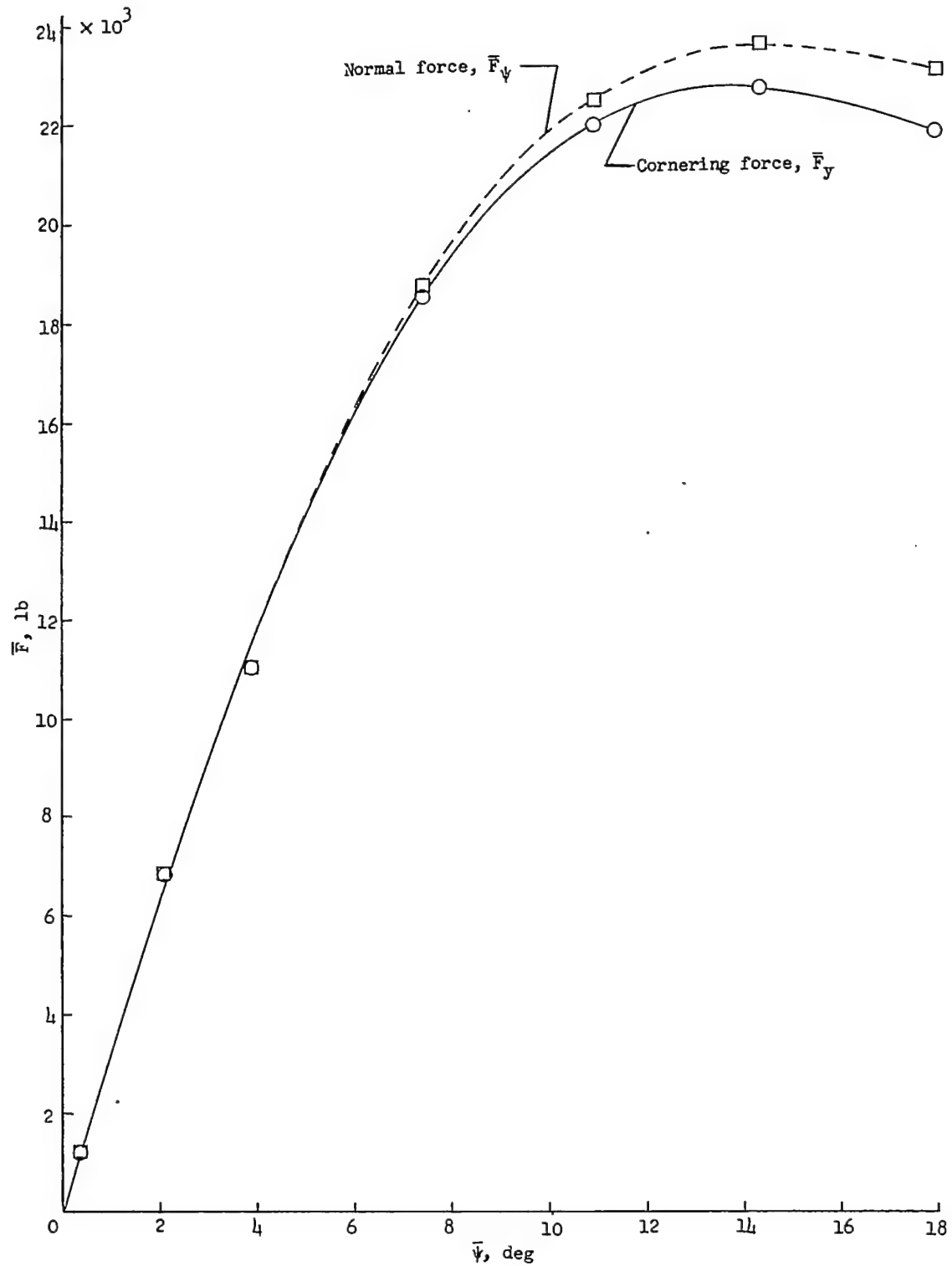
Figure 23.- Comparison of cornering-force and normal-force variations
with yaw angle for a typical loading condition. (Test series D:
$\overline{F}_Z = 39,800$ pounds; $\overline{p} \approx 230$ pounds per square inch; $\delta_o \approx 2.7$ inches.)
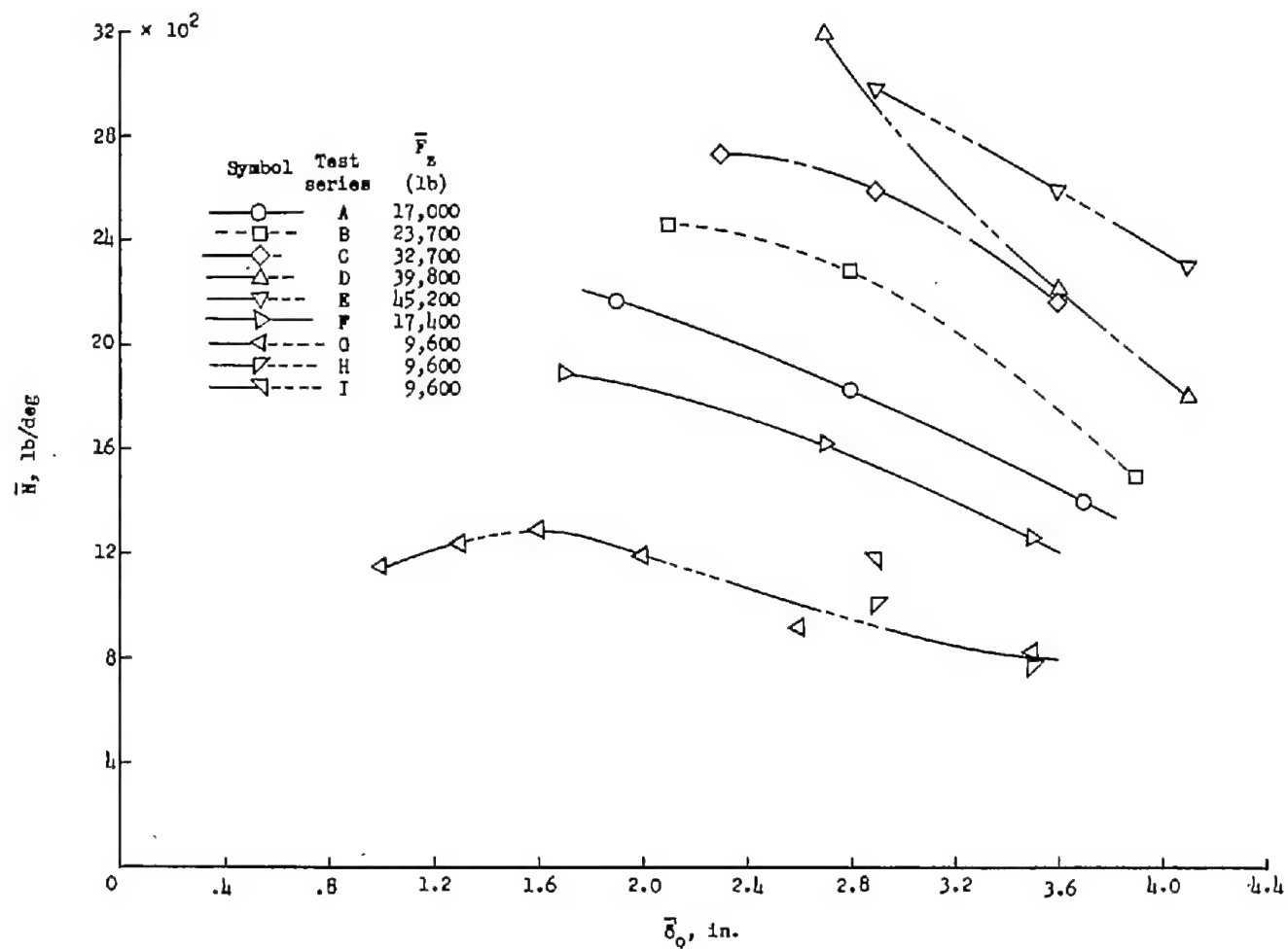
(a) Variation of cornering power with vertical tire deflection.

Figure 24.- Variation of cornering power with vertical tire deflection
and inflation pressure.
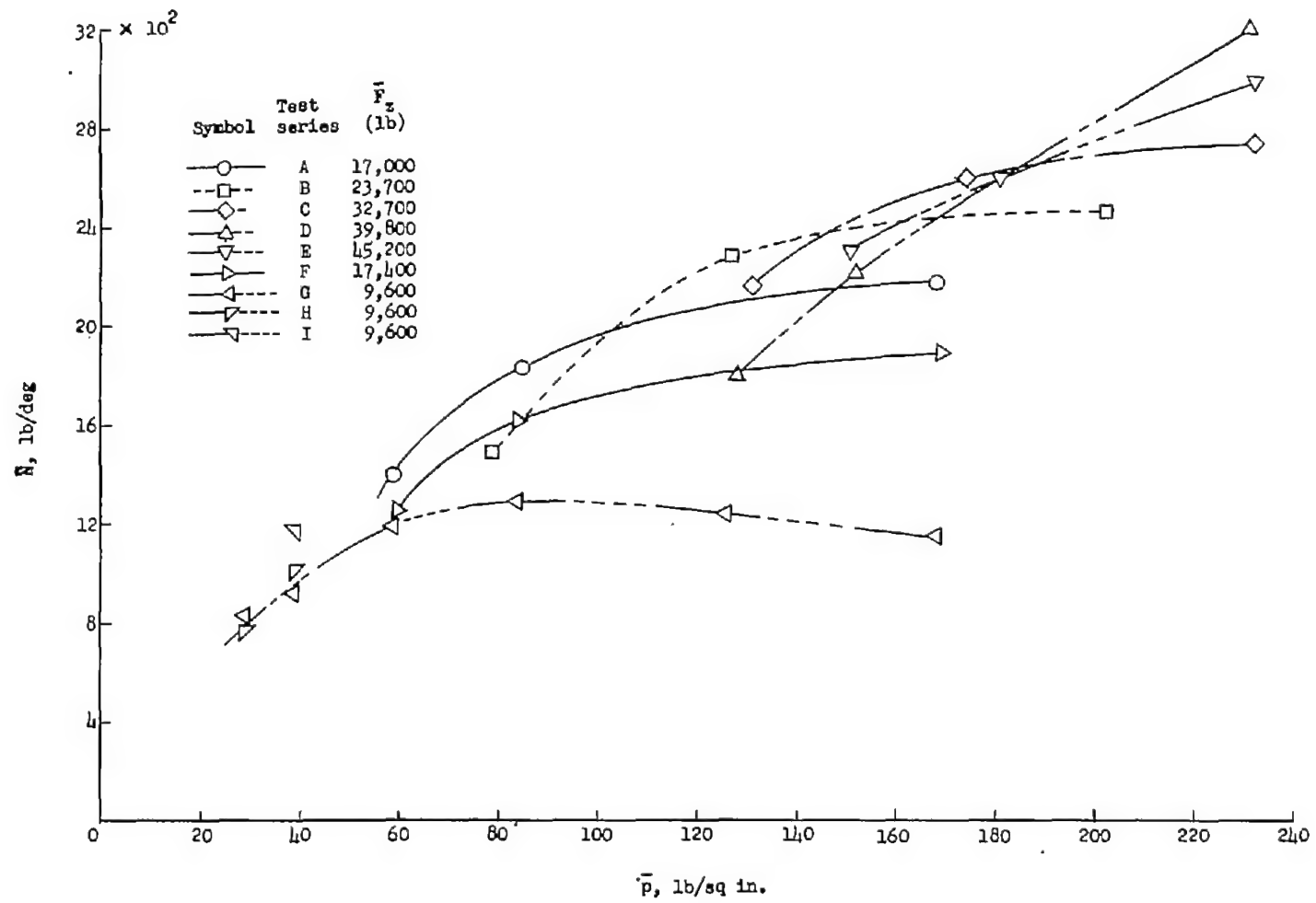
(b) Variation of cornering power with inflation pressure.

Figure 24.- Concluded.
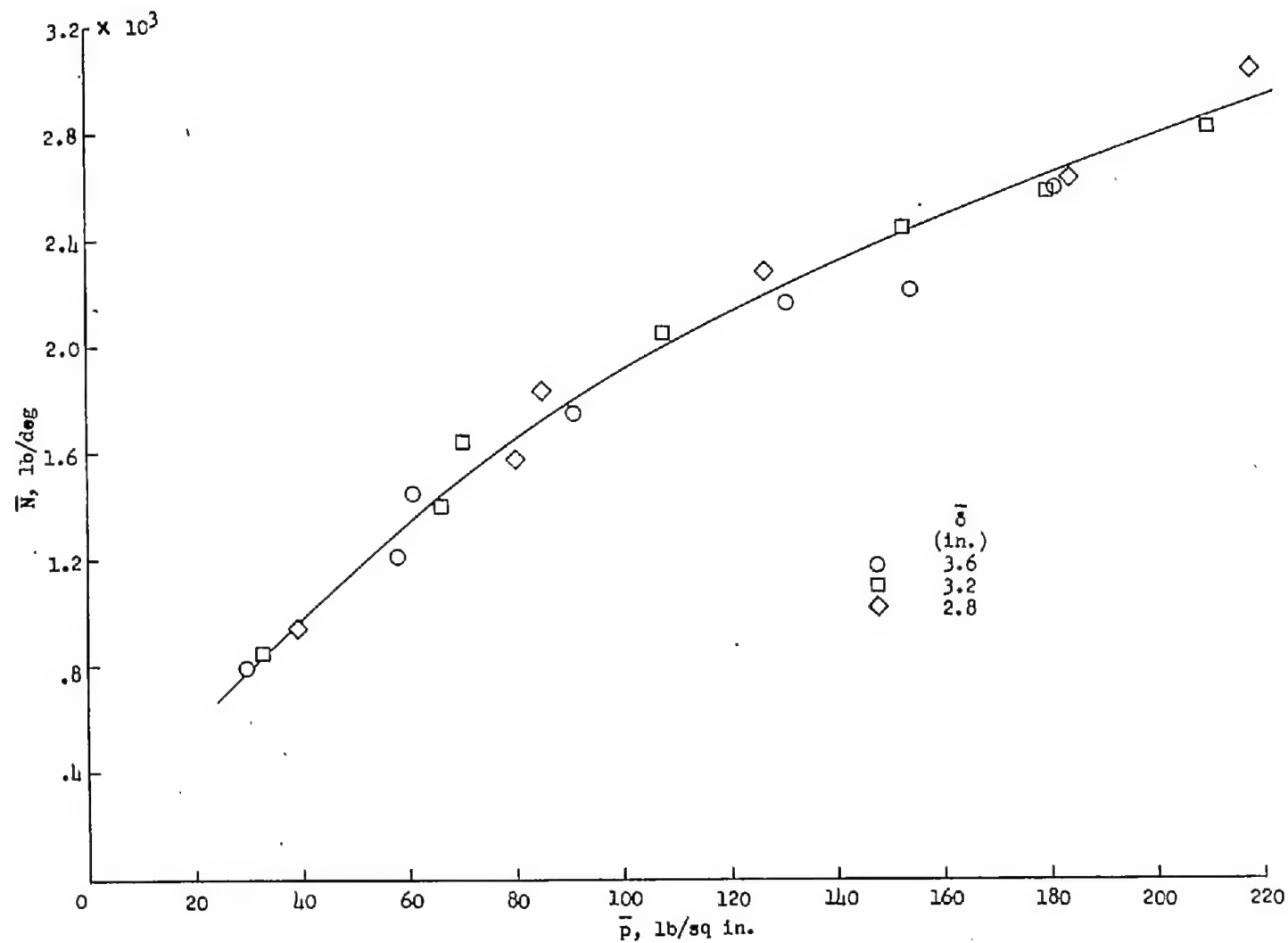
Figure 25.- Variation of cornering power with inflation pressure for
several constant vertical deflections.
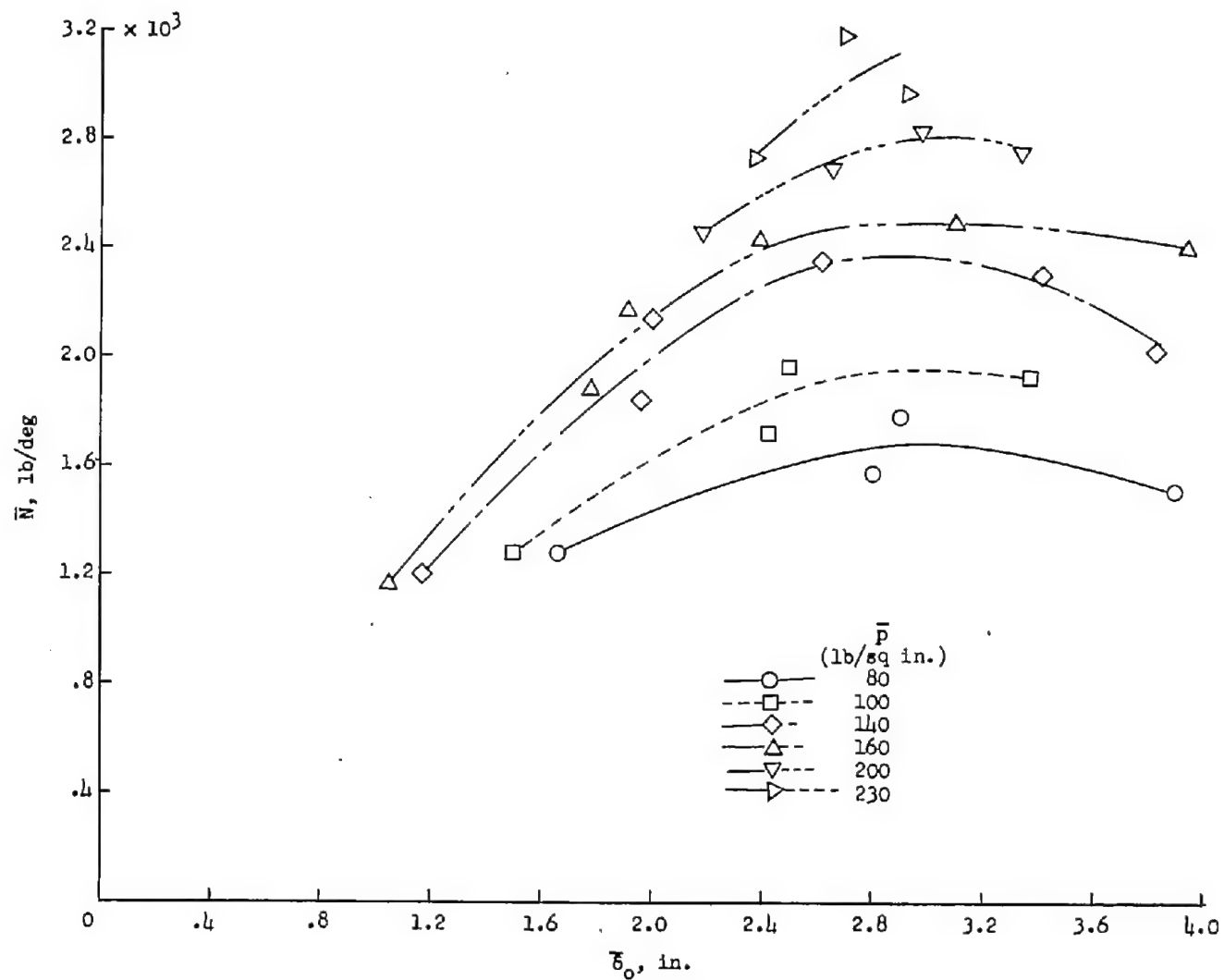
Figure 26.- Variation of cornering power with vertical tire deflection for several constant inflation pressures.
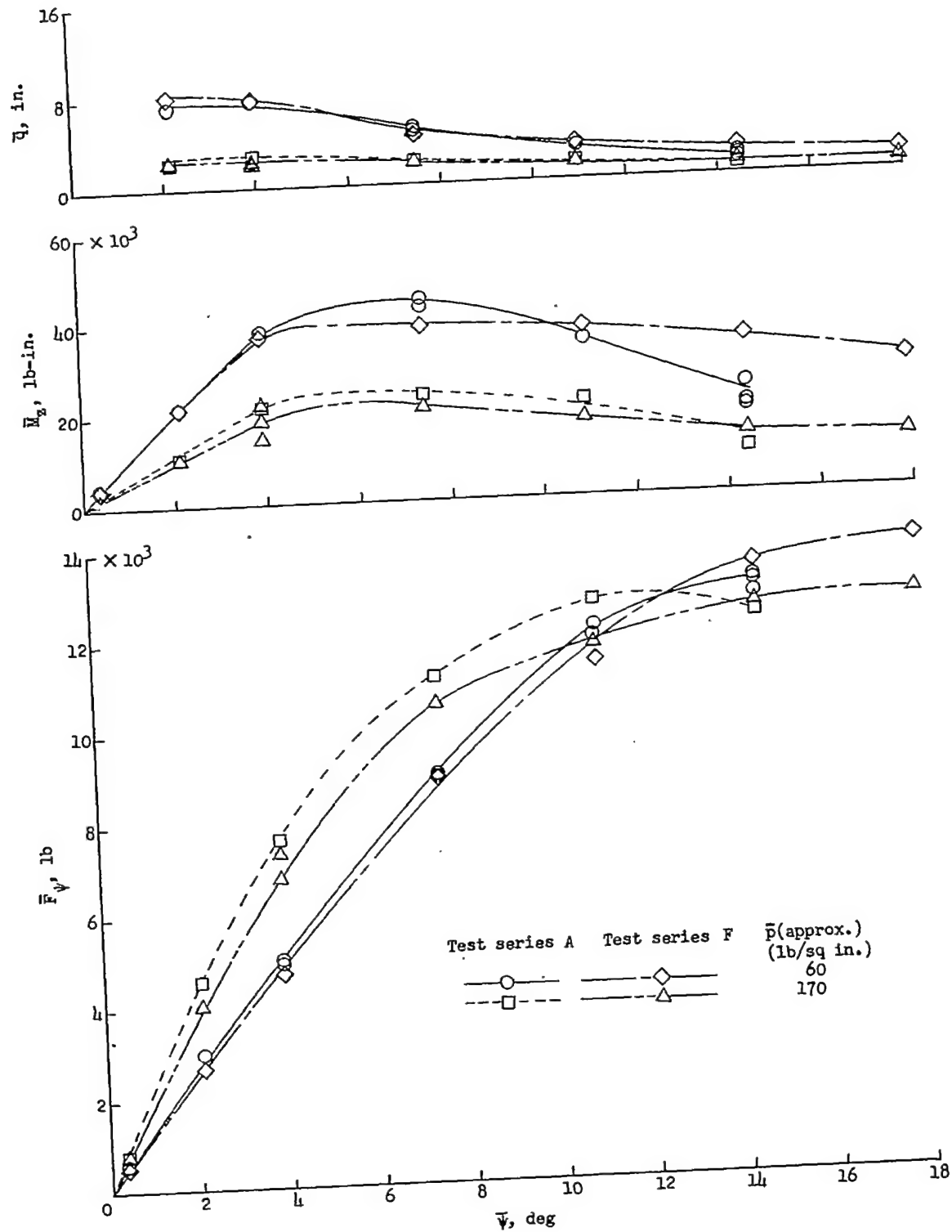
Figure 27.- Effect of tire wear on normal force, self-alining torque, and pneumatic caster for $\bar{F}_z \approx 17,000$ pounds.
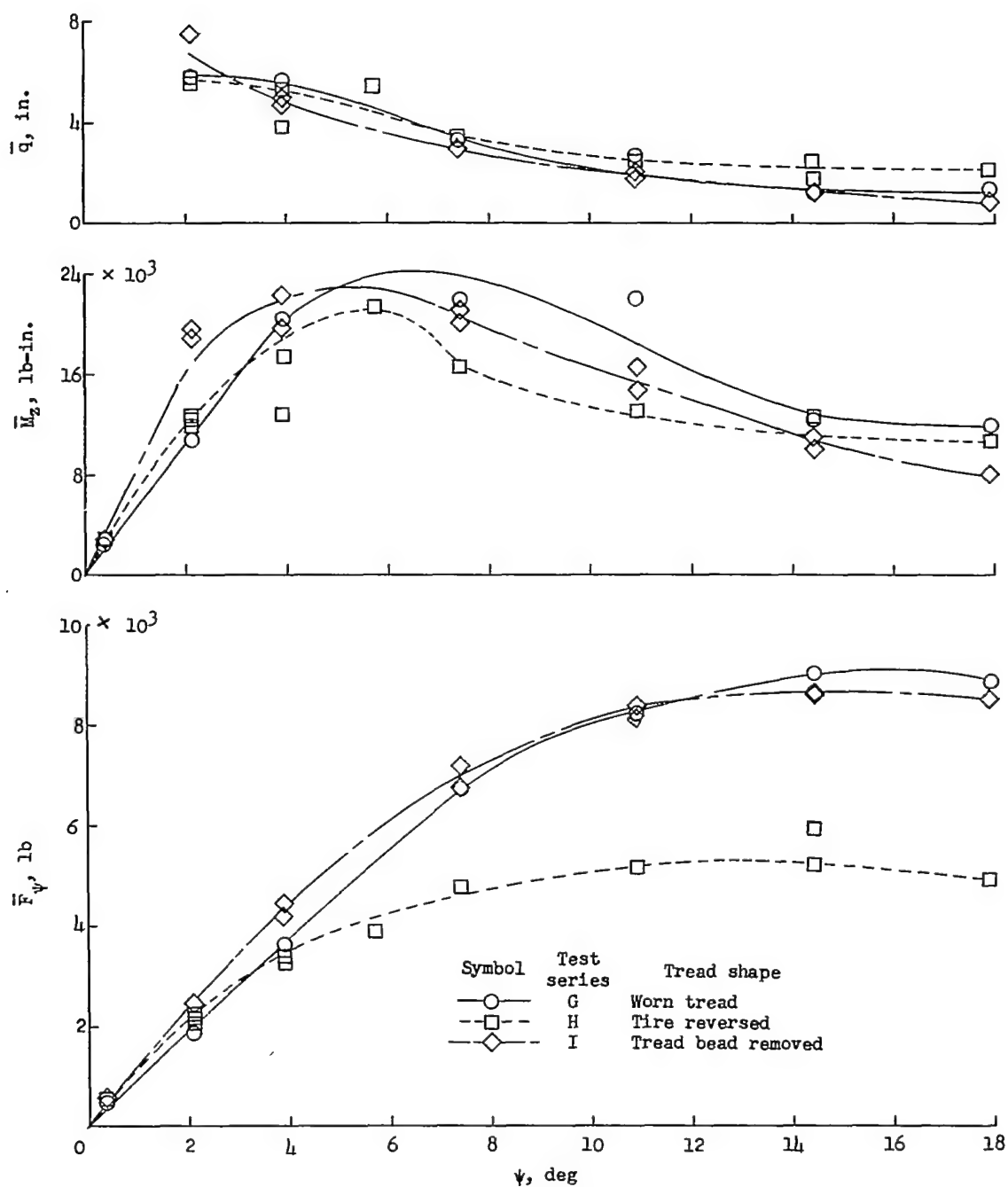
Figure 28.- Effect of tread shape on normal force, self-alining torque, and pneumatic caster for $\bar{F}_z = 9,600$ pounds and $\bar{p} \approx 39$ pounds per square inch.

(a) Tire unloaded.

(b) Tire under normal towing conditions (test series A to G).

(c) Tire under reversed towing conditions (test series H).
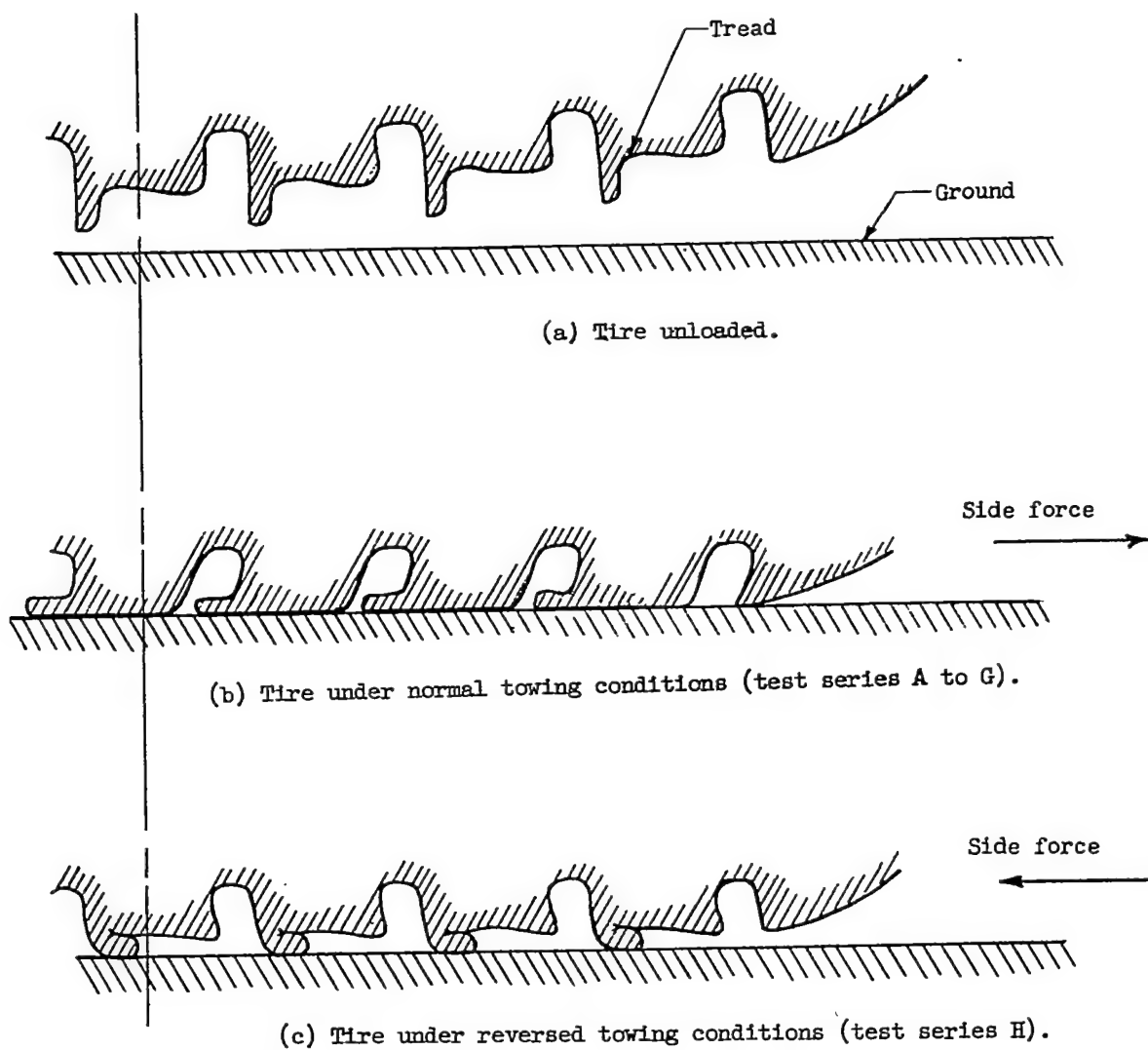
Figure 29.- Tread bead position.
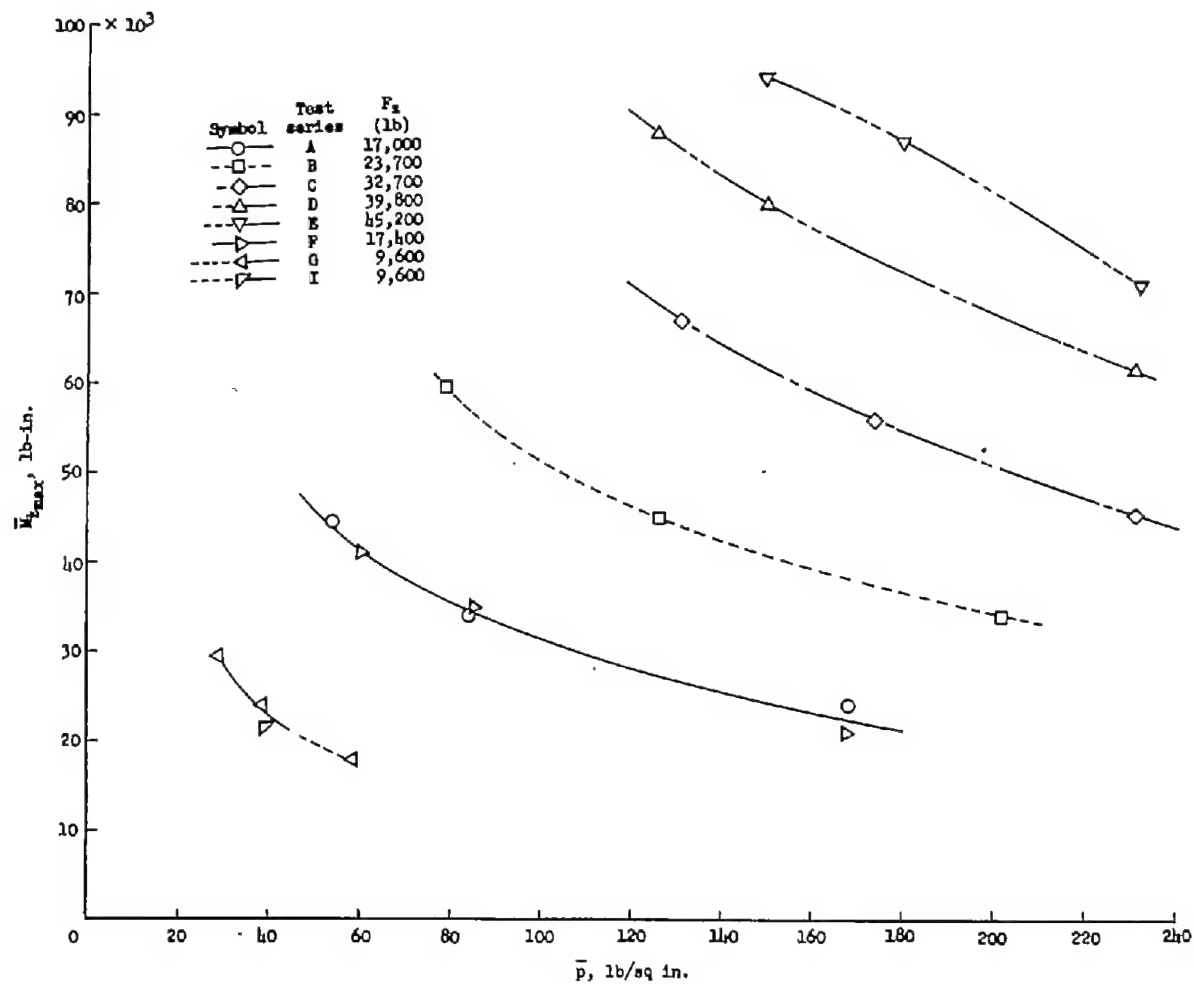
(a) Variation of maximum self-alining torque with inflation pressure.

Figure 30.- Variation of maximum self-alining torque with inflation pressure and vertical tire deflection.
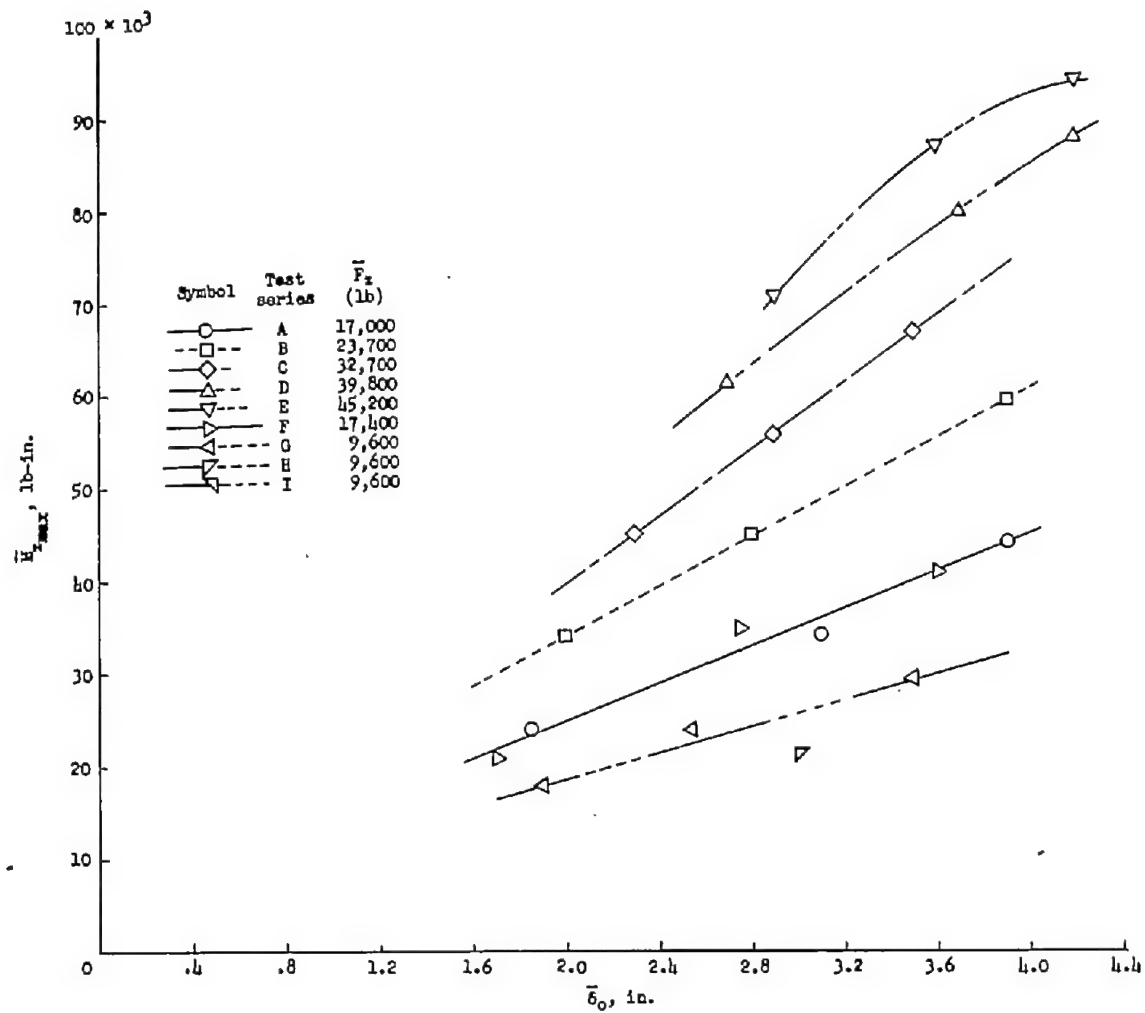
(b) Variation of maximum self-alining torque with vertical tire deflection.

Figure 30.- Concluded.
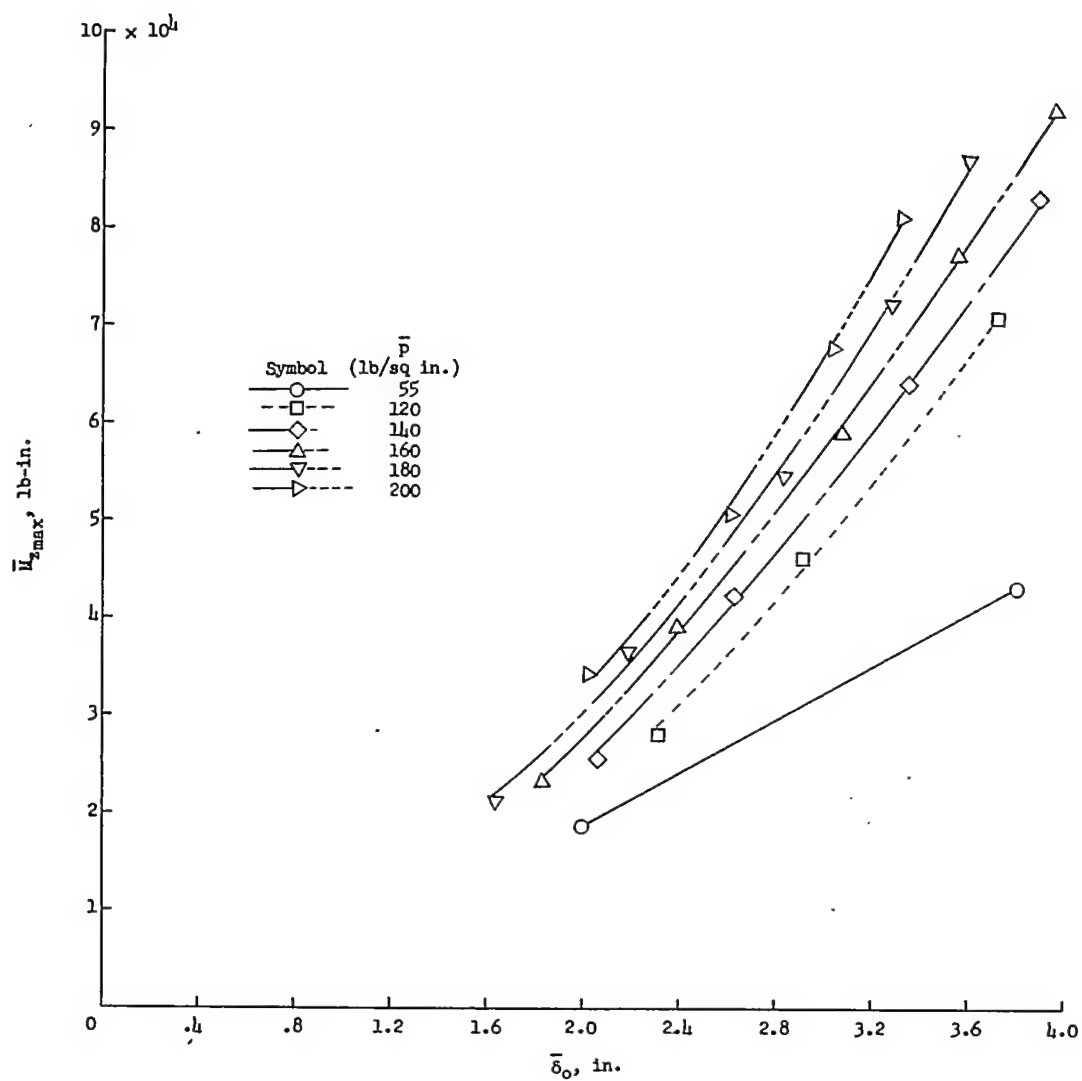
Figure 31.- Variation of maximum self-alining torque with vertical tire deflection for several constant inflation pressures.
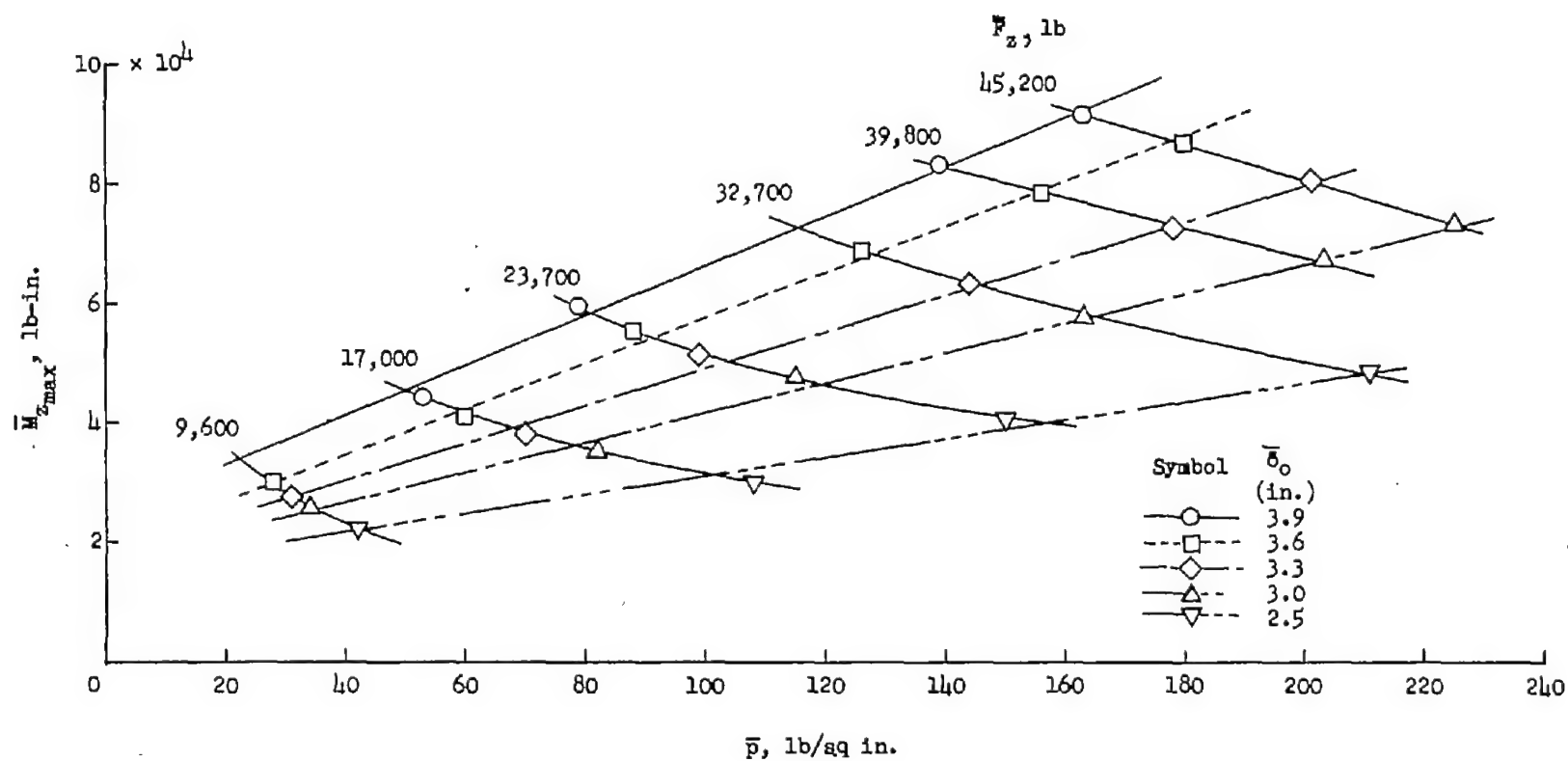
Figure 32.- Variation of maximum self-alining torque with inflation pressure for several constant vertical tire deflections.

| Symbol | Test series | $F_z$ (lb) |
|--------|-------------|------------|
| O | A | 17,000 |
| □ | B | 23,700 |
| ◇ | C | 32,700 |
| △ | D | 39,800 |
| ▽ | E | 45,200 |
| ▷ | F | 17,400 |
| ◁ | G | 9,600 |
| ▽ | H | 9,600 |
| ▽ | I | 9,600 |

(a) $\Psi = 2.1°$.

(b) $\Psi = 3.9°$.
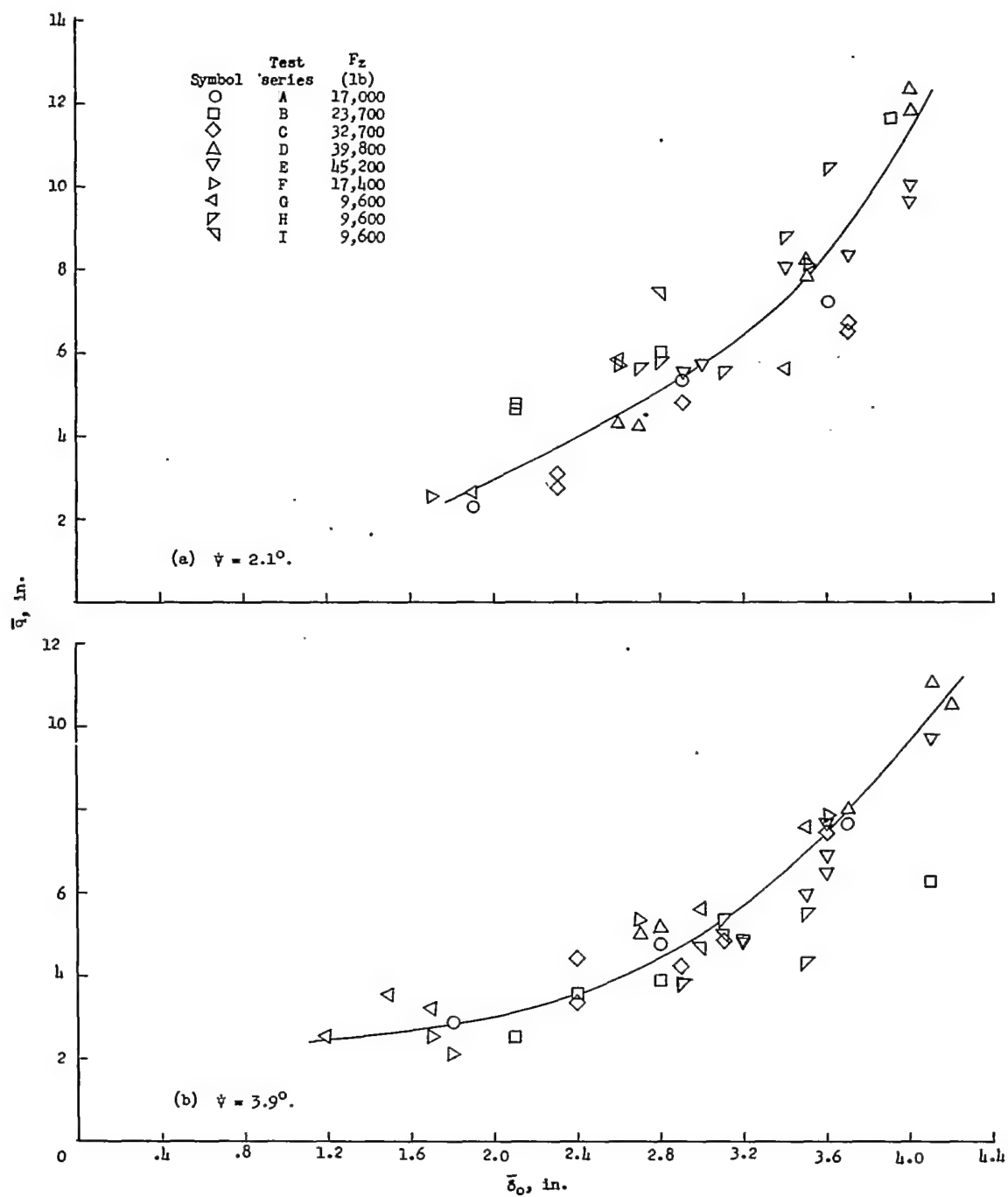
Figure 33.- Variation of pneumatic caster with vertical tire deflection for the vertical-load and yaw-angle ranges tested.

| Symbol | Test series | $F_z$ (lb) |
|--------|------------|-----------|
| ○ | A | 17,000 |
| □ | B | 23,700 |
| ◇ | C | 32,700 |
| △ | D | 39,800 |
| ▽ | E | 45,200 |
| ◁ | F | 17,400 |
| ▷ | G | 9,600 |
| ▽ | H | 9,600 |
| ◁ | I | 9,600 |

(c)  $\forall = 7.4^\circ$.

(d)  $\forall = 10.9^\circ$.

(e)  $\forall = 14.4^\circ$.

(f)  $\forall = 17.9^\circ$.

$\bar{q}$, in.

$\bar{\delta}_o$, in.
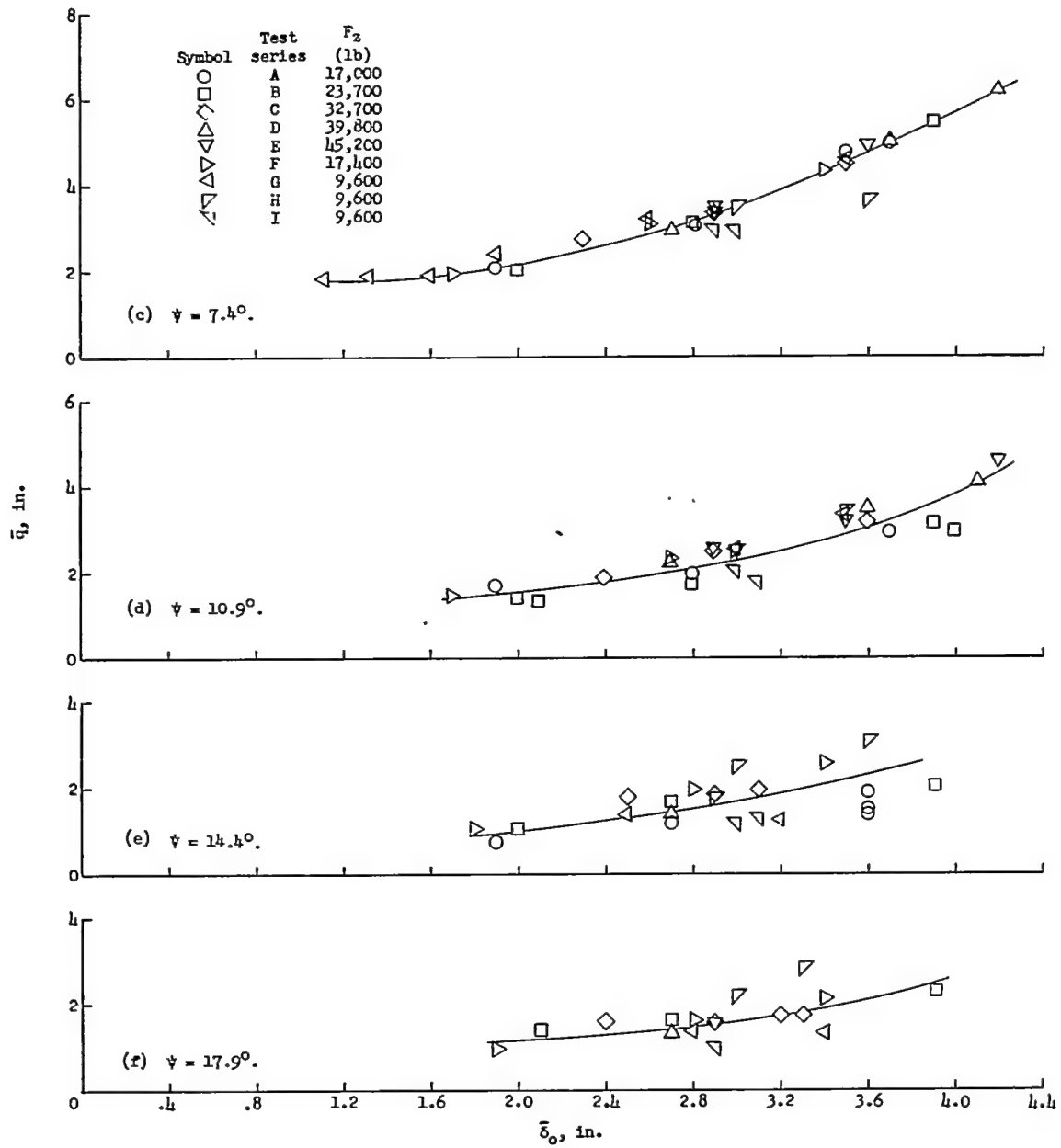
Figure 33.- Concluded.
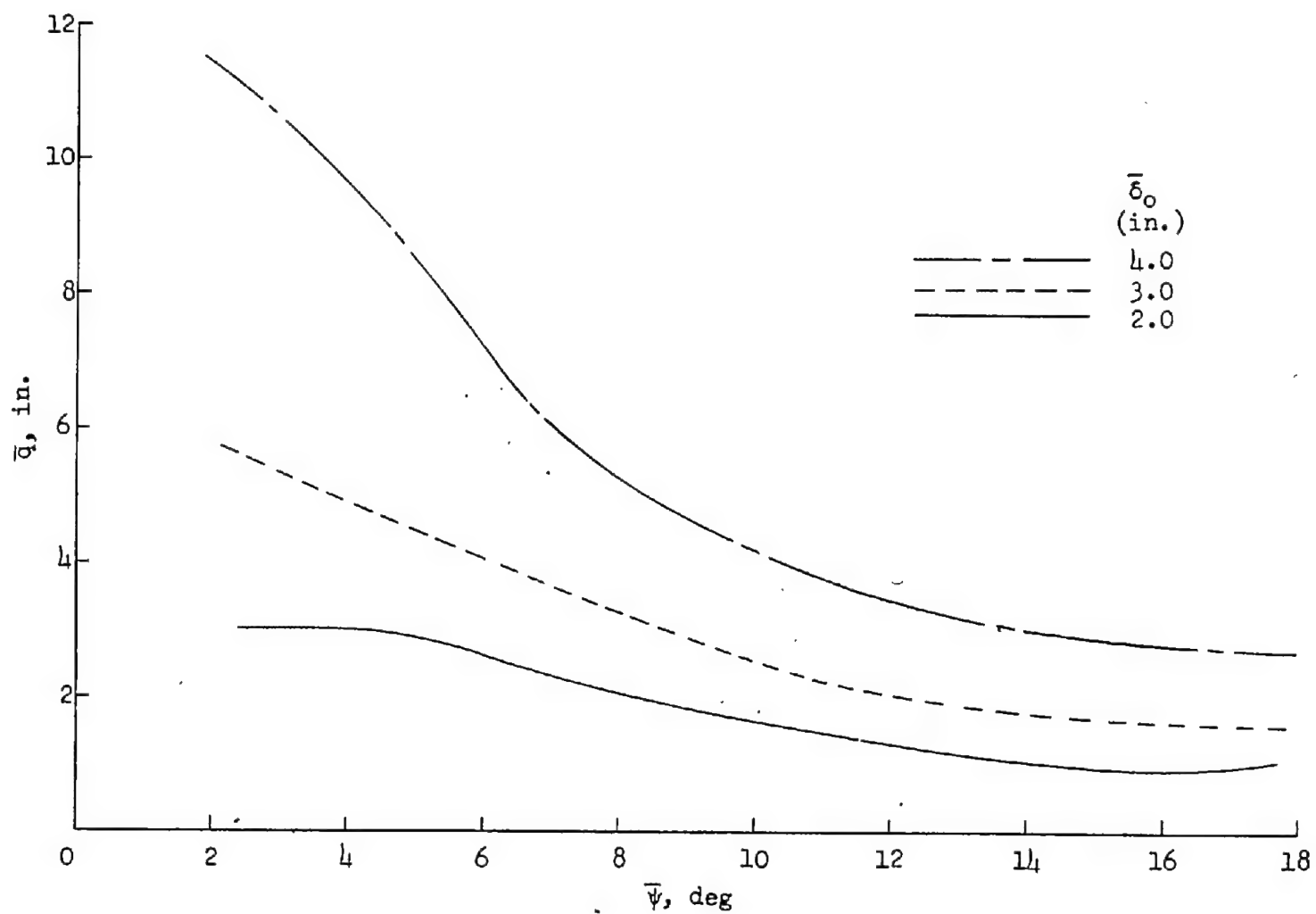
Figure 34.- Variation of pneumatic caster with yaw angle for several constant vertical tire deflections.
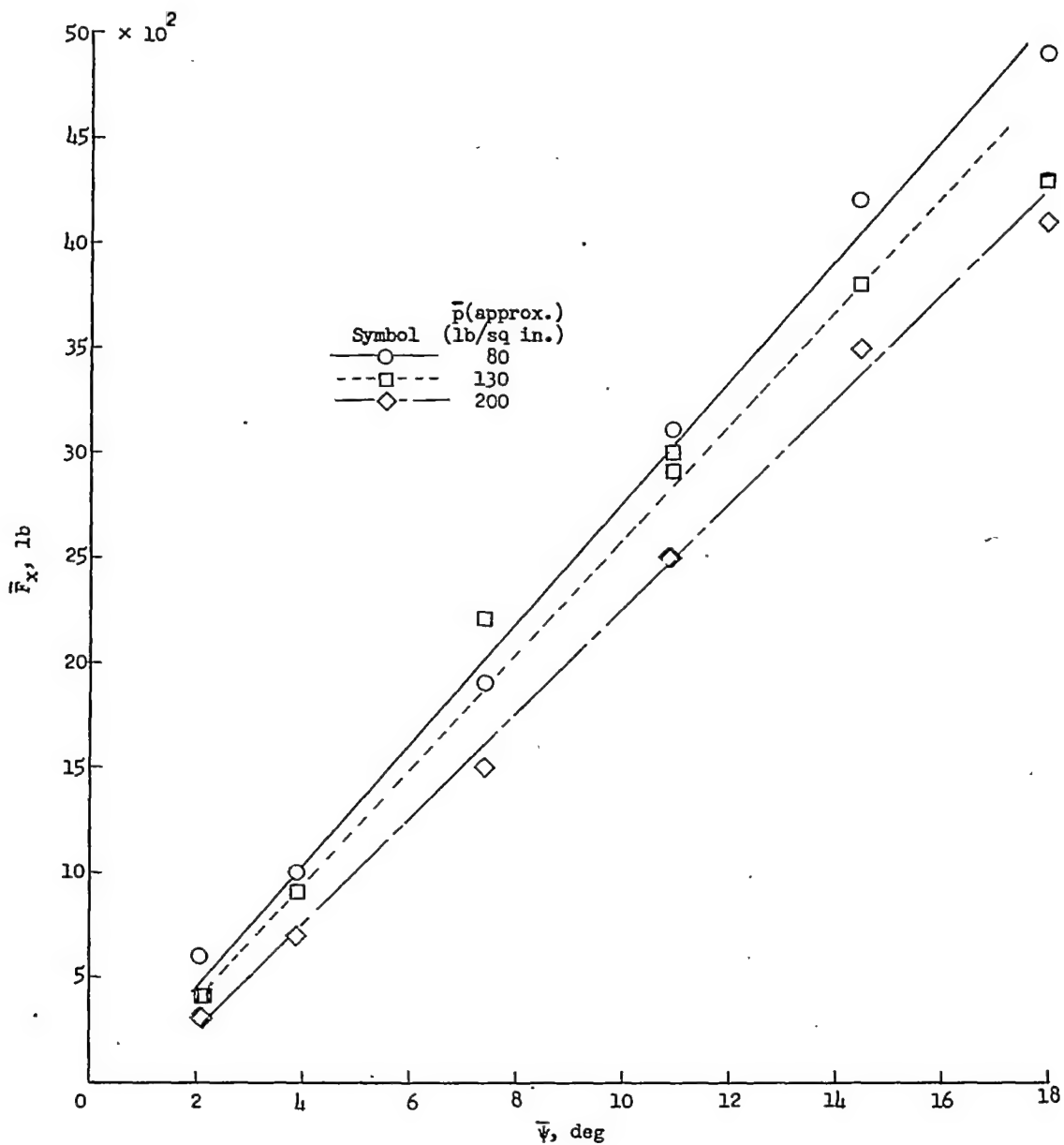
Figure 35.- Variation of drag force with yaw angle for several tire
inflation pressures.  (Yawed-rolling tests, test series B;
$\overline{F}_z$ = 23,700 pounds.)

(a) Test series A; $\overline{F}_z = 17,000$ pounds.

(b) Test series B; $\overline{F}_z = 23,700$ pounds.

(c) Test series C; $\overline{F}_z = 32,700$ pounds.

(d) Test series D; $\overline{F}_z = 39,800$ pounds.

(e) Test series E; $\overline{F}_z = 45,200$ pounds.
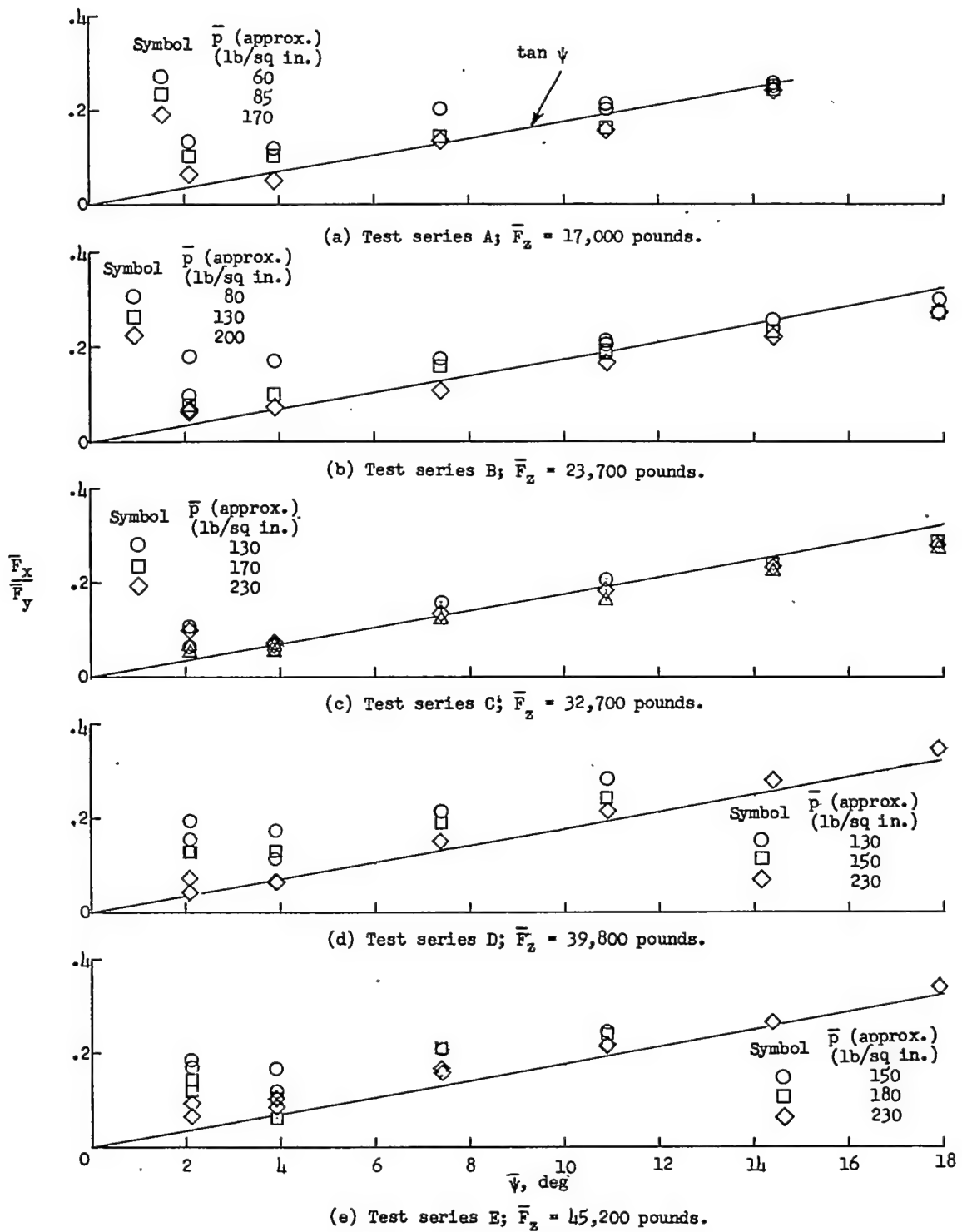
Figure 36.- Variation of the ratio of drag force to cornering force with yaw angle.

(f) Test series F; $\overline{F}_z$ = 17,400 pounds.

(g) Test series G; $\overline{F}_z$ = 9,600 pounds.

(h) Test series H; $\overline{F}_z$ = 9,600 pounds.

(i) Test series I; $\overline{F}_z$ = 9,600 pounds.

Figure 36.- Concluded.

$\bar{\mu}_\psi = \dfrac{\bar{F}_{Rmax}}{\bar{F}_z}$

| Symbol | Test series | $\bar{F}_z$ (lb) |
|--------|-------------|--------|
| ○ | A | 17,000 |
| □ | B | 23,700 |
| ◇ | C | 32,700 |
| △ | D | 39,800 |
| ▽ | E | 45,200 |
| ▷ | F | 17,400 |
| ◁ | G | 9,600 |
| ▽ | I | 9,600 |

$\bar{p}_n$, lb/sq in.
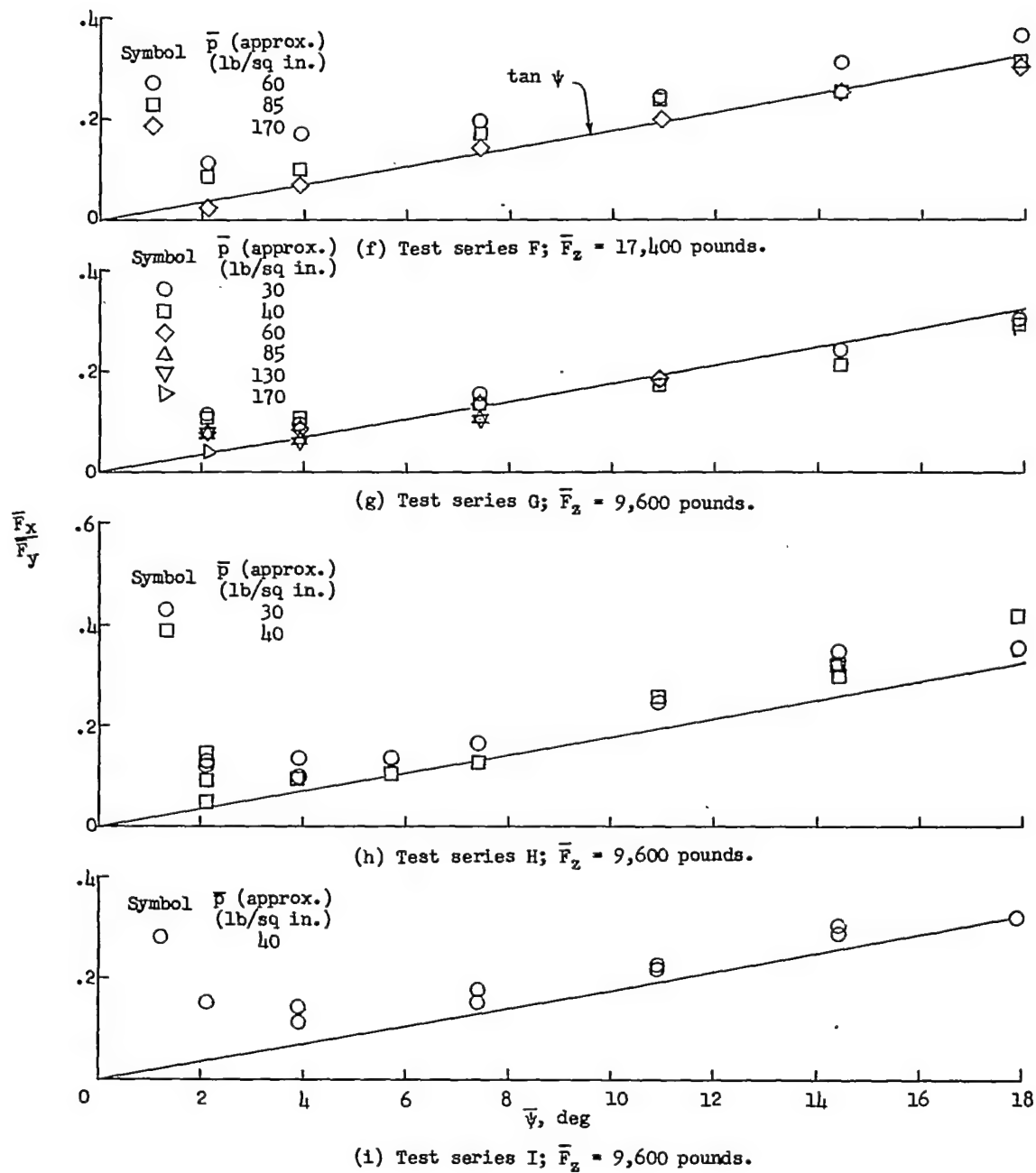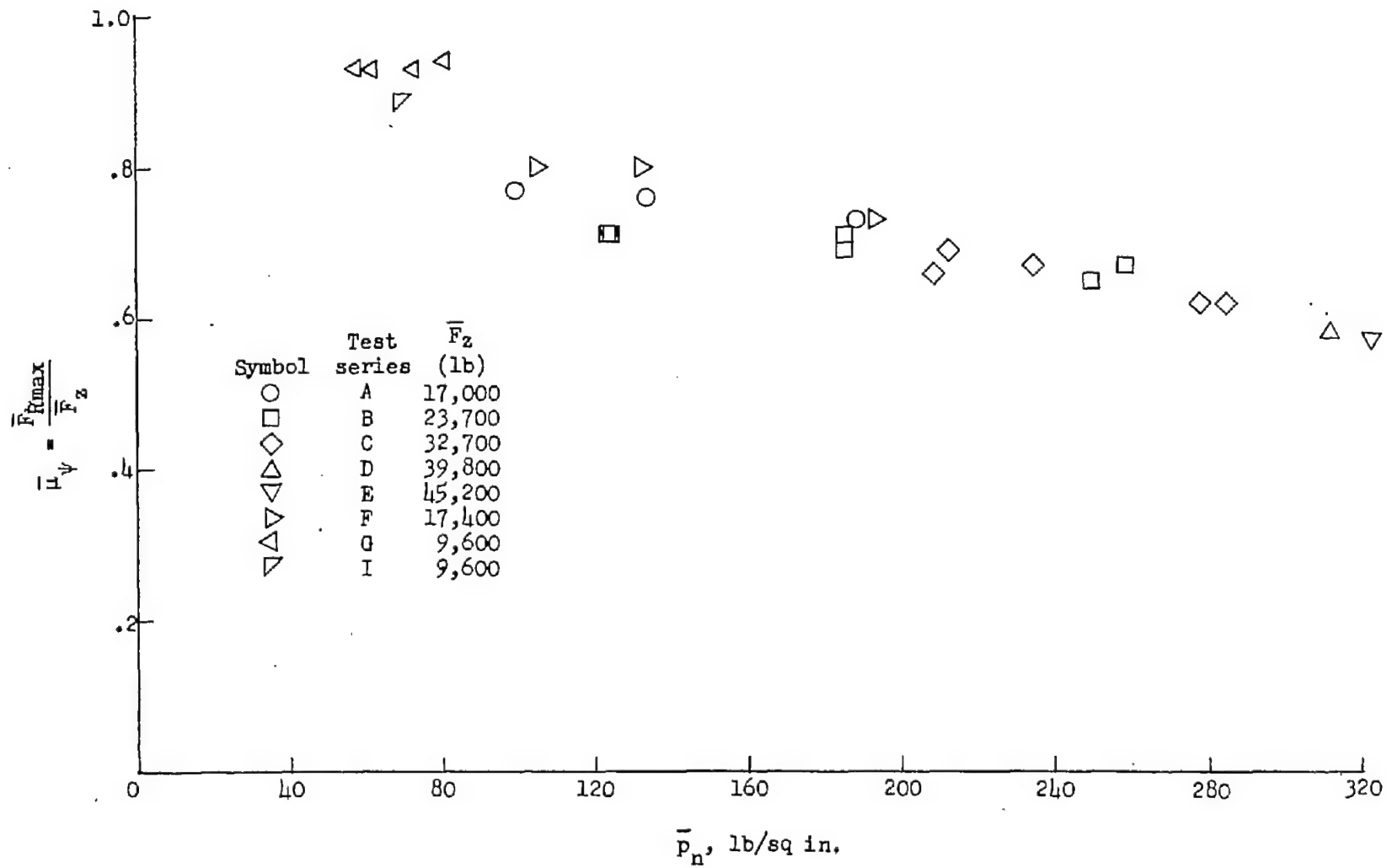
Figure 37.- Variation of yawed-rolling coefficient of friction with average bearing pressure.
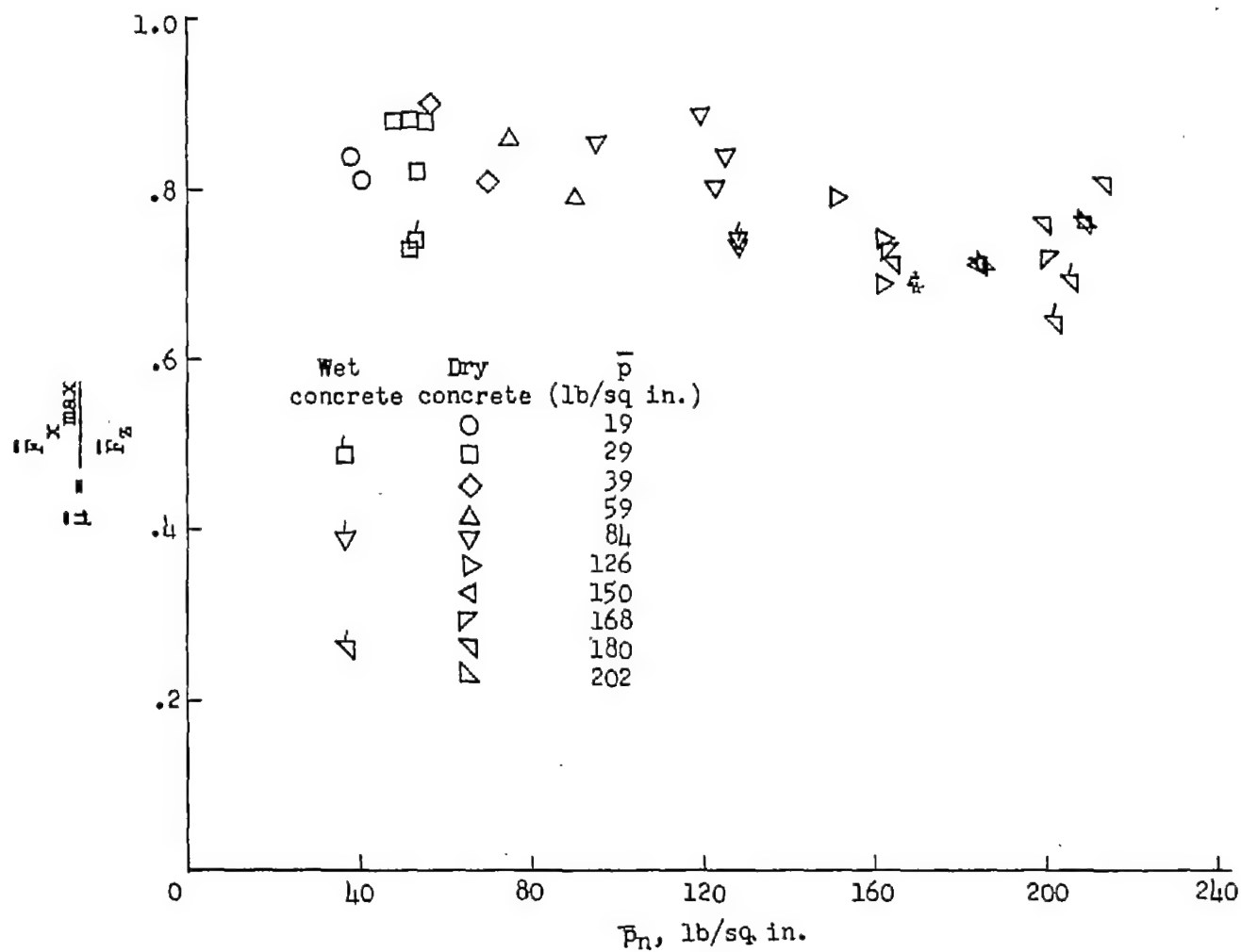
Figure 38.- Variation of sliding drag coefficient of friction with average bearing pressure. $\bar{F}_Z = 9{,}730 - 0.068F_{x_{max}}$ pounds.
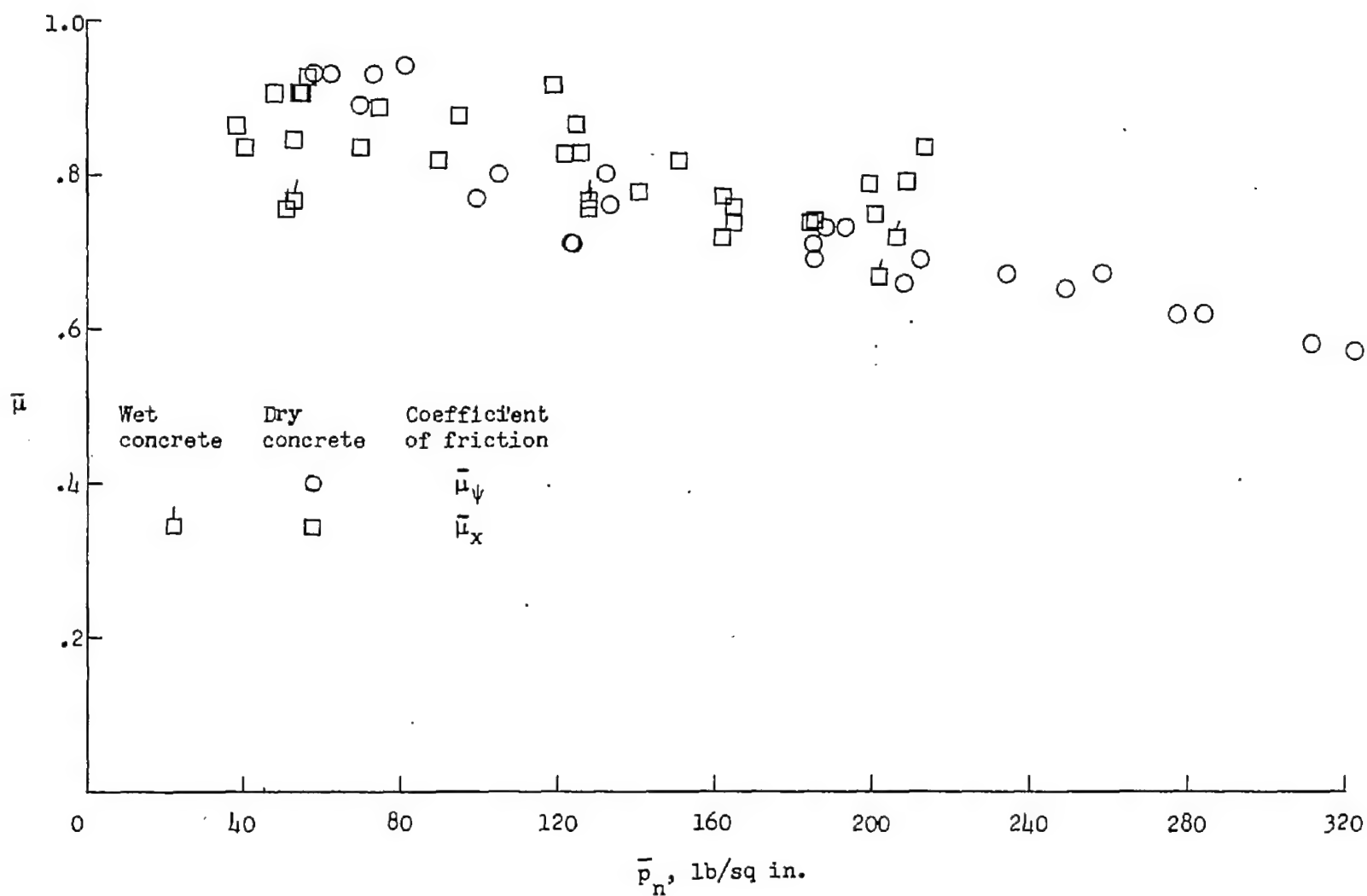
Figure 39.- Comparison of sliding drag and yawed-rolling coefficients
of friction.
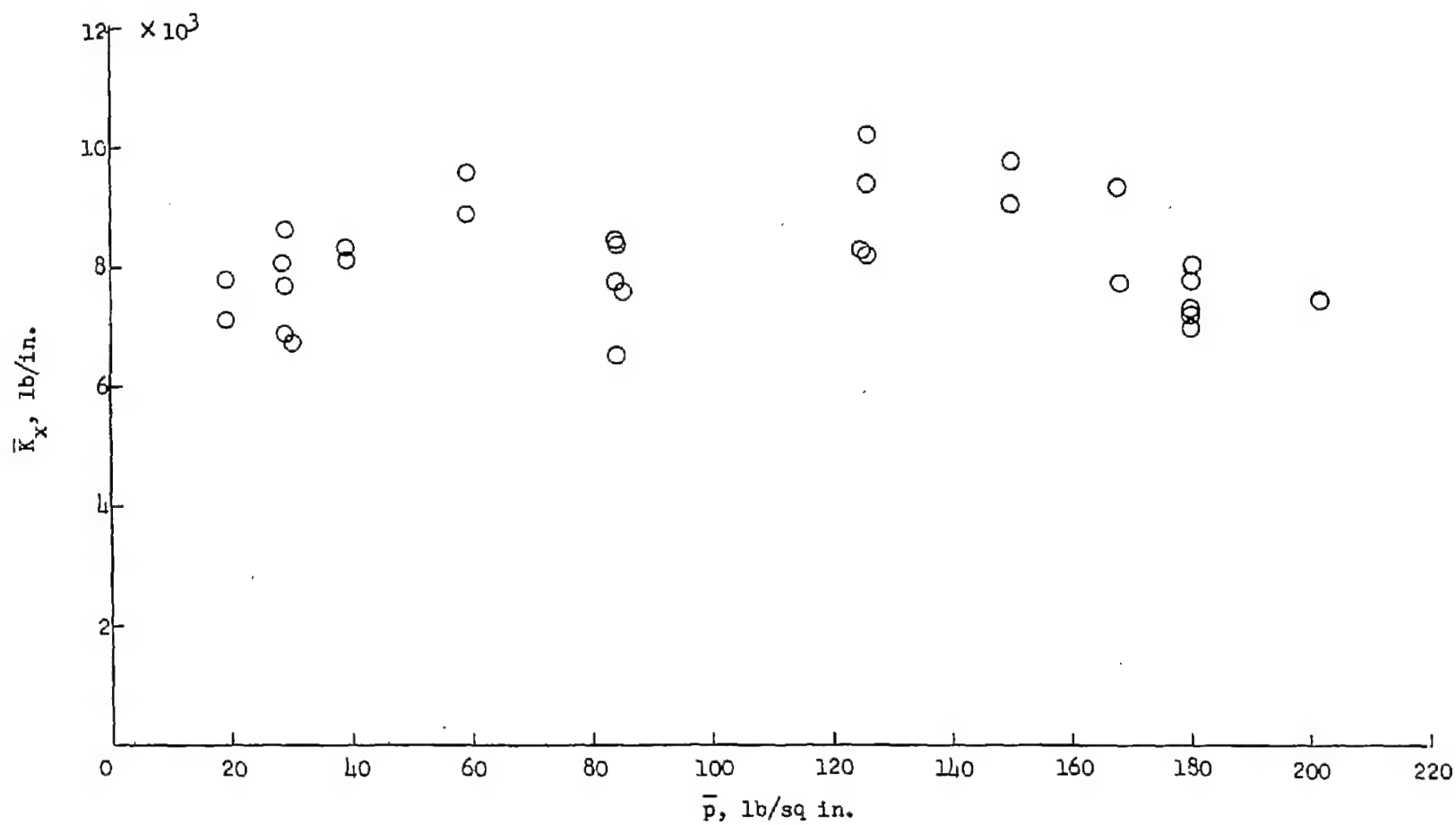
Figure 40.- Variation of fore-and-aft spring constant with tire inflation pressure.
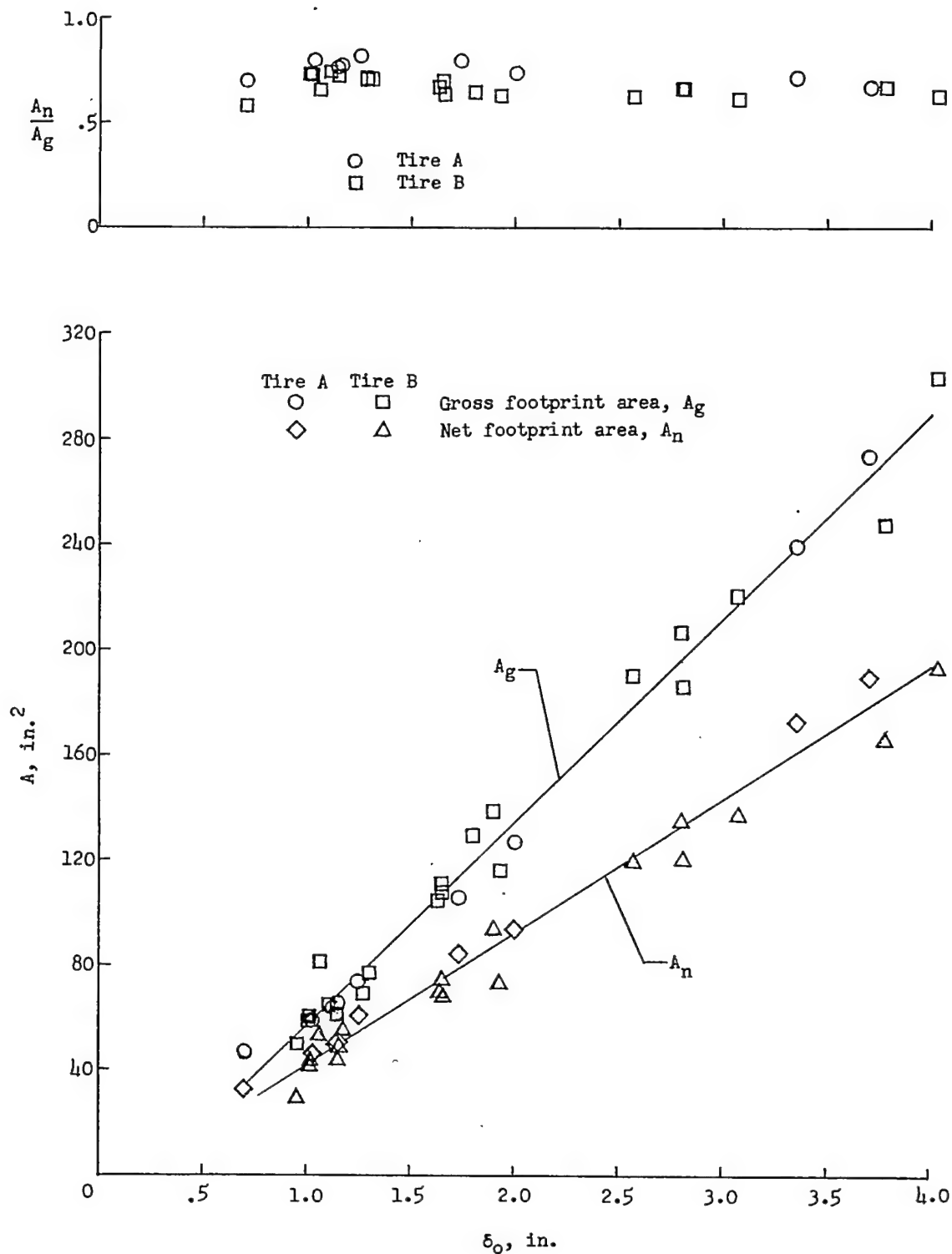
Figure 41.- Variation of gross footprint area, net footprint area, and
the ratio of net footprint area to gross footprint area with vertical
tire deflection for tires A and B.
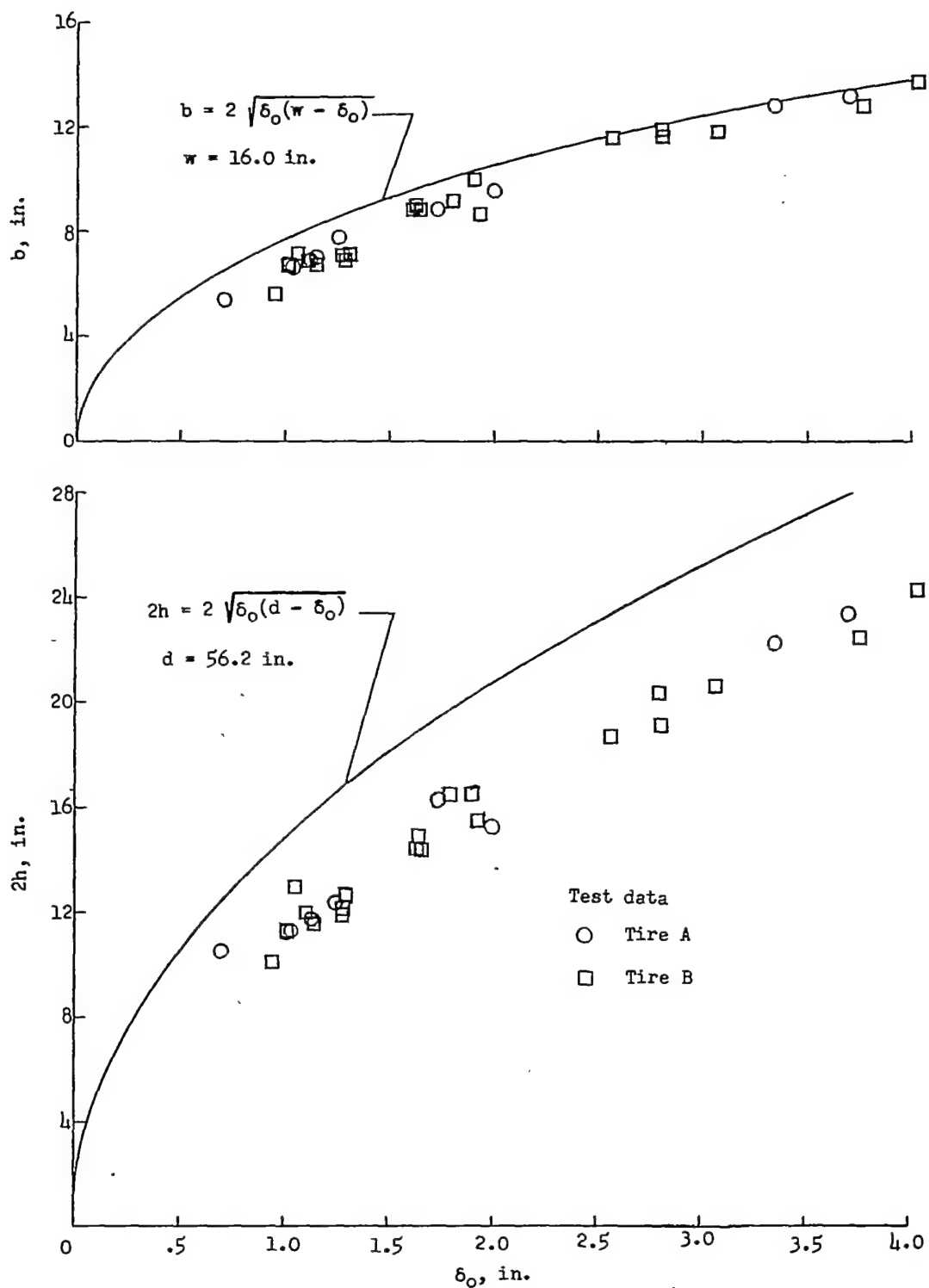
Figure 42.- Variation of footprint length and width with vertical tire
deflection. (Solid lines represent chord lengths of circles having
diameters equal to the diameter and width at rated inflation pressure.)
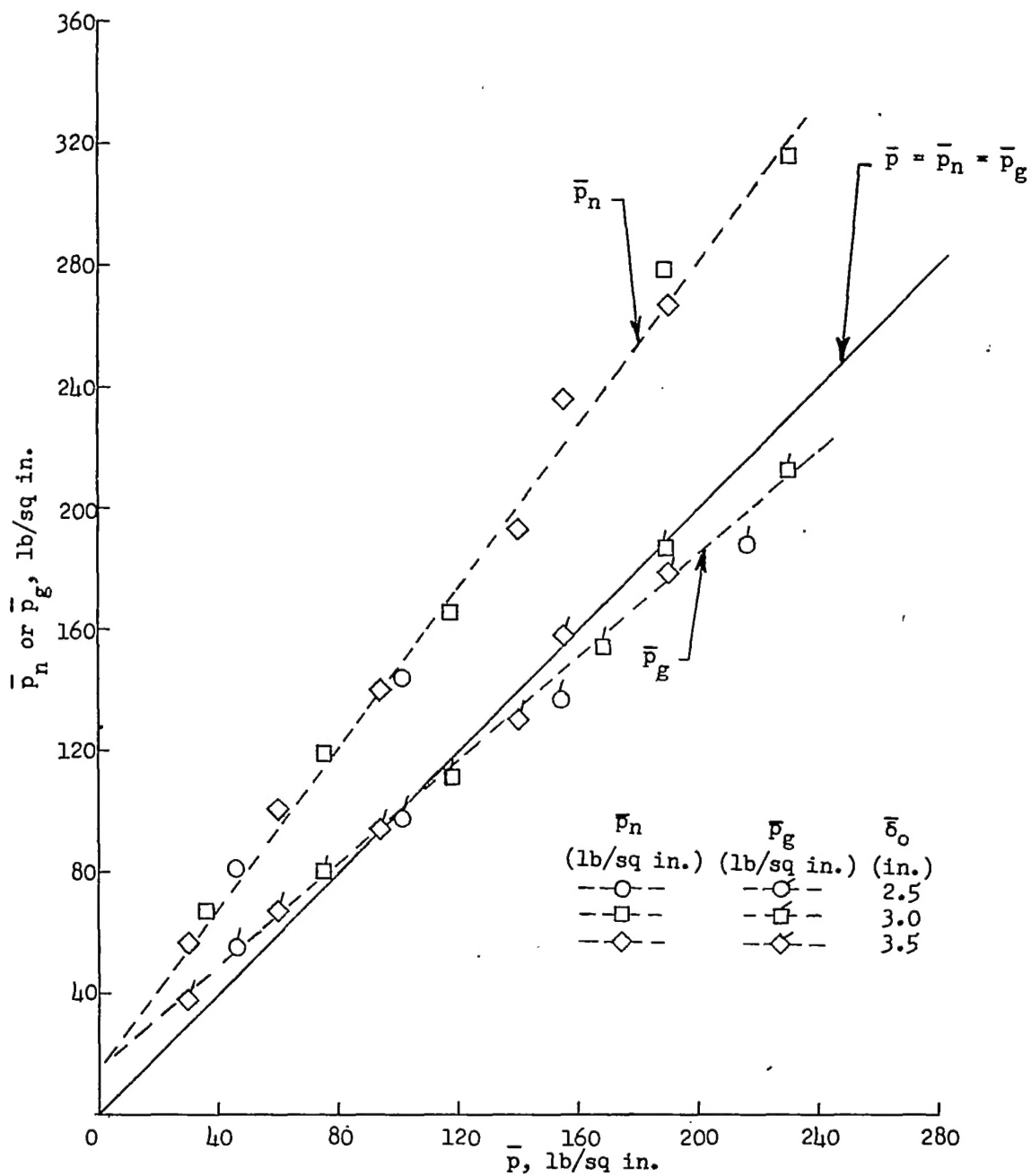
Figure 43.- Variation of average bearing and average gross footprint
pressures with tire inflation pressure for several constant vertical
tire deflections.
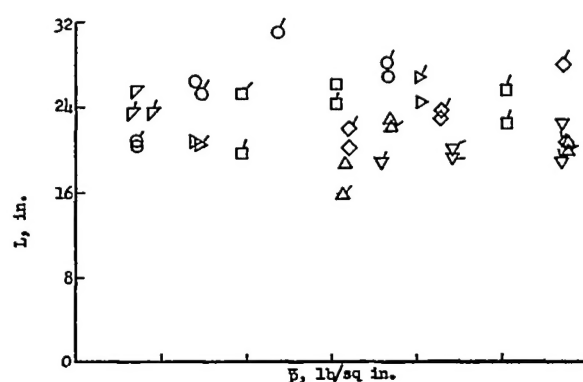
(a) Static-deflection relaxation length  $L_s$ .  Symbols without flags denote
tire A values; symbols with flags, tire B values.
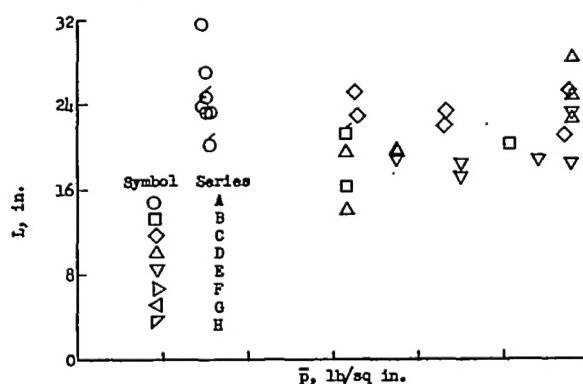


(b) Unyawed-rolling-force relaxation length  $\bar{L}_f$   and unyawed-rolling-
deflection relaxation length  $\bar{L}_\lambda$ .  Symbols without flags are for
the unyawed-rolling-force relaxation length; symbols with flags,
unyawed-rolling-deflection relaxation length.
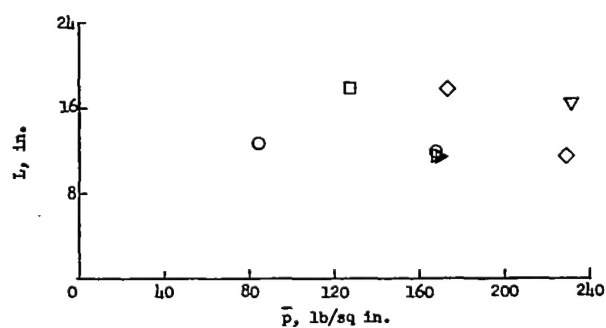


(c) Yawed-rolling relaxation length  $\bar{L}_y$ .

Figure 44.- Variation of the four types of relaxation length with tire
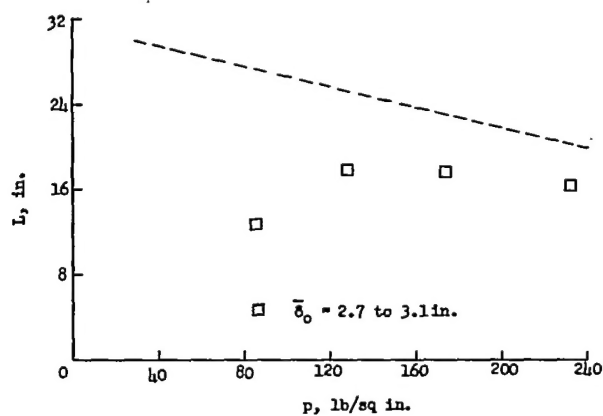inflation pressure.
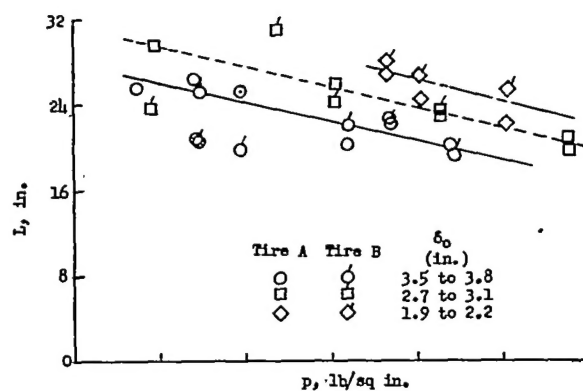
(a) Static-deflection relaxation length $L_s$.
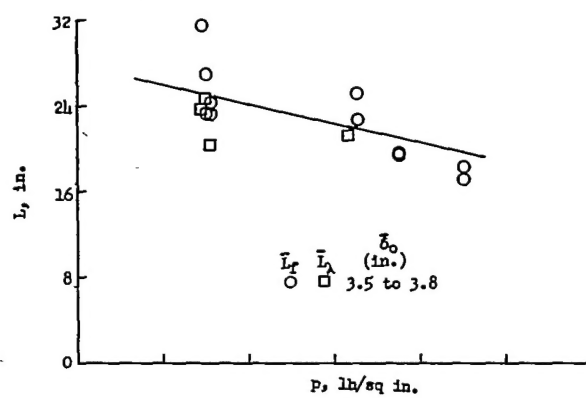


(b) Unyawed-rolling-force relaxation length $\bar{L}_f$ and unyawed-rolling-deflection relaxation length $\bar{L}_\lambda$.



(c) Yawed-rolling relaxation length $L_y$.

Figure 45.- Variation of relaxation length with tire inflation pressure for several constant vertical tire deflections.
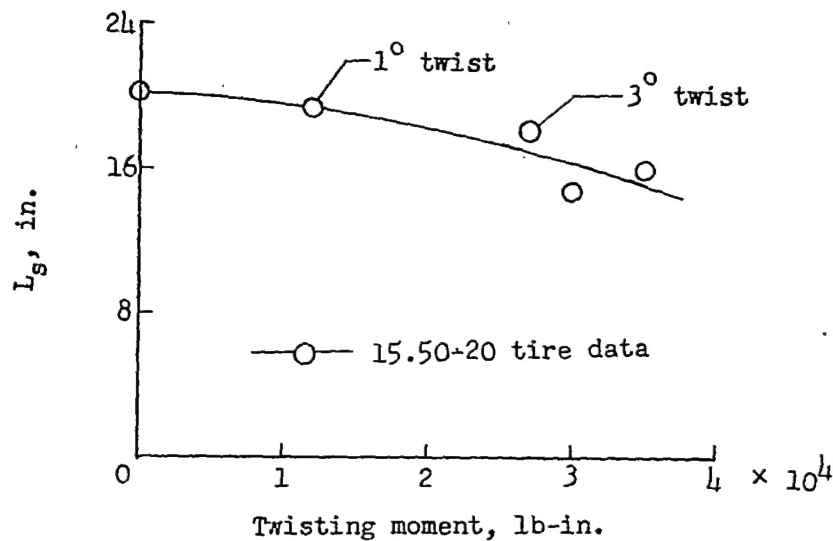
Figure 46.- Variation of static relaxation length with twisting moment or twist for a 15.50-20, type III, low-pressure tire (tire C of ref. 2). $F_s$ = 3,000 pounds; $F_z$ = 20,000 pounds; $p_0$ = 81 pounds per square inch; p = 84 pounds per square inch.
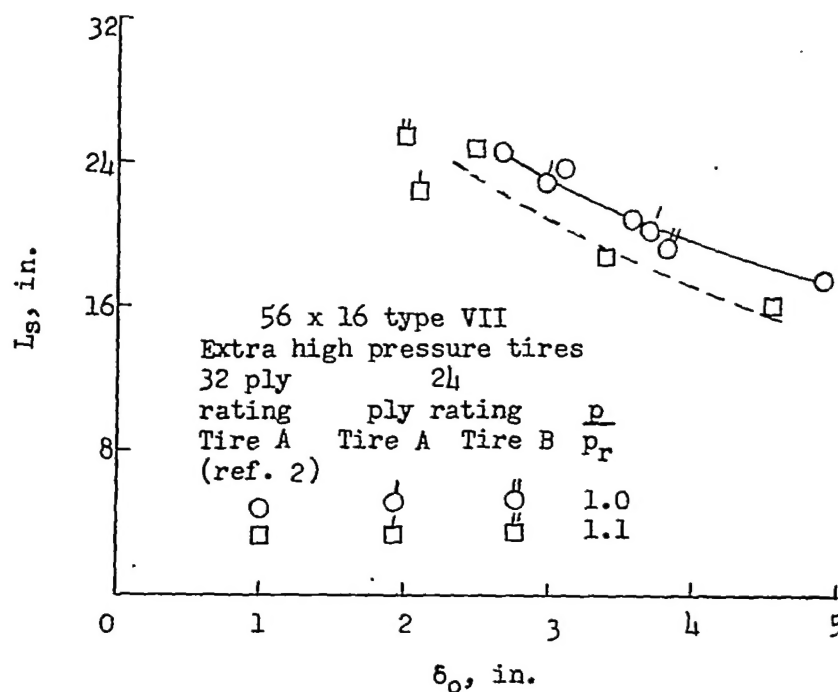


Figure 47.- Comparison of static relaxation lengths obtained from a 56 × 16, type VII, extra high pressure, 32-ply-rating tire (tire A of ref. 2) with test data.